

**NAVAL POSTGRADUATE SCHOOL
MONTEREY, CALIFORNIA**



THESIS

**TURBINE PERFORMANCE MAPPING
OF THE SPACE-SHUTTLE MAIN ENGINE
HIGH-PRESSURE FUEL TURBOPUMP**

Philip Andrew Greco

September 1995

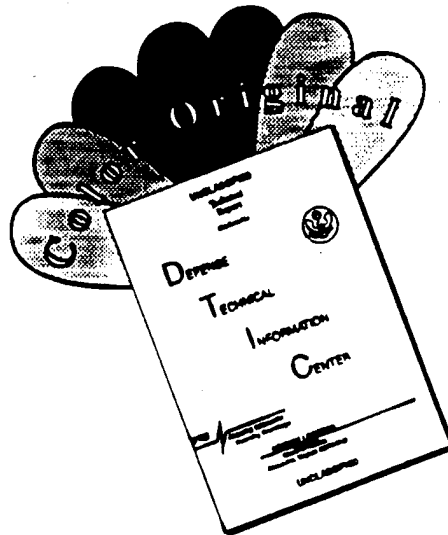
Thesis Advisor: Garth V. Hobson

Approved for public release; distribution is unlimited

DTIC QUALITY INSPECTED 1

19960326 086

DISCLAIMER NOTICE



THIS DOCUMENT IS BEST QUALITY AVAILABLE. THE COPY FURNISHED TO DTIC CONTAINED A SIGNIFICANT NUMBER OF COLOR PAGES WHICH DO NOT REPRODUCE LEGIBLY ON BLACK AND WHITE MICROFICHE.

REPORT DOCUMENTATION PAGE

Form Approved
OMB No. 0704-0188

Public reporting burden for this collection of information is estimated to average 1 hour per response, including the time for reviewing instructions, searching existing data sources, gathering and maintaining the data needed, and completing and reviewing the collection of information. Send comments regarding this burden estimate or any other aspect of this collection of information, including suggestions for reducing this burden, to Washington Headquarters Services, Directorate for Information Operations and Reports, 1215 Jefferson Davis Highway, Suite 1204, Arlington, VA 22202-4302, and to the Office of Management and Budget, Paperwork Reduction Project (0704-0188), Washington, DC 20503.

1. AGENCY USE ONLY (Leave blank)	2. REPORT DATE September 1995	3. REPORT TYPE AND DATES COVERED Master's Thesis
---	---	--

4. TITLE AND SUBTITLE TURBINE PERFORMANCE MAPPING OF THE SPACE-SHUTTLE MAIN ENGINE HIGH-PRESSURE FUEL TURBOPUMP	5. FUNDING NUMBERS
---	---------------------------

6. AUTHOR(S) Philip Andrew Greco	
--	--

7. PERFORMING ORGANIZATION NAME(S) AND ADDRESS(ES) Naval Postgraduate School Monterey, CA 93943-5000	8. PERFORMING ORGANIZATION REPORT NUMBER
---	---

9. SPONSORING / MONITORING AGENCY NAME(S) AND ADDRESS(ES)	10. SPONSORING / MONITORING AGENCY REPORT NUMBER
--	---

11. SUPPLEMENTARY NOTES
The views expressed in this thesis are those of the author and do not reflect the official policy or position of the Department of Defense or the U.S. Government.

12a. DISTRIBUTION / AVAILABILITY STATEMENT Approved for public release; distribution is unlimited	12b. DISTRIBUTION CODE
---	-------------------------------

13. ABSTRACT (Maximum 200 words)
The redesign, data acquisition system installation, and software development for the cold-flow Turbine Test Rig is reported. The turbine tested was the Space Shuttle Main Engine High Pressure Fuel Turbopump first stage 'Alternate Turbopump Development' model designed and manufactured by Pratt & Whitney. The purpose of this research was to establish a continuously operating, cold-flow, turbine test facility which could be used for future laser-Doppler-velocimetry measurements in the tip leakage region of the turbine rotor blades. Also, to determine both the single and two stage turbine performance parameters, and to provide a test model for comparison with numerical simulations using a three-dimensional viscous flow code. A throttle valve was designed and installed at the turbine exit to control the pressure ratio in order to map the turbine performance. Data acquisition, reduction and display programs were developed using LabVIEW Visual Instrument software in order to collect, and process the data. The first-stage turbine exit velocity profile was measured using a cobra probe. Also, the first-stage turbine performance characteristics were determined. Flow-field characteristics of the first stage turbine were predicted using a three-dimensional viscous flow code.

14. SUBJECT TERMS Performance Mapping, Turbine, Data Acquisition, Laser Doppler Velocimetry, Numerical Simulation, Space Shuttle Main Engine, High Pressure Fuel Turbopump	15. NUMBER OF PAGES 162
	16. PRICE CODE

17. SECURITY CLASSIFICATION OF REPORT Unclassified	18. SECURITY CLASSIFICATION OF THIS PAGE Unclassified	19. SECURITY CLASSIFICATION OF ABSTRACT Unclassified	20. LIMITATION OF ABSTRACT UL
--	---	--	---

Approved for public release; distribution is unlimited.

TURBINE PERFORMANCE MAPPING OF THE
SPACE-SHUTTLE MAIN ENGINE
HIGH-PRESSURE FUEL TURBOPUMP

Philip A. Greco
Lieutenant, United States Navy
B.S., The Cooper Union, 1986

Submitted in partial fulfillment of the requirements for
the degree of

MASTER OF SCIENCE IN AERONAUTICAL ENGINEERING

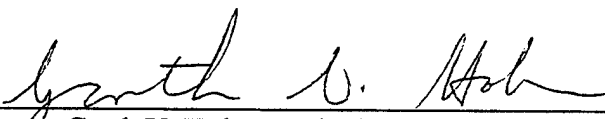
from the

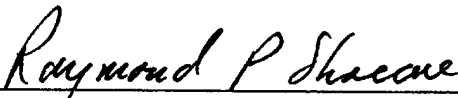
NAVAL POSTGRADUATE SCHOOL
September 1995

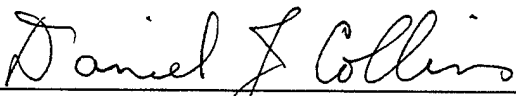
Author:


Philip A. Greco

Approved by:


Garth V. Hobson, Thesis Advisor


Raymond P. Shreeve, Second Reader


Daniel J. Collins, Chairman,
Department of Aeronautics and Astronautics

ABSTRACT

The redesign, data acquisition system installation, and software development for the cold-flow Turbine Test Rig is reported. The turbine tested was the Space Shuttle Main Engine High Pressure Fuel Turbopump first stage 'Alternate Turbopump Development' model designed and manufactured by Pratt & Whitney. The purpose of this research was to establish a continuously operating, cold-flow, turbine test facility which could be used for future laser-Doppler-velocimetry measurements in the tip leakage region of the turbine rotor blades. Also, to determine both the single and two stage turbine performance parameters, and to provide a test model for comparison with numerical simulations using a three-dimensional viscous flow code. A throttle valve was designed and installed at the turbine exit to control the pressure ratio in order to map the turbine performance. Data acquisition, reduction and display programs were developed using LabVIEW Visual Instrument software in order to collect, and process the data. The first-stage turbine exit swirl and velocity profiles were measured using a cobra probe. Also, the first-stage turbine performance characteristics were determined. Flow-field characteristics of the first stage turbine were predicted using a three-dimensional viscous flow code.

TABLE OF CONTENTS

I.	INTRODUCTION.....	1
	A. PURPOSE.....	1
	B. OVERVIEW.....	2
II.	TURBINE TEST RIG.....	3
	A. TURBINE THROTTLE VALVE AND 1ST/2ND STAGE OUTER CASING UPGRADE.....	3
	B. DYNAMOMETER AUTOMATIC SPEED-CONTROL SYSTEM.....	7
	C. AIRPAX TACHTROL 3 TACHOMETER.....	8
	D. COBRA PROBE INSTALLATION AND POSITIONING.....	9
III.	DATA ACQUISITION SYSTEM.....	11
	A. GENERAL DESCRIPTION.....	11
	B. HARDWARE DESCRIPTION.....	11
	1. PC-486 Computer.....	11
	2. AT-GPIB/TNT Interface Board.....	13
	3. PC-DIO-24 I/O Board.....	13
	4. PC-LPM-16 Multifunction I/O Board.....	14
	5. Scanivalve Digital Interface Unit, Solenoid Controller and Interface Box.....	14
	6. HP Data Acquisition Modules.....	14
IV.	LabVIEW SOFTWARE PACKAGE.....	17

A.	GENERAL DESCRIPTION.....	17
1.	LabVIEW Software Familiarization and Development Method....	17
B.	LabVIEW INSTRUMENT DRIVERS.....	18
1.	HP Digital Voltmeter (DVM) and HP Scanner.....	18
2.	HP 5335 Universal Counter.....	20
3.	Scanivalve Digital Interface Unit (SDIU).....	21
C.	TTR (SSME HPFTP ATD) DATA ACQUISITION.....	21
V.	EXPERIMENTAL SETUP.....	25
A.	TURBINE TEST RIG MEASUREMENTS.....	25
B.	COBRA PROBE CALIBRATION.....	31
C.	EXPERIMENTAL PROCEDURE.....	33
1.	Turbine Test Rig Operation.....	33
a.	<i>Pressure Transducer Calibration</i>	35
b.	<i>Load Cell Calibration</i>	35
c.	<i>Automatic Speed Control</i>	36
2.	SSME HPFTP ATD Real-Time Data Display.....	37
3.	SSME HPFTP ATD Performance Data Collection.....	38
4.	Outlet Velocity Profile Data Collection.....	40
VI.	RESULTS AND DISCUSSION.....	43
VII.	NUMERICAL SIMULATION.....	61
A.	INTRODUCTION.....	61
B.	TURBINE FIRST STAGE GRID GENERATION.....	61
C.	FLOW SOLUTION.....	62

VIII.	CONCLUSIONS AND RECOMMENDATIONS.....	75
A.	EXPERIMENT AND TTR.....	75
B.	DATA ACQUISITION SYSTEM.....	77
C.	COMPUTATIONAL FLUID DYNAMICS.....	78
APPENDIX A.	ENGINEERING DRAWINGS.....	79
APPENDIX B.	WIRING DIAGRAMS.....	87
APPENDIX C.	SOFTWARE PROGRAMMING CODES & HARDWARE DIP SWITCH SETTINGS.....	91
APPENDIX D.	50 PIN CONNECTOR ASSIGNMENTS.....	97
APPENDIX E.	LabVIEW VISUAL INSTRUMENT FUNCTIONS.....	99
APPENDIX F.	LabVIEW TTR DATA ACQUISITION VI's.....	101
APPENDIX G.	COBRA PROBE CALIBRATION.....	121
APPENDIX H.	TTR PRE-OPERATION CHECKLIST and DATA COLLECTION SHEET.....	123
APPENDIX I.	SSME HPFTP ATD PERFORMANCE EQUATIONS.....	127
APPENDIX J.	EXCEL WORKSHEETS.....	127
APPENDIX K.	FORTRAN PROGRAMS.....	133
APPENDIX L.	TCGRID & RVC3D INPUT FILES.....	135
	LIST OF REFERENCES.....	143
	INITIAL DISTRIBUTION LIST.....	147

LIST OF FIGURES

Figure 1.	TTR and SSME HPFTP ATD Assembly.....	4
Figure 2.	Schematic of Automatic Turbine Speed-Control System.....	5
Figure 3.	Turbine Exit Throttle Valve.....	6
Figure 4.	MOTION Systems Ball-Drive Actuator.....	7
Figure 5.	L.C. Smith Probe Actuator.....	9
Figure 6.	TTR Data Acquisition System.....	12
Figure 7.	Scanivalve Control and Pressure Port Designation.....	15
Figure 8.	HP_DVM.VI Icon.....	19
Figure 9.	SCANNER2.VI Icon.....	19
Figure 10.	HP 5335A.VI Icon.....	20
Figure 11.	SVCONTRL.VI.....	21
Figure 12.	LabVIEW Hierarchy Diagram for the SSME_TTR.VI Data Acquisition VI.....	22
Figure 13.	SSME_TTR.VI Front Panel.....	23
Figure 14.	TTR Seven Channel Thermocouple Set-up.....	27
Figure 15.	5th Order and Linear Curve Fits for the Type-J Thermocouple.....	28
Figure 16.	Lebow Load Cell Calibration.....	29
Figure 17.	Cox Flow Meter Calibration.....	30
Figure 18.	Cobra Probe Calibration Set-up and Scanivalve Port Designation.....	32
Figure 19.	Control and Read Out for the Ball Drive and L.C. Smith Probe Actuators.....	42

Figure 20.	Efficiency vs. Referred RPM.....	44
Figure 21.	Efficiency vs. Total-to-Total Pressure Ratio.....	45
Figure 22.	Referred Horsepower vs. Referred RPM.....	46
Figure 23.	Referred Mass Flow vs. Total-to-Total Pressure Ratio.....	47
Figure 24.	Mass Flow Rate vs. RPM.....	48
Figure 25.	Efficiency vs. Total-to-Total Pressure Ratio.....	50
Figure 26.	Referred Mass Flow Rate vs. Total-to-Total Pressure Ratio.....	51
Figure 27.	Referred Horsepower vs. Referred RPM.....	52
Figure 28.	Turbine Characteristics [from Ref. 21].....	54
Figure 29.	Dynamometer Power Absorption Curve.....	55
Figure 30.	Absolute and Relative Velocity Vectors [from Ref. 23]	57
Figure 31.	Radial Position vs. Swirl Angle.....	58
Figure 32.	Radial Position vs. Mach Number.....	60
Figure 33.	3-D First Stage Stator Grid.....	63
Figure 34.	2-D First Stage Stator Hub Grid.....	64
Figure 35.	3-D First Stage Rotor Grid.....	65
Figure 36.	2-D First Stage Rotor Hub Grid.....	66
Figure 37.	General Fitted Body System.....	67
Figure 38.	Stator Exit Plane Mach Number Contours.....	69
Figure 39.	Stator Exit Plane Stagnation Pressure Contours.....	70
Figure 40.	Stator Residual History.....	71

Figure 41.	Rotor Exit Plane Relative Mach Number Contours.....	72
Figure 42.	Rotor Exit Plane Stagnation Pressure Contours.....	73
Figure 43.	Rotor Residual History.....	74
Figure A1.	Stage 1 Casing.....	79
Figure A2.	Stage 2 Casing	80
Figure A3.	Nozzle Flange.....	81
Figure A4.	Movable Back-Pressure Plate.....	82
Figure A5.	Shaft Cover.....	83
Figure A6.	Throttle Guide Rod.....	84
Figure A7.	Dynamometer Flange Actuator Mounting Plate.....	85
Figure A8.	Actuator Mounting Bracket.....	86
Figure B1.	Automatic Load-Control System Wiring Diagram.....	87
Figure B2.	AIRPAX TACHTROL 3 Terminal Bus Connections.....	88
Figure B3.	Scanivalve Interface Box.....	89
Figure B4.	AIRPAX TACHTROL 3 Flow Diagram.....	90
Figure D1.	PC-DIO-24 50 Pin Connector Assignments.....	97
Figure D2.	PC-LPM-16 50 Pin Connector Assignments.....	99
Figure F1.	SSME_TTR.VI Block Diagram.....	101
Figure F2.	COBR_CAL.VI Front Panel and Block Diagram.....	114
Figure F3.	TTR_TEST.VI Front Panel and Block Diagram.....	115
Figure F4.	ACTUATOR.VI Front Panel and Block Diagram.....	118

Figure F5.	VEL_PRFL.VI Front Panel and Block Diagram.....	119
Figure G1	Cobra Probe Calibration.....	122
Figure H1.	TTR Pre-Operation Check List.....	123
Figure H2.	TTR Data Collection Sheet.....	124
Figure J1.	SSMETTR Excel Data Collection Worksheet (TTR Raw Data).....	127
Figure J2.	SSME_TTR Excel Reduced Data Collection Worksheet.....	130
Figure J3.	VEL_PRFL Excel Data Collection Worksheet (TTR Exit Data).....	131
Figure K1.	PXY.F.....	133
Figure K2.	SHRINK99.F.....	134
Figure L1.	STATOR.IN.....	135
Figure L2.	ROTOR.IN.....	138
Figure L3.	RVC3D.IN for both the Stator and Rotor.....	141

I. INTRODUCTION

A. PURPOSE

The purpose of this research was to establish a continuously operating, cold-flow, Turbine Test Rig (TTR) which could be used for future laser-Doppler-velocimetry (LDV) measurements in the tip-leakage region of the turbine rotor blades. The TTR was modified in order to test the Space Shuttle Main Engine High Pressure Fuel Turbopump (HPFTP) Alternate Turbopump Development (ATD) model. Previous work as reported by Studevan [Ref. 1], incorporated the original TTR modification and installation of the ATD. The follow-on work reported by Rutkowski [Ref. 2], included modifications to the turbine bearing housing and initial shake-down tests. Numerical modeling of the first stage turbine stator using a three-dimensional viscous flow code was also reported. The purpose of this thesis was to further modify the TTR, install the data acquisition system, automate the data collection and reduction process using a Personal Computer (PC)-based graphical data-acquisition software package, and map the first-stage turbine performance. Also, the flow through the first-stage turbine was simulated using a three-dimensional (3-D) viscous flow code. The most significant modification to the turbine was the design, manufacture and installation of a back-pressure throttle valve aft of the turbine. Follow-on work would include measuring the first stage inlet velocity profile, LDV measurements of the flow field at the first stage turbine rotor immediately adjacent to the endwall in the tip clearance region, incorporating the second stage onto the TTR, and mapping the two-stage turbine performance.

B. OVERVIEW

The redesign of the TTR included cobra probe measurement access at the first-stage inlet and exit planes, installation of the redesigned first- and second-stage outer casings, inclusion of a LDV optical window in the first-stage outer casing, and installation of a turbine-exit throttle valve in order to control the turbine pressure ratio. The TTR modifications also included connection of additional sensors and the complete commissioning of a data acquisition system. These sensors included all TTR pressure probes, thermocouples, a magnetic speed pick-up, a dynamometer load cell and water flow-rate meter. Also, software was developed in order to automatically collect, store, and reduce turbine performance data.

Turbine tests were conducted in order to shake down the TTR and to map the first-stage model. The turbine tests were conducted using two different configurations. First, the turbine exit was exposed to atmosphere, and second, a turbine exit throttle valve was installed.

The cobra probe measurements with the turbine exit exposed to atmosphere and with the exit throttle valve installed were conducted in order to determine the rotor exit plane velocity profile for comparison to numerical flow solutions using a code developed by Roderick V. Chima. The code, Rotor Viscous Code 3-D (RVC3D) [Ref. 3], was used for numerical computation of the flow field through the first-stage turbine.

II. TURBINE TEST RIG

A schematic showing a cross section of the turbine test rig is shown in Figure 1. Various sensor locations are annotated on the figure which also shows the flow direction of air through the turbine. Figure 2 shows a schematic of the water dynamometer system, which was used to apply a load to the turbine. Also shown is the magnetic speed sensor, digital readout and automatic controller of the dynamometer outlet valve. The torque produced by the turbine was determined using the Lebow load cell mounted on the water dynamometer. Dynamometer water flow measurement was obtained from the Cox flow meter connected to the inlet water line.

The TTR set-up reported in [Ref. 1] and [Ref. 2] was modified to include housing changes, a turbine exit throttle valve, speed control system upgrades, and additional turbine performance sensors.

A. TURBINE THROTTLE VALVE AND 1ST/2ND STAGE OUTER CASING UPGRADE

The first- and second-stage outer turbine casings were redesigned and manufactured in order to incorporate the following changes. The first-stage casing included a LDV window at the 9:00 position when viewed from the rear of the turbine, and an inlet probe slot at the 11:30 position. This probe slot was needed in order to measure the inlet velocity profile. The second-stage casing included a probe slot at the 1:00 position and 4 axially-aligned static pressure ports at the 7:00 position. The second-stage probe slot was

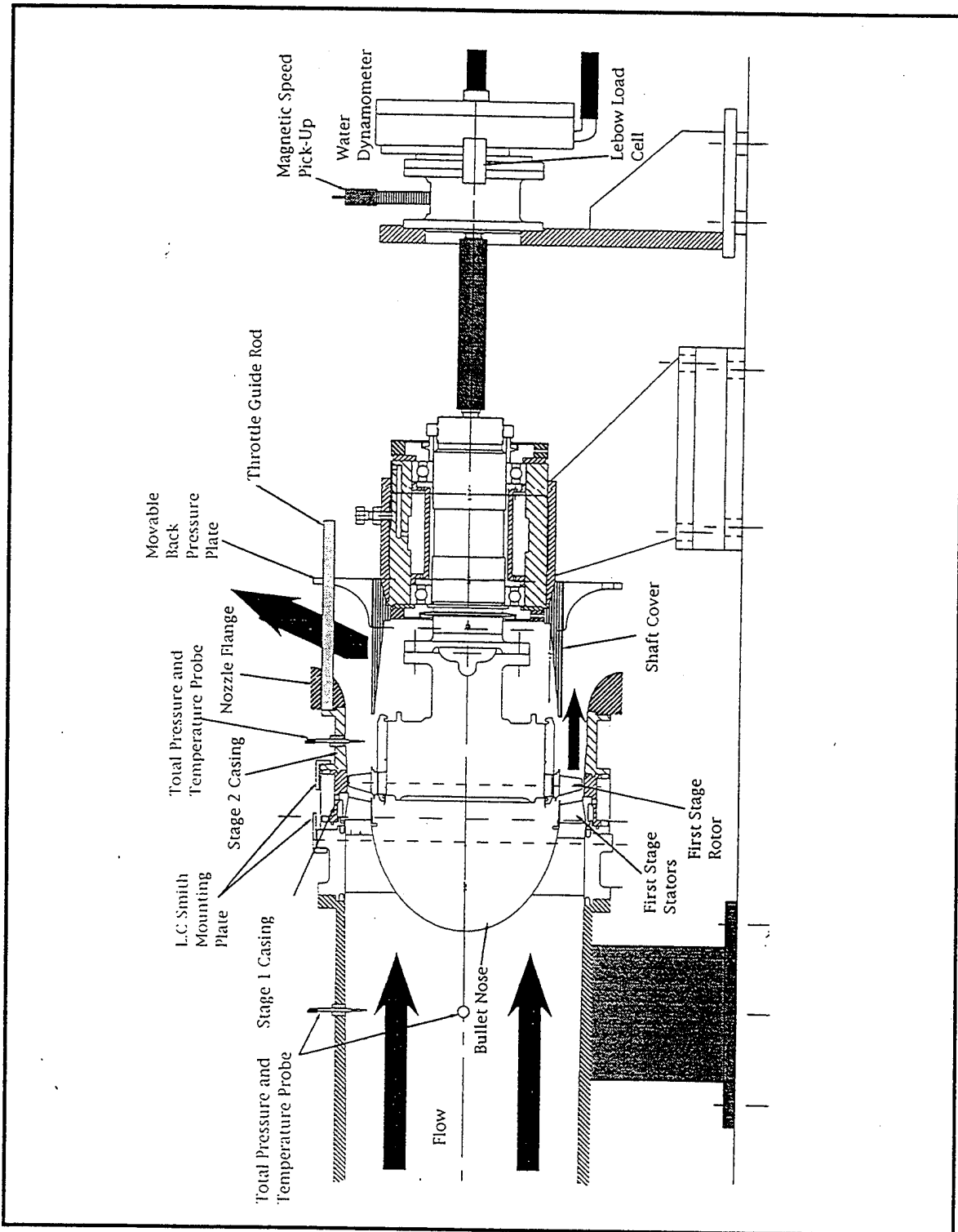


Figure 1. TTR and SSME HPFTP ATD Assembly

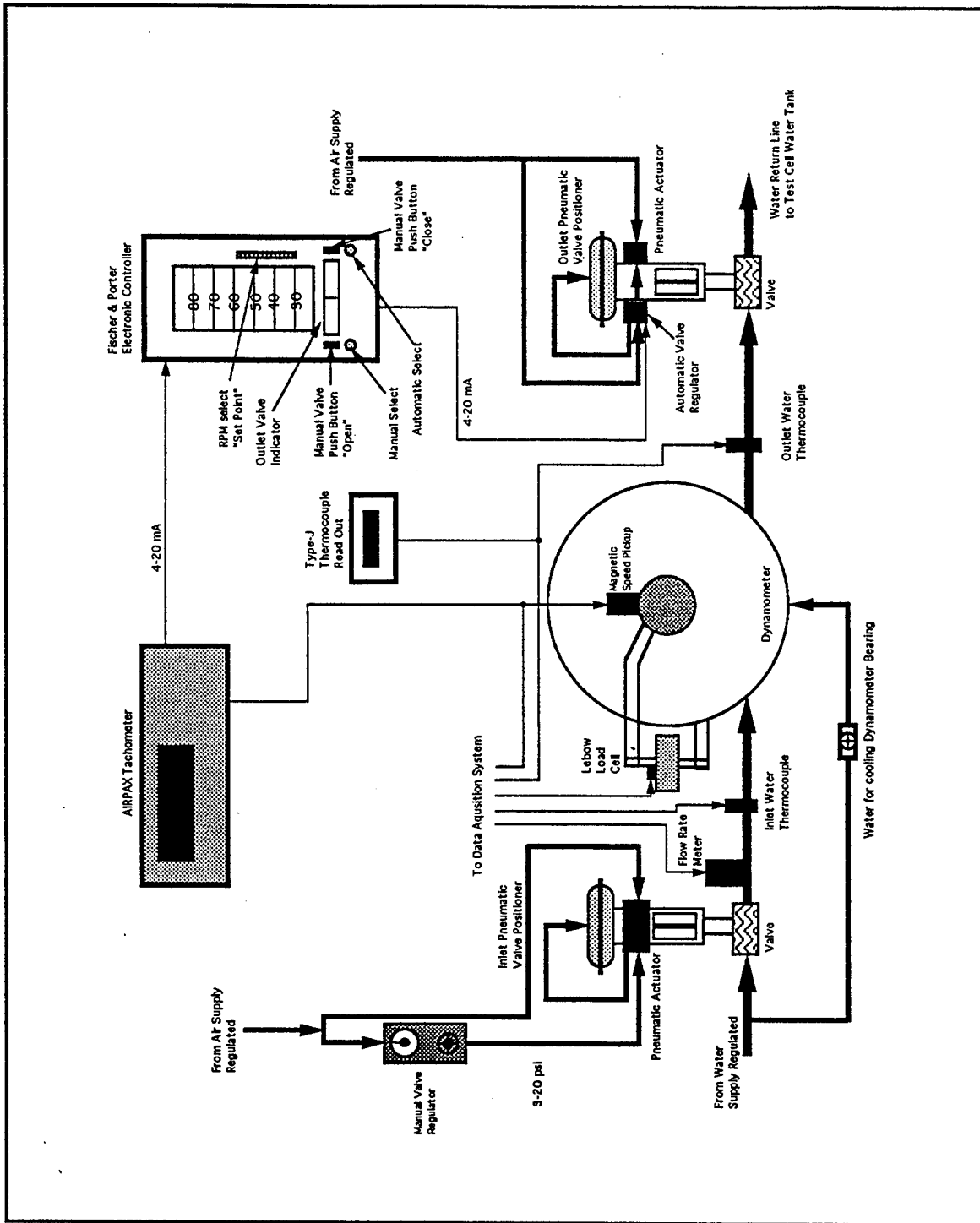


Figure 2. Schematic of Automatic Turbine Speed-Control System

used to measure the first-stage turbine exit velocity profile. Engineering drawings for all the TTR modifications are shown in Appendix A.

The TTR exit throttle valve was designed and manufactured in order to control the turbine pressure ratio, and to increase the upstream total pressure. This was accomplished by a movable plate which varied the turbine exit area, thus creating a back pressure. The throttle valve also turned the flow 90 degrees, a photograph of the turbine exit throttle valve assembly is shown Figure 3.

The turbine throttle valve was positioned using a linear ball-drive actuator. The Motion Systems ball-drive actuator (Model 85151), shown in Figure 4, was connected between the back pressure plate and the mounting flange of the dynamometer. It had a stroke of six inches with a 40:1 gear ratio and could supply an axial force of 500 lbs.

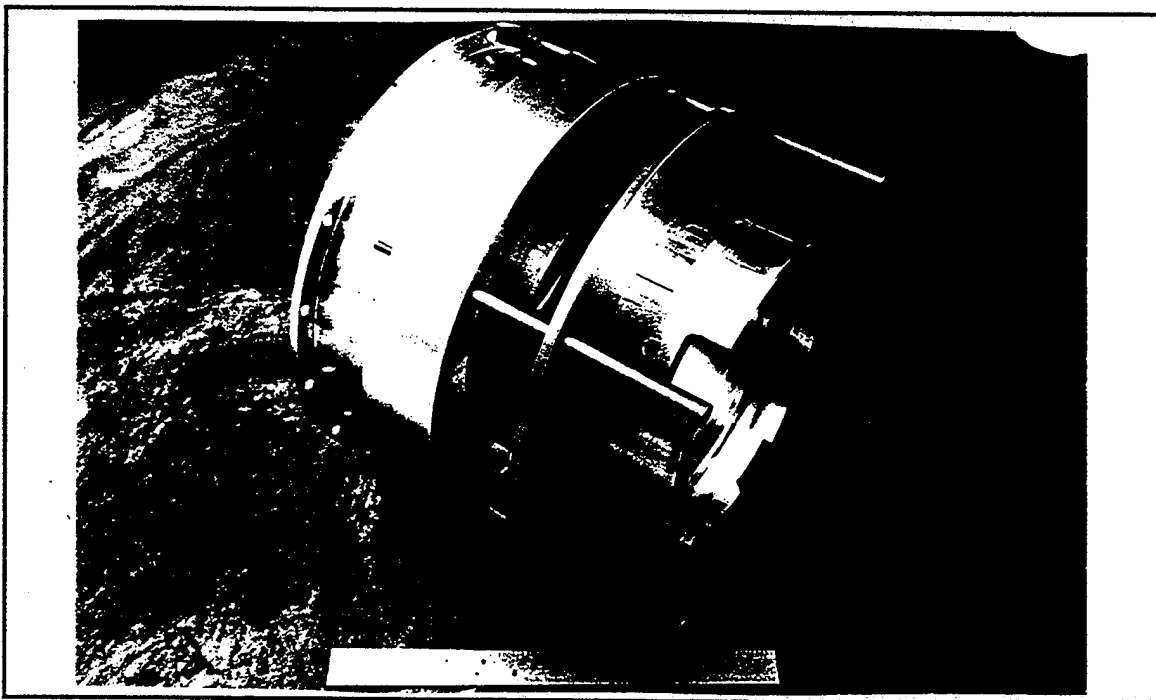


Figure 3. Turbine Exit Throttle Valve Assembly

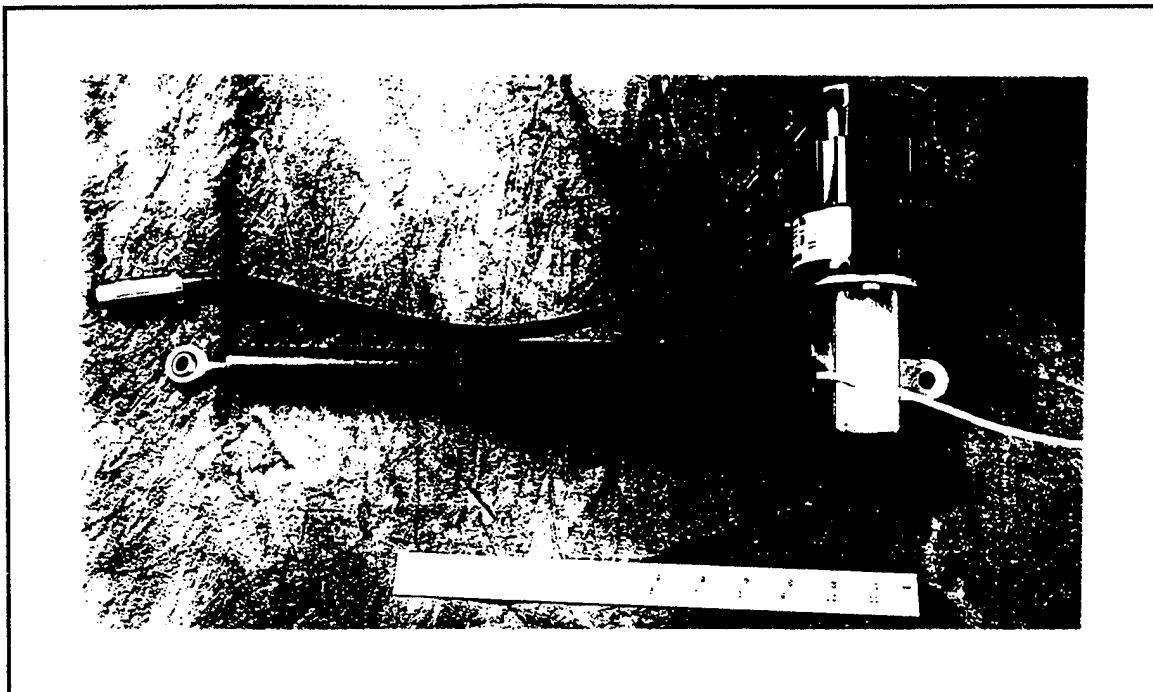


Figure 4. MOTION Systems Ball-Drive Actuator

B. DYNAMOMETER AUTOMATIC SPEED-CONTROL SYSTEM

The automatic load-control system is shown in Figure 2 where the torque in (in-lbs) was measured using the Lebow load cell. The original dynamometer turbine load system set-up, as reported by Studevan [Ref. 1], was operated manually and consisted of an electronic controller (Fischer and Porter series 53EL4000), a water dynamometer, two pneumatic valve positioners, and a magnetic speed pick-up. A tachometer (AIRPAX TACHROL 3) was added to the system in order to operate the load-control system in automatic mode and to obtain a digital readout of the turbine rotational speed in revs/min (RPM). The tachometer provided an analog output that produced a linear relationship of output current in mA vs. turbine RPM. This current output, 4-20 mA, corresponded to 0-10000 RPM which was connected to terminal #10 of the electronic controller and was

used as the signal "process variable". A wiring diagram of the electronic controller is shown in Appendix B, Figure B1. Because the analog signal from the TACHTROL 3 was a current output (4-20 mA), shown in Appendix B, Figure B2, and the electronic controller needed a 1-5 Vdc source, a 250Ω resistor was connected between terminals 10 and 11 of the electronic controller. By adjusting the thumb wheel on the Fischer & Porter Electronic Controller, an output voltage was generated between 1-5 Vdc which was the controller "set point". The electronic controller drove the difference between the set point and process variable output to zero by positioning the outlet dynamometer water valve to meet the desired condition. The outlet water valve was connected to terminal #4 of the electronic controller. Positioning the outlet water valve changed the water level in the dynamometer, which changed the load on the turbine causing a change in turbine speed.

C. AIRPAX TACHTROL 3 TACHOMETER

The turbine speed display consisted of the AIRPAX TACHTROL 3 tachometer unit with digital readout, analog output and a magnetic speed sensor. The TACHTROL 3 had two channels; A and B, where only channel A was used for turbine RPM. The magnetic speed sensor shown in Figures 1 and 2 was located over a thirty-toothed gear mounted on the input dynamometer shaft. The sensor generated a repeating AC electrical pulse proportional to the speed of the shaft in pulses per second (Hz). This electrical pulse was used as input to the AIRPAX TACHTROL 3 tachometer and was connected to channel A with terminals 1, 2, and 3 as shown in Appendix B, Figure B2.

D. COBRA PROBE INSTALLATION AND POSITIONING

Total pressure, Mach number and flow angle measurements at the turbine exit were incorporated into the TTR instrumentation using a 3-hole cobra probe. Cobra probe radial position and yaw angle movement were obtained using a L.C. Smith probe actuator, which is shown in Figure 5. The L.C. Smith probe actuator and the Motion Systems ball-drive actuator were operated from the same control box. The control box was designed to house the L.C. Smith actuator DC-to-AC power conversion and the Motion Systems actuator circuitry. Also, the radial, rotational and linear control circuits and toggle switches were mounted on the control box's front panel.

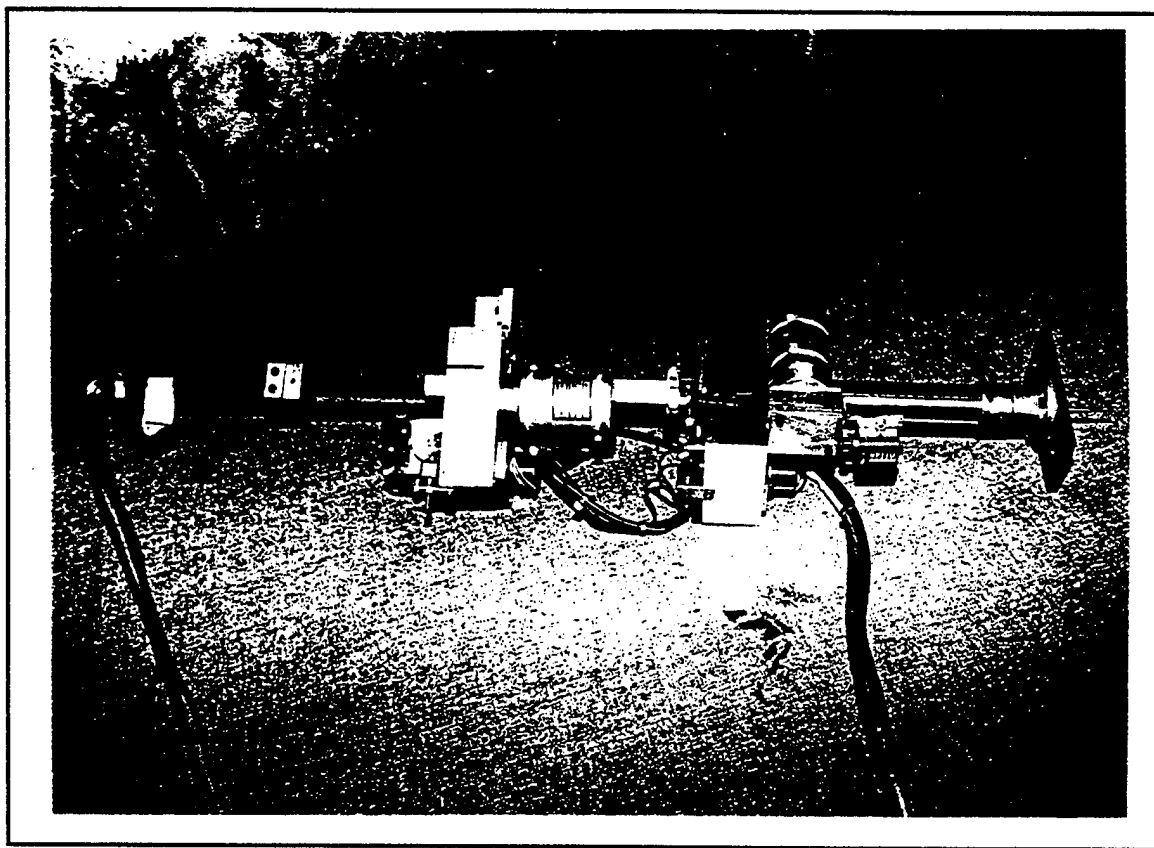


Figure 5. L.C. Smith Probe Actuator

III. DATA ACQUISITION SYSTEM

A. GENERAL DESCRIPTION

The TTR data acquisition system consisted of a personal computer (PC-486) and the Turbopropulsion Laboratory Hewlett-Packard (HP) data acquisition modules. All turbine sensor measurements were obtained by controlling the data acquisition system using the PC-486 computer via the GPIB/IEEE data bus and LabVIEW software programs. A schematic of the data acquisition system control and sensor designation is shown in Figure 6.

The PC-486 computer, controlled the data acquisition system via the AT-GPIB/TNT interface board. The instruments addressed on the GPIB were the HP 3495A Scanner, HP 3456A Digital Voltmeter, HP 5335A Universal Counter and Scanivalve Digital Interface Unit. The PC also had an internally-mounted PC-LMP-16 multifunction I/O A/D Board which monitored the potentiometers on the L.C. Smith and ball drive actuator. Table C1 in Appendix C summarizes all the data acquisition equipment binary dip switch settings/GPIB addressees.

B. HARDWARE DESCRIPTION

1. PC 486 Computer

The PC-486 computer was added to the data acquisition system in order to provide an increased capability in software availability, interactive control of measuring devices, real-time measurement display, and data reduction. The PC-486

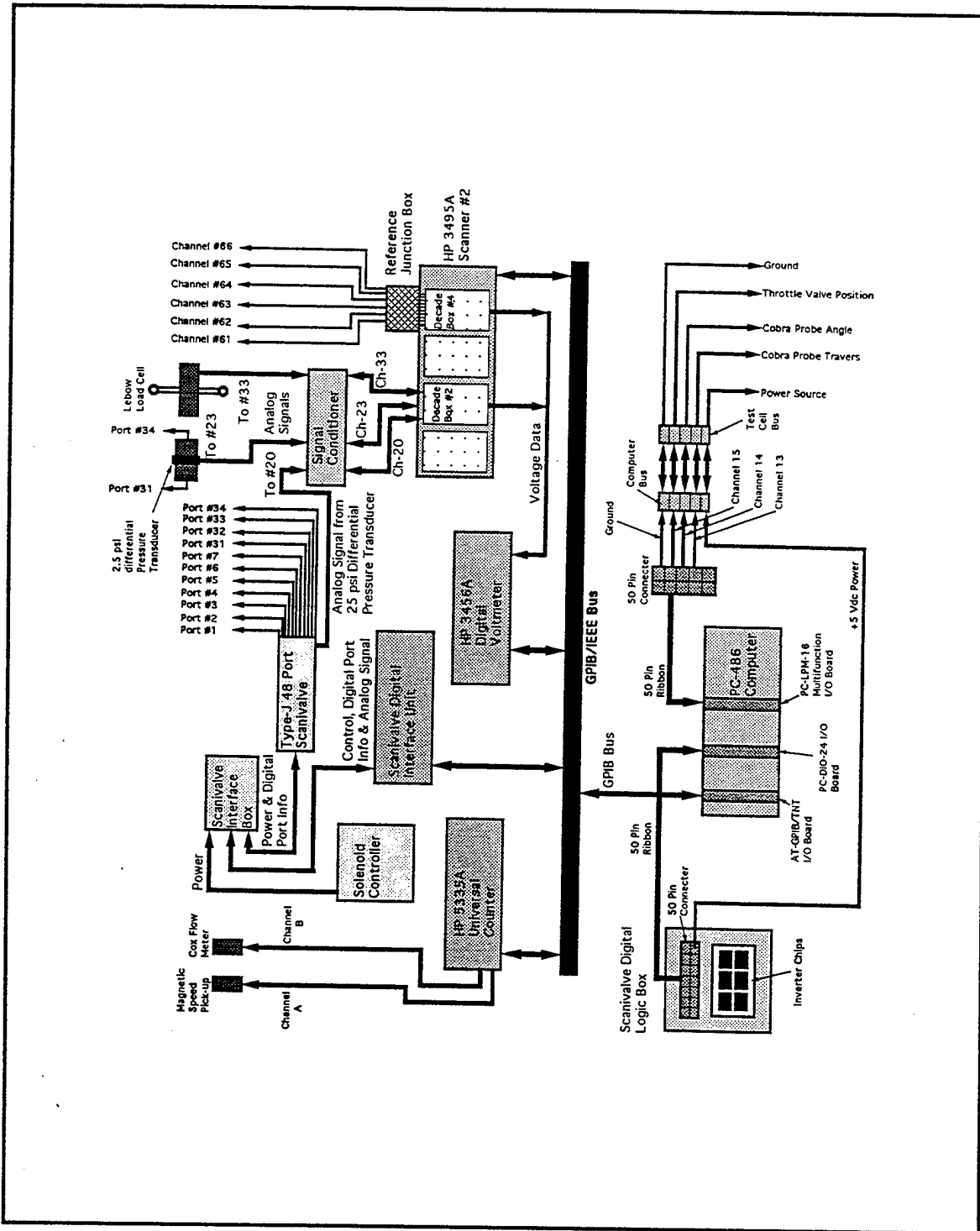


Figure 6. TTR Data Acquisition System

computer was incorporated into the data acquisition system via the AT-GPIB/TNT Interface I/O board.

2. AT-GPIB/TNT Interface Board

The AT-GPIB/TNT board allowed the PC-486 computer to function as a GPIB Talker/Listener/Controller via the GPIB/IEEE bus shown in Figure 6. The GPIB board was set up as computer device GPIB0 using the LabVIEW GPIB icon located in the Windows\Program Manager\Main\Control Panel window. The default settings found in [Ref. 4] were changed due to conflict with another device. The current dip switch settings are shown in Table C2 of Appendix C.

3. PC-DIO-24 I/O Board

The PC-DIO-24 board was a 24-bit parallel, digital I/O interface for the PC. All digital I/O was through a standard 50-pin male connector. Pin assignments are shown in Appendix D, Figure D1. The DIO board was purchased in order to read digital Scanivalve port information directly from the encoder via the seven digital lines using the Scanivalve digital logic box shown in Figure 6, bypassing the HG-78K Scanivalve Controller. This feature was not used. The board was also used as a +5 Vdc (pin 49) power source to three linear potentiometers. The DIO board was set up as computer device #1 using the LabVIEW WDAQ config. The default settings found in [Ref. 5] were changed due to a conflict with another device. The current settings are shown in Table C3 of Appendix C.

4. PC-LPM-16 Multifunction I/O Board

The PC-LPM-16 was a low power analog input, digital, and timing I/O board for the PC. The board contained a self-calibrating analog-to-digital converter (ADC) with sixteen analog inputs, eight lines of digital I/O and two 16-bit counter/timer channels for timing I/O. All digital I/O was through a standard 50-pin male connector. Pin assignments are shown in Appendix D, Figure D2. The analog board was used to continuously or selectively read DC voltage from three different linear potentiometers, two from the L.C. Smith gear for cobra probe radial and rotational position and one from the ball-drive actuator for throttle valve position. The analog board was set up as computer device #2 using the LabVIEW WDAQ config icon. The default settings found in [Ref. 6] were used and are shown in Table C4 of Appendix C.

5. Scanivalve Digital Interface Unit, Solenoid Controller and Interface Box

The required pressure measurements were obtained using the Scanivalve Digital Interface Unit (SDIU), Solenoid Controller (CTLR2/S2-S6), and the Interface Box to control the 48 port Type-J Scanivalve. A wiring diagram of the SDIU, CTLR2/S2-S6, Interface Box and pressure port designation is shown in Figure 7. A detailed wiring diagram of the Interface Box is shown in Appendix B as Figure B3.

6. HP Data Acquisition Modules

The HP data acquisition modules consisted of the HP 3495A Scanner, HP 3456A Digital Voltmeter (DVM), and the HP 5335A Universal Counter.

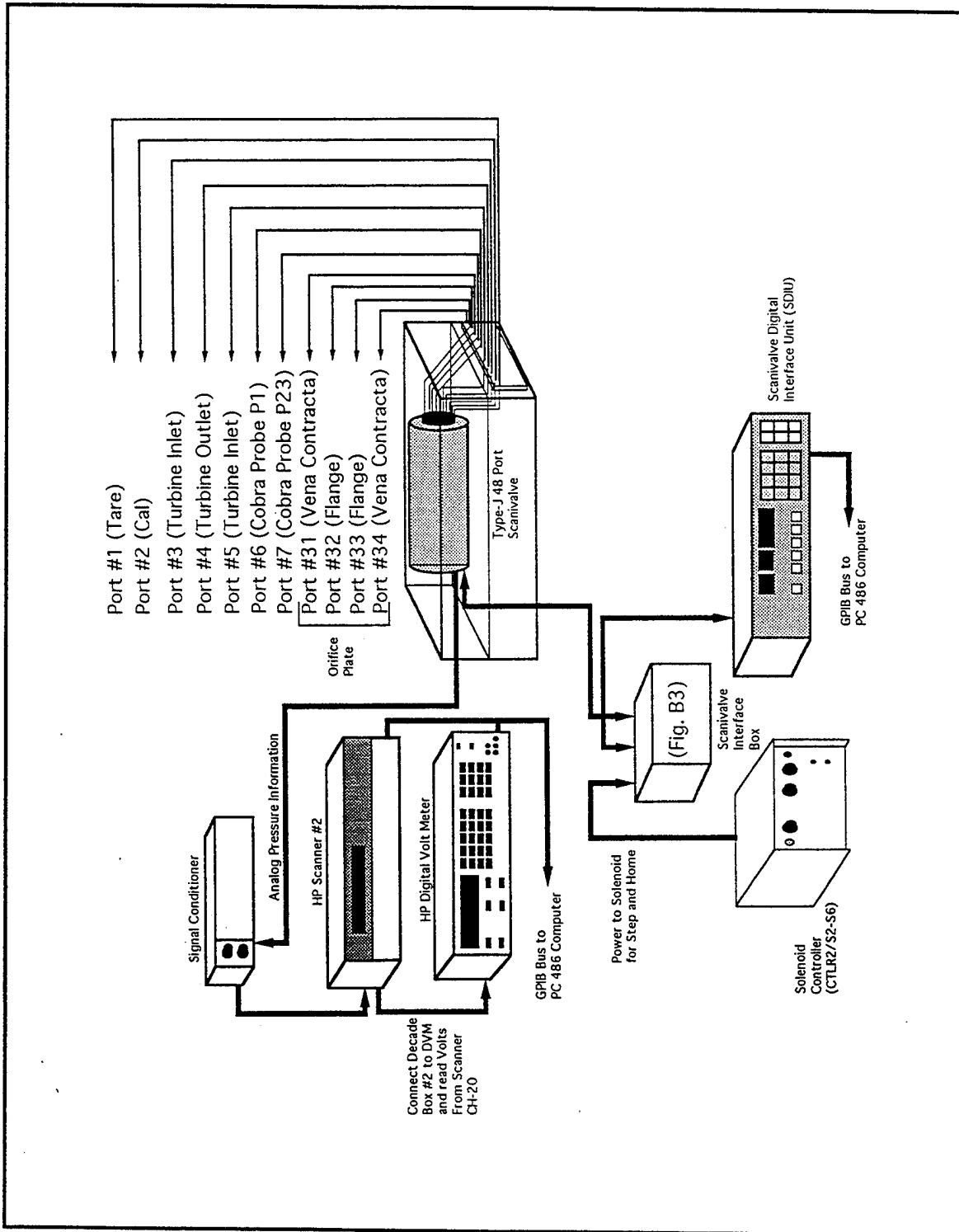


Figure 7. Scanivalve Control and Pressure Port Designation

The HP Scanner consisted of four 20-channel duo-decade boxes (1-4). Decade boxes two and four were utilized for pressure, torque, and temperature measurements as illustrated in Figure 6. The HP Scanner was used to connect a specific Scanner channel to the HP DVM for voltage measurement. The digital voltmeter was used to measure voltage data from the TTR transducers. Signal conditioning was used to calibrate the ± 25 psi Scanivalve and the ± 2.5 differential pressure transducers in inches of water and to calibrate and check the span of the Lebow load cell. The HP 5335A Universal Counter was used to measure frequency from the magnetic speed pick-up and the Cox flow meter as shown in Figure 6. The magnetic speed and flow rate sensors were connected to channels A and B respectively, on the front panel of the counter.

IV. LabVIEW SOFTWARE PACKAGE

A. GENERAL DESCRIPTION

LabVIEW (Laboratory Virtual Instrument Engineering Workbench) for Windows was the graphical software package used for data acquisition, interactive control and data display. Programming was done using a block diagram approach, with virtual instruments (VI's). A VI consisted of a front panel and a block diagram and could include one or more sub-blocks. The front panel specified the inputs, outputs, and features needed for interactive operation and was analogous to a physical instrument's front panel. Behind the front panel was the block diagram which was analogous to the circuitry of an instrument and was the source code of the VI. The icon/connector was the programmatic interface of the VI. Each icon could be used as a lower level VI that could be called by higher level VI's. Icons were wired together to indicate data flow in the block diagram. Data could be passed from a sub-VI to a calling VI using the VI's icon which was located in the upper right hand corner of the front panel. The data were available to the icon by wiring the desired information on the front panel (display indicators) to the icon, as described in [Ref. 7]. The sub-VI was called by the higher-level VI by placing the sub-VI icon in the higher-level VI's block diagram. To run a VI, all that was needed was to click on the arrow icon in the upper left hand corner of the front panel.

1. LabVIEW Software Familiarization and Development Method

The data acquisition software for the TTR was developed by initially using LabVIEW to acquire the data for a turbocharger experiment described in [Ref. 8] and

[Ref. 9]. The turbocharger laboratory setup provided the hardware and instrumentation needed to develop a data acquisition program. The turbocharger data acquisition/data reduction LabVIEW program was similar to the HP Basic program presented in [Ref. 9]. Both programs collected the same input data and produced the same compressor and turbine performance data. The LabVIEW Turbocharger data acquisition program output was validated by comparing the results obtained using the HP Basic version. Both programs produced the same turbine and compressor performance parameters. Some of the programming techniques used to develop the Turbocharger program were used to develop the SSME HPFTP data acquisition program

B. LabVIEW INSTRUMENT DRIVERS

Instrument drivers, or LabVIEW VI's, were developed in order to control a specific programmable instrument interactively through the front panel or from a higher-order VI through the instrument drivers icon.

1. HP Digital Voltmeter (DVM) and HP Scanner

This combined instrument driver was used to connect a specific HP Scanner channel to the DVM and obtain a voltage measurement. The voltage information was obtained from instruments such as the Scanivalve pressure transducer, the differential pressure transducer, the Lebow load cell and six thermocouples. Input settings used to program the Scanner/DVM and output measurement are displayed in the icon shown in Figure 8.

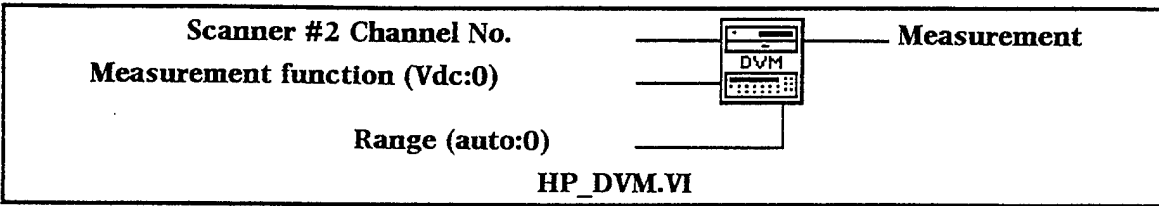


Figure 8. HP_DVM.VI Icon

The initializations for HP_DVM.VI were channel designation, measurement function (Vdc:0), and range (auto:0), and the output was the voltage measurement. The channel # designation was used to connect the sensor of interest to the DVM.

Measurement function was used to program the DVM to measure a specific function.

Range was used to set the measurement scale and units. HP 3456A DVM program codes from [Ref. 10] available in the HP_DVM.VI are shown in Table C5 of Appendix C.

The SCANNER2.VI was used as a subroutine in the HP_DVM.VI. Input to the HP Scanner was the desired channel number. A list of the sensor Scanner channel number designations are presented in Table 1 and shown in Figure 6. Scanner #2 VI was programmed using the icon shown in Figure 9.

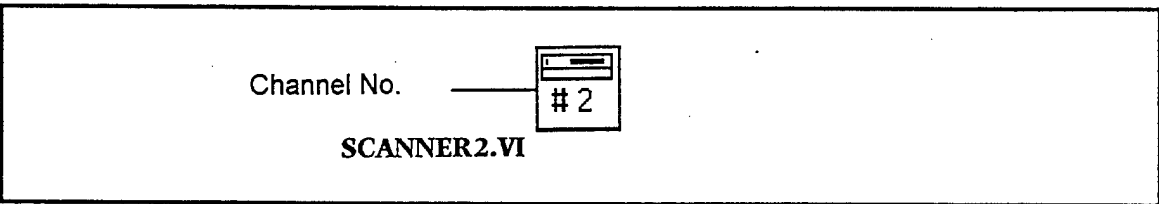


Figure 9. SCANNER2.VI Icon

Sensor	Channel No.
Scanivalve Differential Pressure Transducer (All Ports)	20
2.5 psi Differential Pressure Transducer (Ports 31 & 34)	23
Lebow Load Cell	33
Reference Junction Temperature	60
Turbine Inlet Temp	61
Turbine Inlet Temp	62
Turbine Outlet Temp	63
Dynamometer Water Inlet	64
Dynamometer Water Outlet	65
Orifice Temperature	66

Table 1. Sensor/Scanner Channel Designations

2. HP 5335 Universal Counter

This instrument driver was used to control and measure frequency displayed on the universal counter (HP 5335.VI) as discussed in section III.B.6. Input settings used to program the counter and output measurement is displayed in the HP 5335A icon shown in Figure 10.

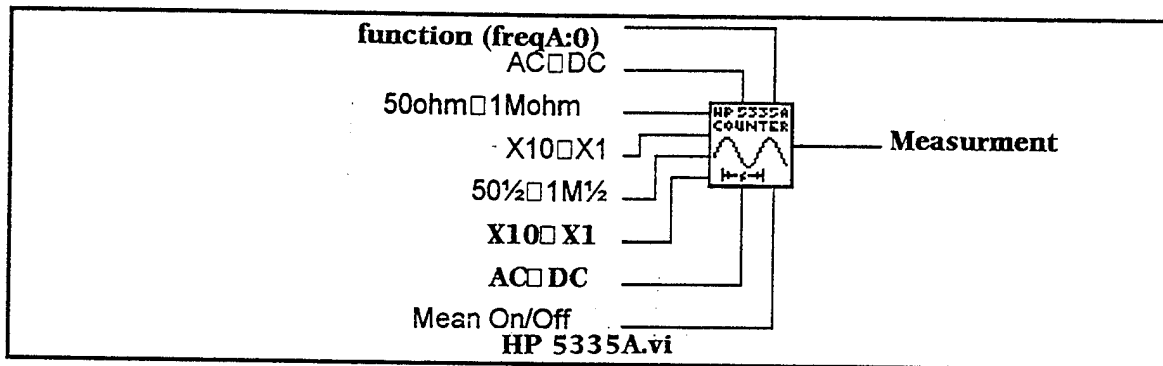


Figure 10. HP 5335A.VI Icon

The VI initializations were function (freqA:0), channel A and B coupling (AC-DC), channel A and B impedance (50ohm-1Mohm), channel A and B attenuation (X10-

X1), and mean (On/Off). A list of the HP Universal Counter device commands available to the HP 5335A.VI are shown in Table C6 of Appendix C, from [Ref. 11].

3. Scanivalve Digital Interface Unit (SDIU)

This instrument driver was used to control the SDIU (SVCONTROL.VI) in order to step, or home the Scanivalve, and advance to any port. The Scanivalve port number was also displayed using this instrument driver. The SDIU icon is shown in Figure 11, which was used to program the instrument.

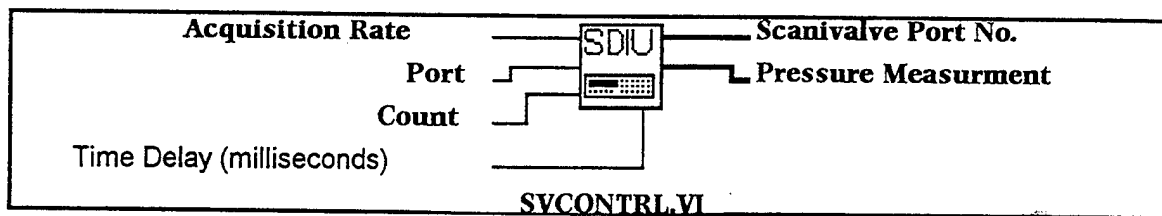


Figure 11. SVCONTROL.VI Icon

The programming features were acquisition rate, port, count, time delay and the VI's output was Scanivalve Port No. and pressure measurement from the internal A/D card (not used). A list of the SDIU commands from [Ref. 12] available to the SVCONTROL.VI are listed in Table C7 of Appendix C.

C. TTR (SSME HPFTP ATD) DATA ACQUISITION

The SSME HPFTP ATD data acquisition program was developed using the instrument drivers as sub-VI's and the LabVIEW sub-VI's illustrated in Figure 12. Figure 12 is an icon hierarchy diagram generated by LabVIEW as part of the SSME_TTR.VI data acquisition program. A general description of the sub-VI input, output and functions are discussed in Appendix E.

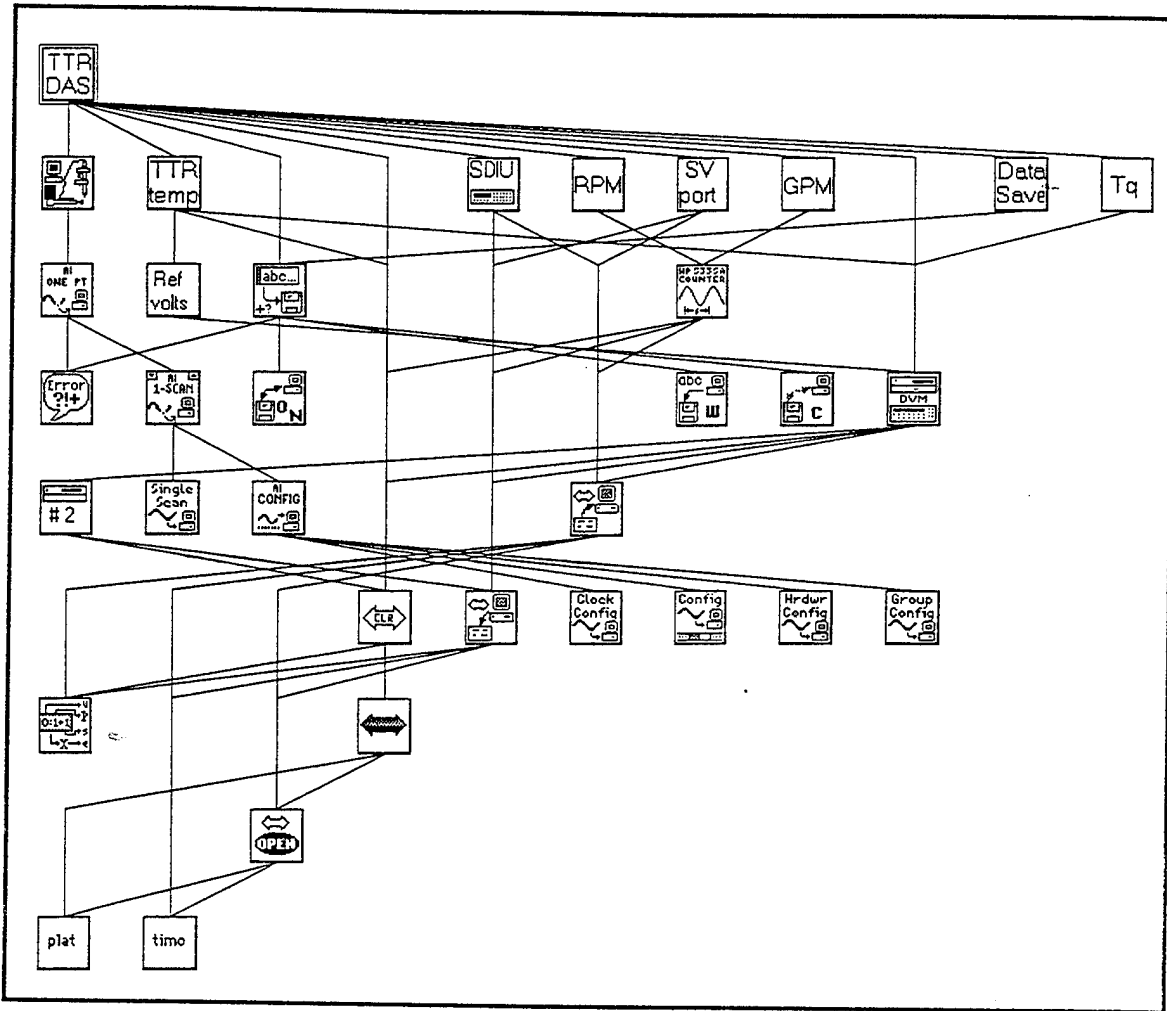


Figure 12. LabVIEW Hierarchy Diagram for the SSME_TTR.VI Data Acquisition VI

The SSME_TTR.VI data acquisition program (Block diagram) shown in Appendix F, Figure F1 controlled the data acquisition system shown in Figure 6 and displayed measured and reduced turbine data on the front panel (Figure 13). Input to the SSME_TTR.VI was atmospheric pressure in inches of mercury. The SSME_TTR.VI was separated into 13 different sections by sequence structures or frames. Frames were used in programming to specify an order of execution, similar to lines of BASIC code.

Frame #0 was used to read all the required Scanivalve port number's, advance to a specified port number, home, obtain pressure information (in inches of water) and save the pressure information to a spreadsheet file TTRDATA.DAT (defaulted to appear in c:\labview\ttr\) for permanent record. Frame #1 was used to acquire pressure information (in inches of water) from the ± 2.5 psi differential pressure transducer and save it to the

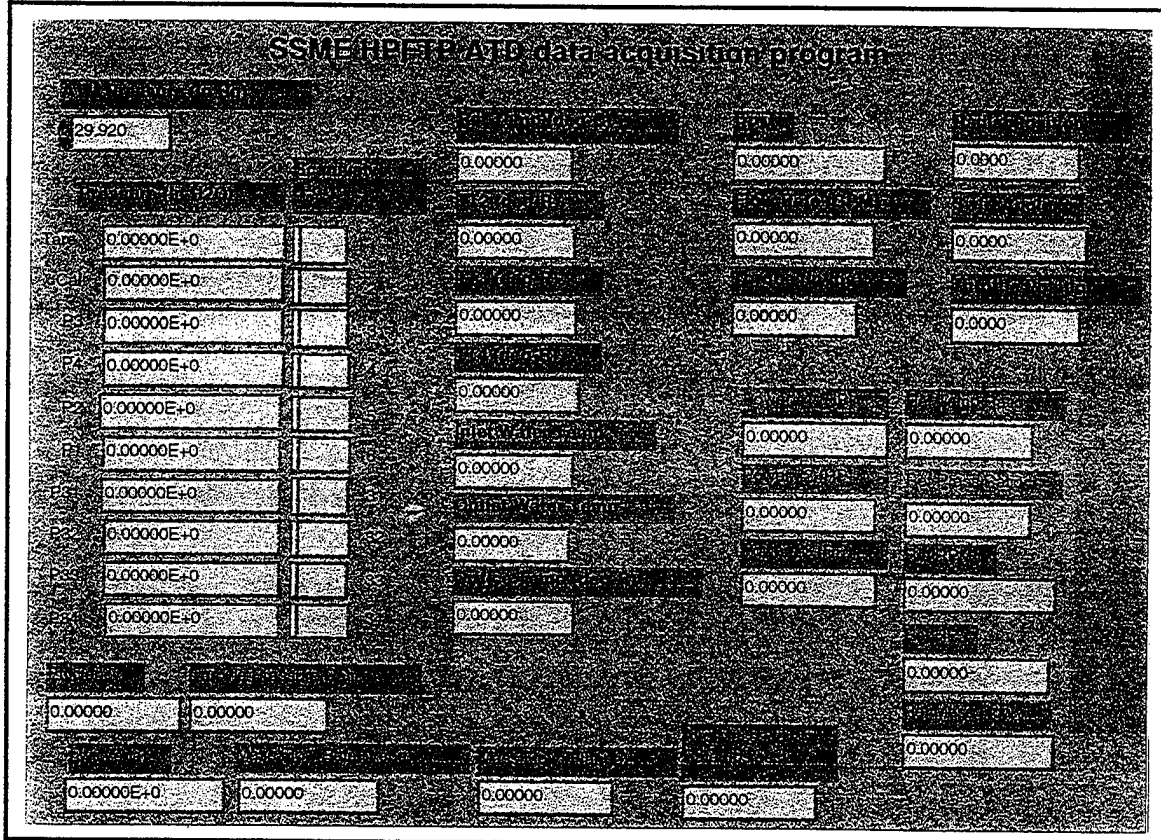


Figure 13. SSME_TTR.VI Front Panel

spreadsheet file. Frame #2 was used to acquire thermocouple temperature data from the reference junction connector in Scanner #2, decade box #4, and save it to the spreadsheet file. Frame #3 was used to measure frequency data using the “mean” function on the HP 5335A Universal Counter, convert the information to RPM and save it to the spreadsheet

file. Frame #4 was used to measure dynamometer flow rate, convert the information to gallons/min (GPM) and save the data to the spreadsheet file. Frame #5 was used to measure voltage information from the Lebow load cell, convert it to torque (in in-lbs), and save the data to the spreadsheet file. Frame #6 was used to measure and record cobra probe radial position, swirl angle, and TTR throttle position. Frame #7 was used to route the measured quantities, pressures, temperatures, RPM, GPM, and torque to the data reduction sub-section for performance calculations. Frame #8 was used for front panel display of the reduced turbine performance parameters. Frame #9 was used to format the spreadsheet file TTRDATA.DAT. Frame #10 was used to record all the calculated parameters to a spreadsheet file SSMEDATA.DAT for permanent record. Frame #11 was used to delete the temporary file JUNCK.DAT. The final frame, Frame #12, was used to clear devices 8 and 22 (Scanner #2 and DVM).

V. EXPERIMENTAL SETUP

A. TURBINE TEST RIG MEASUREMENTS

The original TTR configuration, without the back-pressure throttle valve, and the redesigned TTR configuration shown in Figure 1 was operated to determine the SSME HPFTP ATD single-stage performance characteristics. Pressure, temperature, torque, dynamometer water flow rate, and turbine rotational speed sensors were connected to the data acquisition system as shown in Figure 6.

The Scanivalve (± 25 psi) differential pressure transducer was connected to Scanner decade box #2 channel 20 via the Signal Conditioner. TTR pressure ports shown in Figure 1 were connected to the 48-port type-J Scanivalve as shown in Figure 7. Also, a ± 2.5 psi differential pressure transducer was connected to decade box #2 channel 23 via the signal conditioner. This differential-pressure transducer was added to the data acquisition system in order to measure the pressure drop across the orifice plate using the vena contracta taps (ports 31 and 34).

Six thermocouple leads were connected to the Scanner decade box #4, channels 61-66, via the Thermocouple Reference Connector 03495-64115 (Option 005), [Ref. 13]. Temperature measurement was obtained using type-J (Iron-Constantan) thermocouples by determining the voltage drop between the thermocouple, J1, and the reference junctions, J2 and J3. J2 and J3 were connected to the DVM when the HP Scanner channels 60-66 were addressed. The reference junction temperature was known,

therefore the temperature of interest could be determined. Figure 14 shows a simplified seven-channel schematic of the thermocouple setup. Using the data acquisition system and LabVIEW, the absolute temperatures T_T were determined by the following procedure.

1) The resistance R_T at the reference junction was measured to find the reference temperature T_{REF} using Equation 1 from [Ref. 13]:

$$T_R = \frac{5041.6}{\ln(R) + 7.15} - 314.052 \quad (1)$$

2) The reference temperature from Equation 1 was converted to its equivalent reference junction voltage V_R using Equation 2, obtained from the 5th order

$$V_R = (5.01059E - 5)T_R + 8.01446E - 6 \quad (2)$$

type-J thermocouple calibration curves found in the Omega Thermocouple Catalog [Ref. 14]. Because the reference temperatures of interest was between 20-40 Deg-C, a linear curve fit was used for this calculation only, in order to simplify the LabVIEW programming. A comparison of the 5th order and linear fit is shown in Figure 15.

3) Thermocouple voltage V_S was measured and a correction made using Equation 3 to find V_1 . V_1 was converted to temperature using the 5th order curve fit found in [Ref. 14] for the type-J thermocouple given by Equation 4.

$$V_R + V_S = V_T \quad (3)$$

$$T_T = a_0 + a_1V_T + a_2V_T^2 + a_3V_T^3 + a_4V_T^4 + a_5V_T^5 \quad (4)$$

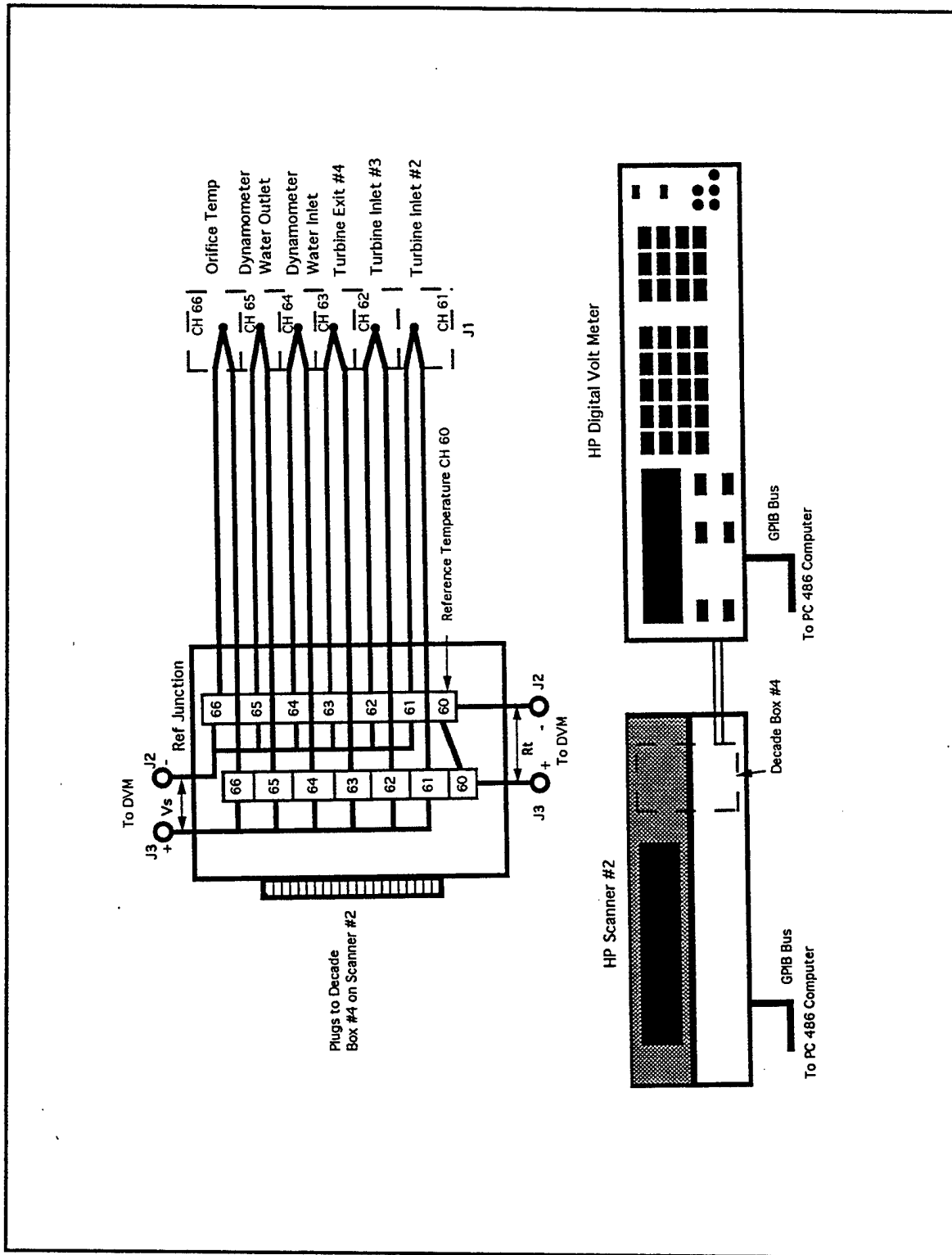


Figure 14. TTR Thermocouple Set-up

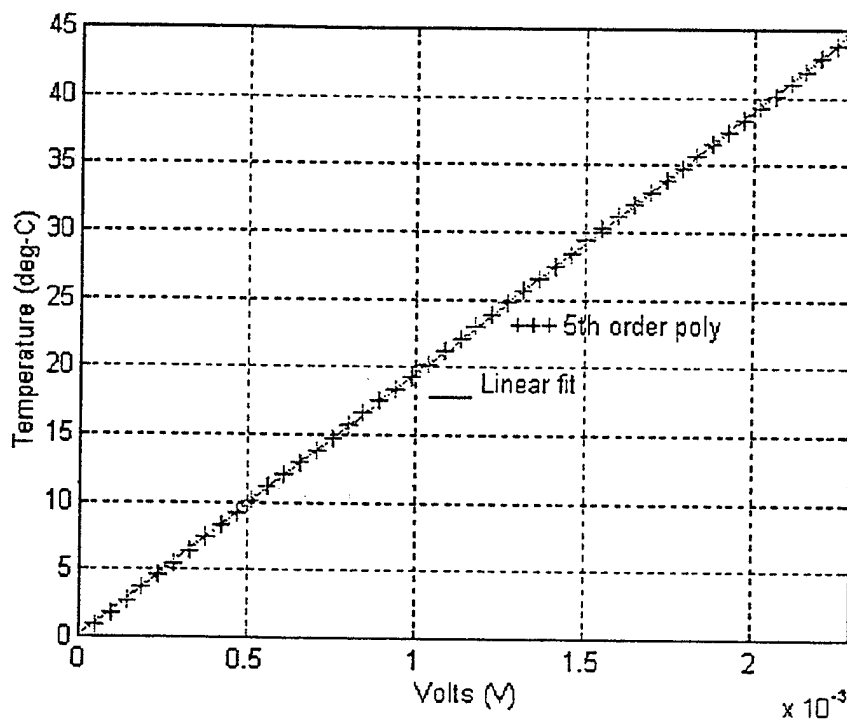


Figure 15. 5th Order and Linear Curve Fits for the Type-J Thermocouple

where:

$$\begin{aligned}
 a_0 &= -0.048868252 \\
 a_1 &= 19873.14503 \\
 a_2 &= -218614.5353 \\
 a_3 &= 11569199.78 \\
 a_4 &= -264917531.4 \\
 a_5 &= 2018441314
 \end{aligned}$$

The above procedure was programmed using LabVIEW to measure and calculate thermocouple temperatures for the turbine inlet (2), turbine outlet, dynamometer inlet water temperature, dynamometer outlet water temperature, and orifice stagnation temperature T_1 .

Torque measurements were incorporated into the experiment by calibrating the Lebow load cell and programming the results of torque vs. voltage using the LabVIEW VI (TORQUE.VI). The Lebow load cell was connected to Scanner decade box #2 channel 33 via the Signal Conditioner.

The load cell was calibrated in compression using a cantilever beam bolted to the dynamometer and a weight pan. Weights were added to the beam up to 75 ft-lbs and the load cell voltage output and weight were recorded. The load cell calibration data and linear curve fit are shown in Figure 16.

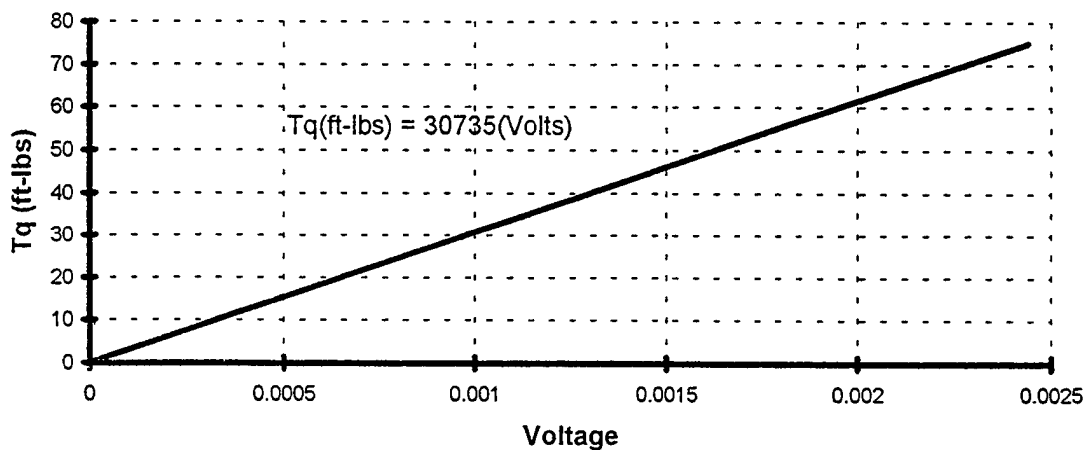


Figure 16. Lebow Load Cell Calibration

Dynamometer flow rate was determined by connecting the Cox flow meter to channel B of the HP Universal Counter front panel in order to measure the frequency

output. The frequency output was converted to gallons/min (GPM) using the calibration data obtained from the Power Machine Co. [Ref. 15] and is shown in Figure 17.

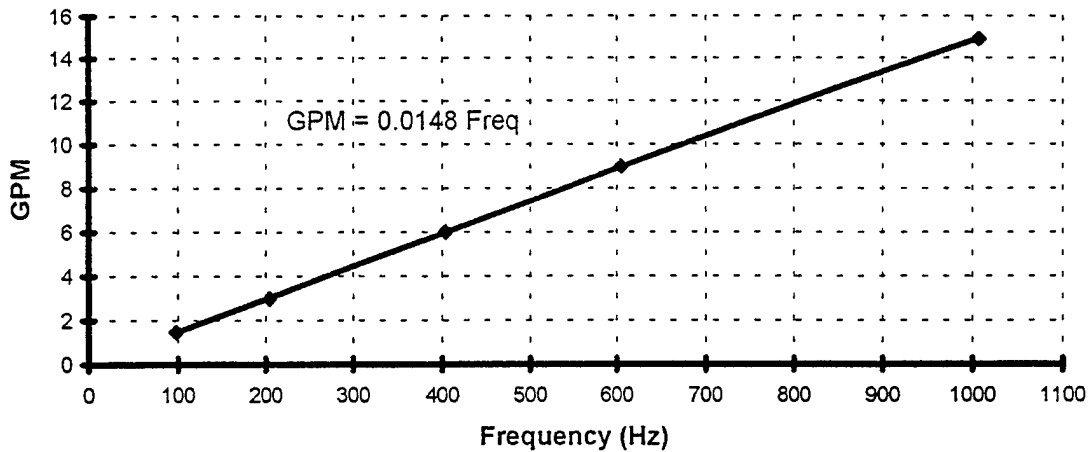


Figure 17. Cox Flow Meter Calibration

The frequency signal from the magnetic speed pick-up was used as input to channel A of the HP Universal Counter's front panel in order to record the turbine RPM using the data acquisition system and LabVIEW. The frequency signal was also used as input to the TACHTROL 3 tachometer which was scaled by a factor of 2 to read out in units of RPM. The TACHTROL 3 could be programmed using constants to generate and display desired units, functions, display, analog output, set points and serial output. Table C8 of Appendix C shows the current TACHTROL 3 constant settings. The operation flow and programmable constants diagram for the TACHTROL 3 is shown in Appendix B, Figure 4B. A complete description of the TACHTROL 3 theory of operation, programming, and constant's definition can be found in the operations manual [Ref. 16].

The up-stream and down-stream vena contracta and flange tap pressures were connected to Scanivalve ports 31, 34 and 32, 33 respectively, (see Figure 7). The orifice up-stream temperature T_1 was determined by connected a type-J thermocouple to the temperature reference connector, channel 66. Mass-flow rate calculations were obtained using the procedure outlined in [Ref. 17].

B. COBRA PROBE CALIBRATION

Cobra probe calibration was accomplished using two different free-jet nozzles with exit diameters of 4.25 and 7 inches in the free-jet calibration facility as described in [Ref. 18]. The probe was mounted in the L.C. Smith actuator with the angle set at 90 degrees (probe directly into the flow) and then calibrated between Mach numbers from 0.15 to 0.80. Once the probe was mounted in the L.C. Smith actuator, the probe was not moved with respect to the actuator. The angle read-out was offset -90 degrees to indicate zero degrees of rotation with the probe directly into the flow. The L.C. Smith actuator and cobra probe setup was then mounted on the TTR at the first-stage turbine exit plane. Because the L.C. Smith actuator was capable of traversing 10 inches and the full down position did not correspond to the turbine hub position, an offset of -2.66 was used so that the computer read-out indicated zero inches with the cobra probe head at the rotor hub. This offset for radial probe position will need to be changed when the probe is mounted to the first-stage stator-inlet plane.

Calibration data collection was obtained using the LabVIEW VI, (PROB_CAL.VI). This VI controlled the data acquisition setup shown in Figure 18 to

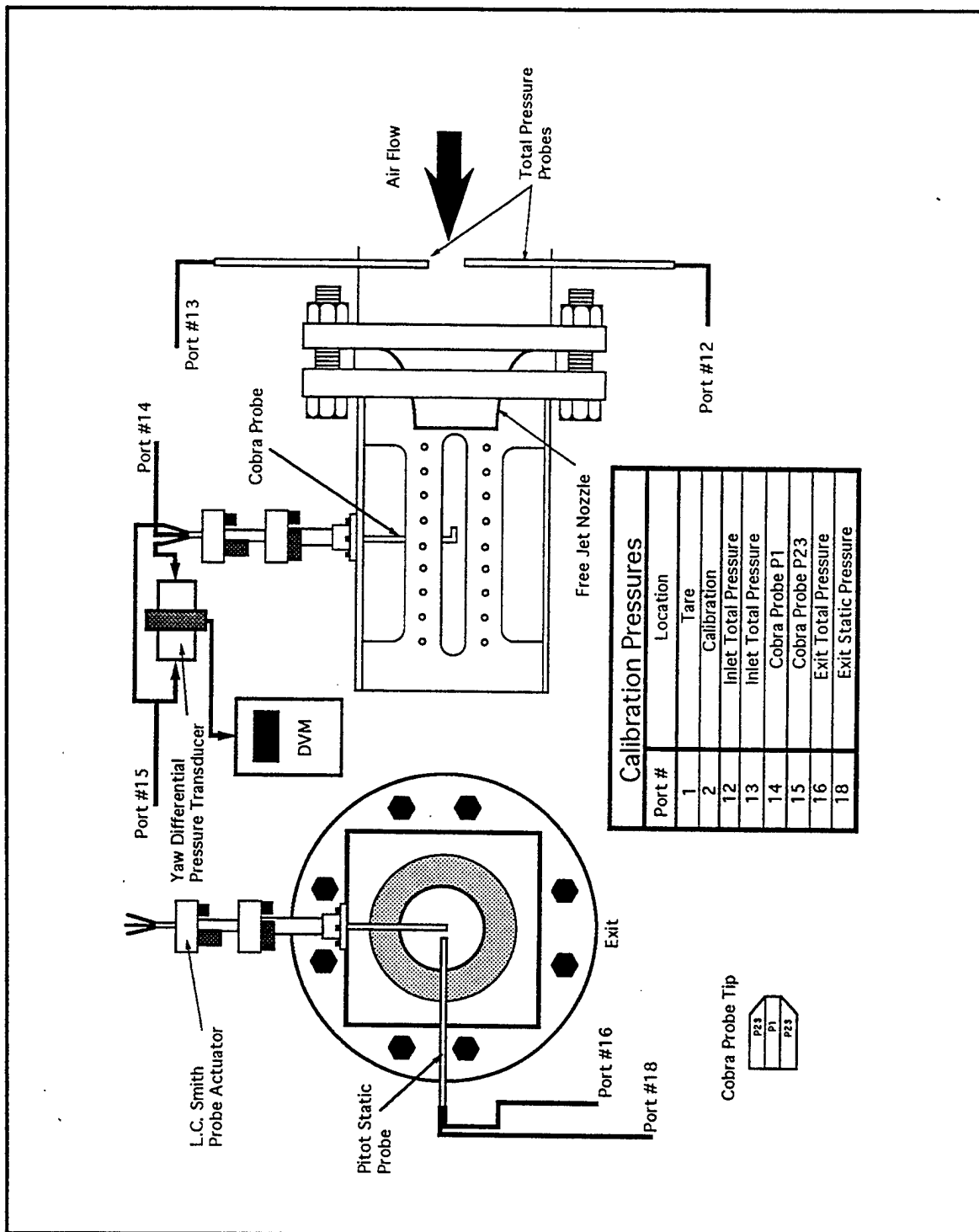


Figure 18. Cobra Probe Calibration Set-up and Scanivalve Port Designation

obtain pressure measurements and calculate the dimensionless variables β , X , and Mach number. A copy of the PROB_CAL.VI front panel is shown in Appendix F, Figure F2. Appendix G contains a description of the calibration variables and the cobra probe calibration data and curve fit. A sixth order curve was used to fit the data and is shown in Figure G1.

C. EXPERIMENTAL PROCEDURE

The TTR was operated extensively in order to obtain repeatable turbine performance data and to document controls such as compressor dump-valve settings, dynamometer water-supply pressure, oil-mist lubrication supply pressure, speed control response, and dynamometer water inlet and exit valve positions. The TTR was operated manually from the control console as reported by Studevan [Ref. 1] in two different configurations. The two configurations were with the turbine exit exposed to atmosphere and with the turbine-exit throttle valve installed. Turbine speed was controlled by the electronic controller in both the manual and automatic modes with the inlet dynamometer water valve fully open. Air at 45 psi was delivered to the SSME HPFTP ATD by the Allis-Chalmers compressor as reported by Rutkowski [Ref. 2].

1. Turbine Test Rig Operation

Prior to operating the TTR, the check list outlined in Appendix H, Figure H1 was completed. The Scanivalve pressure transducer and the ± 2.5 psi differential pressure transducer were calibrated to indicate inches of water. Also, the Lebow load cell's zero adjust and voltage span were checked. The check list was developed from operating the

TTR and documenting the control settings, turbine RPM, valve, and dump positions and atmospheric temperature. During each run, these settings, along with TTR pressure and temperature measurements, were manually recorded. A copy of the manual TTR data collection sheet is shown in Appendix H, Figure H2.

For safe operation of the TTR, the parameters listed in Table 2 were monitored to insure critical limits were not exceeded. Care was taken, at turbine speeds of 7000 RPM and above, that dynamometer outlet water temperature and flow rate through the Cox flow meter did not exceed set limits. With the inlet and outlet dynamometer valves fully open, flow rate could exceed 15 GPM. Also, dynamometer-outlet water temperature could exceed 180 °F as the outlet water valve approached fully closed. With the speed controller in automatic mode both these parameters could be exceeded. The outlet water-valve position was monitored from the display on the Fischer and Porter electronic controller, and the dynamometer outlet water temperature was monitored from the Type-J thermocouple read-out shown in Figure 2. The TTR rotational speed (RPM), water flow rate through the Cox flow meter, and the dynamometer torque were monitored from the PC-486 computer using the real-time display program TTR_TEST.VI. SSME HPFTP ATD data collection was obtained at turbine speeds above 1200 RPM with dump valve number 2 fully closed. Dump valve number 2 needed to be closed in order to obtain meaningful mass-flow rate measurements.

Parameter	Maximum Value
Dynamometer Outlet Water	180 °F
Dynamometer Inlet Water	100 °F
Cox Flow Meter	15 GPM
Dynamometer Torque	900 (in-lbs)
FWD Bearing Temp	150 °F
AFT Bearing Temp	150 °F
Accelerometer #1	Abnormal
Accelerometer #2	Abnormal

Table 2. TTR Operating Limits

a. Pressure Transducer Calibration

The Scanivalve pressure transducer measured gage pressure and was calibrated in inches of water, first manually homing the Scanivalve to port #1 (exposed to atmosphere) from the SDIU front panel. The signal conditioner was manually adjusted until a zero readout on the DVM was obtained. The Scanivalve was then stepped to port #2 which was connected to the shop air source via a pressure regulator. The pressure regulator was adjusted to apply ten inches of mercury (Hg) to port #2 and the signal-conditioner span adjust was used to set 13.59E-3 volts on the DVM. The ± 2.5 differential pressure transducer was calibrated in a similar manner with five inches of Hg applied to one side from a supply line on the front panel of the HP data acquisition unit. The other side of the transducer was exposed to atmosphere and the SPAN adjusted until 6.795e-3 volts was indicated on the DVM.

b. Load Cell Calibration

The Lebow load cell was calibrated as discussed earlier. The signal conditioner was used in order to set the zero adjust and span. The zero adjust was

checked by unloading the dynamometer and manually connecting the signal conditioner to the DVM and adjusting the voltage output to zero. The DVM should indicate 0.002 volts with 61.47 ft-lbs applied to the dynamometer, which was applied to the dynamometer by attaching a cantilever calibration beam and hanging 14.01 lbs of weight on the end of the beam. A setup of the cantilever beam and weight assembly is shown in Appendix C, Table C9.

c. Automatic Speed Control

For automatic turbine speed control, the electronic controller variables were set up in accordance with the operations manual [Ref. 19]. The current settings are listed in Table C10 of Appendix C.

For the TTR set up with the turbine exit exposed to atmosphere, turbine speed was changed using the TTR and dump valves with the electronic controller in the manual mode and the outlet dynamometer water-valve set to 60%. At the desired turbine speed the electronic controller was then placed into automatic mode once the set point had been correctly adjusted. The outlet dynamometer water valve indicator was then monitored to insure the valve was not moving to the fully open or closed position. Also, dynamometer outlet water temperature and water flow rate were monitored to ensure they did not exceed their respective limits.

With the turbine-exit throttle valve installed, the automatic speed-control system was operated as discussed above. With the turbine operating at the desired set-point, the throttle valve was moved inward in steps of approximately 0.30 inches. The

throttle valve was not closed any further once the dynamometer outlet water valve opened to approximately 20%. In order to continue obtaining turbine data on the same constant speed line, the compressor dump valve (#1) was closed until the dynamometer outlet water valve indicated approximately 80% closed. The throttle valve was then closed in steps to a minimum opening of 0.5 inches. An additional limiting factor for throttle valve position was the turbine aft-bearing temperature. The aft-bearing temperature increased as the throttle valve was traversed inward.

2. SSME HPFTP ATD Real-Time Data Display

The real-time data display, LabVIEW VI (TTR_TEST.VI) was used to display dynamometer water flow rate, dynamometer torque, and turbine RPM. These parameters were selected in order to determine the operating conditions for the TTR prior to the data collection, and to monitor critical limiting values as outlined in Table 2. The dynamometer water flow rate was a good indicator in detecting supply-water pressure fluctuations caused by relief valve discharge, and to set supply-water pressure to maintain a constant level in the TTR cell storage tank.

TTR_TEST.VI was operated during run-up operations and prior to each data collection run. The real-time display was used to show the run-up characteristics and to determine that the turbine was operating at a constant speed. TTR_TEST.VI, was executed by clicking the On/Off switch to the On position, then clicking on the arrow icon in the upper left-hand corner of the front panel. The program was terminated by clicking the On/Off switch to the Off position and waiting for the program to stop running, which

took approx. 5-8 sec. No other programs could be activated before TTR_TEST.VI was terminated. A copy of the real-time displays front panel and block diagram is shown in Appendix F, Figure F3.

3. SSME HPFTP ATD Performance Data Collection

Turbine performance parameters were obtained by operating the TTR at different speeds using the TTR control panel dump valves, the Fischer and Porter electronic speed controller, the turbine exit throttle valve, and then executing LabVIEW VI's (TTR_TEST.VI, SSME_TTR.VI, ACTUATOR.VI, AND VEL_PRFL.VI).

With the turbine operating at a constant speed, the cobra probe was moved to midspan and nulled in yaw. The SSME HPFTP ATD performance parameters were calculated and stored in a spreadsheet file by the data acquisition VI (SSME_TTR.VI) discussed in section IV.C. Parameters calculated were; turbine total-to-total pressure ratio ($P2/P1$), turbine efficiency (η_t) using Equation 5 from [Ref. 20], mass-flow rate using the vena contracta and flange taps as reported by Vavra [Ref. 17], and horsepower (HP) using three different methods. Also, the referred quantities of pressure ratio, temperature ratio, HP, and RPM were calculated and stored. Appendix I outlines the equations used in SSME_TTR.VI. The two spreadsheet files TTRDATA.DAT and SSMEDATA.DAT were copied to two separate Excel work sheets for data validation and plotting. The two Excel work sheets are shown in Appendix J.

For TTR data collection with the turbine-exit throttle valve installed the throttle valve's position was determined by measuring the voltage output of the ball-drive

actuator's internal linear potentiometer using the data acquisition system. The potentiometer was powered from the black wire by a +5 Vdc source via the PC -DIO-24 I/O board pin # 49. The potentiometer ground (red wire) was connected to the ground source from the PC-LPM-16 multifunction I/O board pin #50. The potentiometer output voltage was determined from the white wire which was connected to pin # 18 (channel 15) on the PC-LPM-16 I/O board. The potentiometer's voltage output was converted to actuator position (in inches) by Equation 5. The offset of 0.92 was used to indicate zero inches with the throttle valve fully closed.

$$Position = \left(\frac{6}{5}\right) \times Volts + Offset \quad (5)$$

The throttle valve was operated using the control box shown in Figure 19 and the position readout was displayed on the PC-486 computer using the LabVIEW VI (ACTUATOR.VI). Due to the ball-drive actuator mounting points, and its maximum traverse capability of six inches, contact between the throttle-valve back plate and the front bearing thermocouple could occur. Also, with the throttle valve fully closed, the actuator was capable of an additional 0.92 inches of travel, which could cause damage to the TTR.

For safety, four lights on the ACTUATOR.VI front panel were used so that TTR damage did not occur. Two lights (warning and stop) were used for the forward stop and two lights for the aft stop. The forward warning light illuminated orange when the throttle valve was 0.1 inches from the fully closed position. The forward stop light illuminated red when the throttle was fully closed. The aft warning light illuminated

orange when the throttle was opened to 2.3 inches and the stop light illuminated red at 2.5 inches. A copy of the ACTUATOR.VI front panel and block diagram are shown in Appendix F, Figure F4.

4. Outlet Velocity Profile Data Collection

The velocity profile at the first-stage turbine outlet was obtained using the calibrated cobra probe and the LabVIEW VI, (VEL_PRFL.VI). The total pressure port P1 was connected to the Scanivalve port #6 and the left differential pressure port P23 was connected to the Scanivalve port #7. First the cobra probe was positioned radially at the desired blade height. The probe was then nulled in yaw using the ± 10 psi Statham, SCO 277-10 differential pressure transducer. VEL_PRFL.VI was executed to obtain pressure information at the turbine exit, cobra probe port (P1) and (P23). The quantities β , dimensionless velocity X , and Mach number (M) were then calculated. The procedure was repeated for additional radial positions. Both cobra probe radial position and angle were determined using the L.C. Smith probe actuator from the two linear potentiometers. The two potentiometers were powered by a +5 Vdc source from the PC -DIO-24I/O board pin # 49. The potentiometer was connected to the ground source from the PC-LPM-16 I/O board pin #50. The radial and angle position potentiometers output voltage were measured by connecting them to pins 14 and 16 (channels #13 and #14) on the PC-LPM-16 I/O board, respectively (see Figure 19). The potentiometers' voltage outputs were converted to radial position (in inches) and swirl angle (in degrees) by Equations 6 and 7 respectively:

$$Radial = \frac{10}{5} Volts + Offset \quad (6)$$

$$Angle = \left(\frac{180}{5} \right) \times Volts - 90 \quad (7)$$

A copy of the VEL_PRFL.VI front panel and block diagram is shown in Appendix F, Figure F5.

Cobra probe traverse and rotation were performed using the control box shown in Figure 19 and position readout was displayed on the PC-486 computer using the LabVIEW VI (ACTUATOR.VI). For safety, the cobra probe was in the full up position (0.955 inches) for turbine speed changes above 5000 RPM. Also, the cobra probe was not lowered closer than 0.1 inch from the hub. Because probe and hub contact could occur, two lights on the ACTUATOR.VI front panel were used as safety indicators. The first light was a warning which was activated when the probe was 0.2 inches from the hub and the second light was a stop light which was activated at a probe height of 0.1 inch from the hub (see Appendix F, Figure F4).

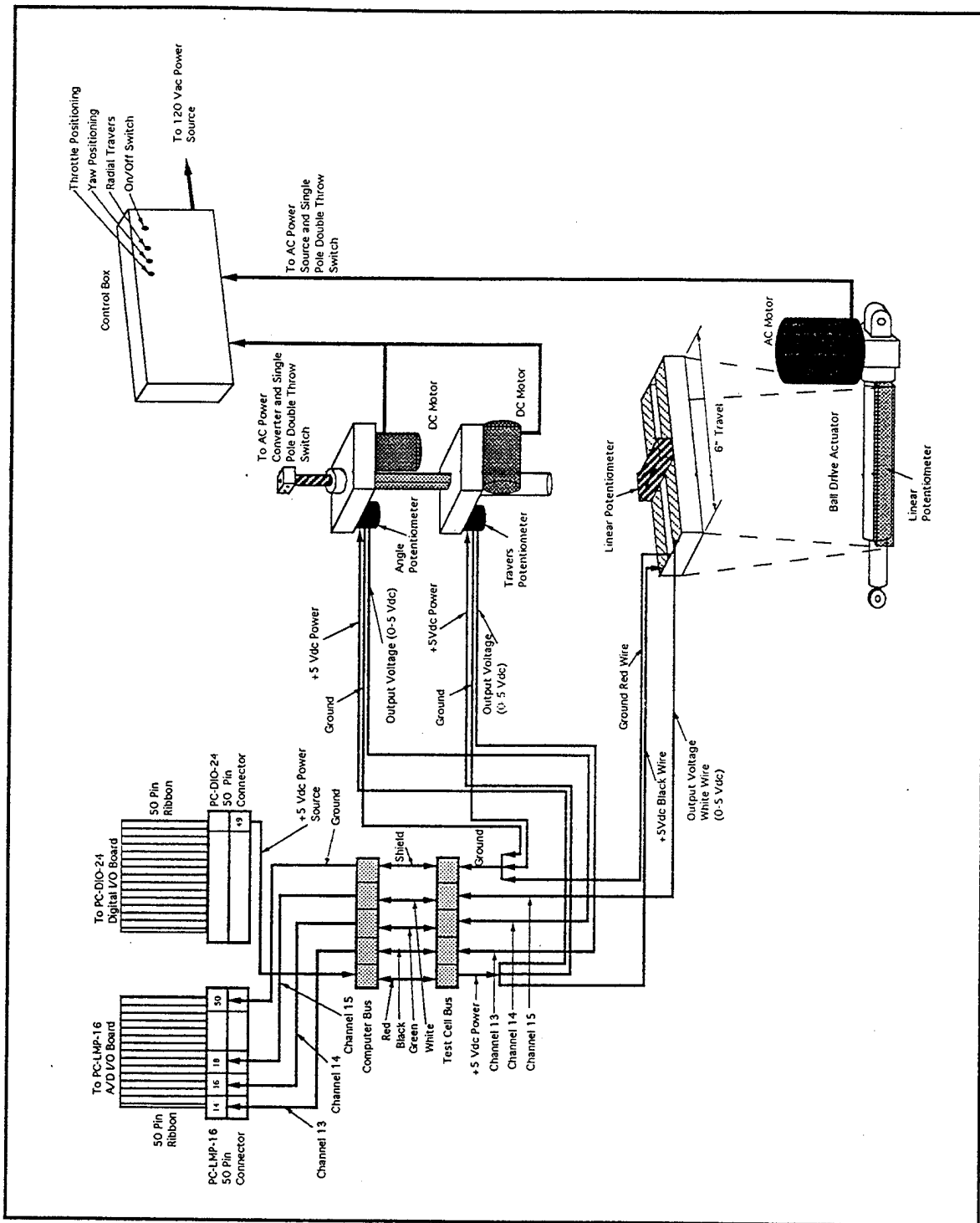


Figure 19. Control and Read Out for the Ball-Drive and L.C. Smith Probe Actuators

VI. RESULTS AND DISCUSSION

The data collected using the LabVIEW VI (SSME_TTR.VI) was transferred to an Excel work sheet for data reduction and display. The values calculated were also used to validate the SSME_TTR.VI's data reduction output. The Excel work sheet (SSMETTR.XLS) shown in Appendix J, Figure J1 was used to plot Figures 20-24. Figures 20-24 were generated by operating the TTR without the exit-plane throttle valve. These turbine performance runs were similar in setup to the runs reported by Rutkowski [Ref. 2]. The plot of referred RPM vs. turbine thermal efficiency, shown in Figure 20, reveals a similar trend as reported by Rutkowski. However, the TTR was also operated with the speed control system in automatic mode in order to obtain constant speed lines. These constant-speed lines are shown at referred speeds of 5600, 5880, 6490, 7200, and 7550. Turbine thermal efficiency vs. total-to-total pressure ratio was plotted for those constant referred-speed lines, and are shown in Figure 21. The plot in Figure 21 shows that the turbine total-to-total pressure ratio (P_{tt}) did not change very much with change in thermal efficiency. The power produced by the turbine was calculated using three different methods. The first method (HP #1) determined power using the thermodynamic measured quantities of the turbine inlet and outlet stagnation temperatures, and mass-flow rate. The second method (HP #2) determined power using the dynamometer mechanical measured quantities of the water temperature increase across the dynamometer and water flow rate. The third method (HP #3) determined power using the turbine mechanical measured quantities of rotational speed in RPM and torque. The three determinations

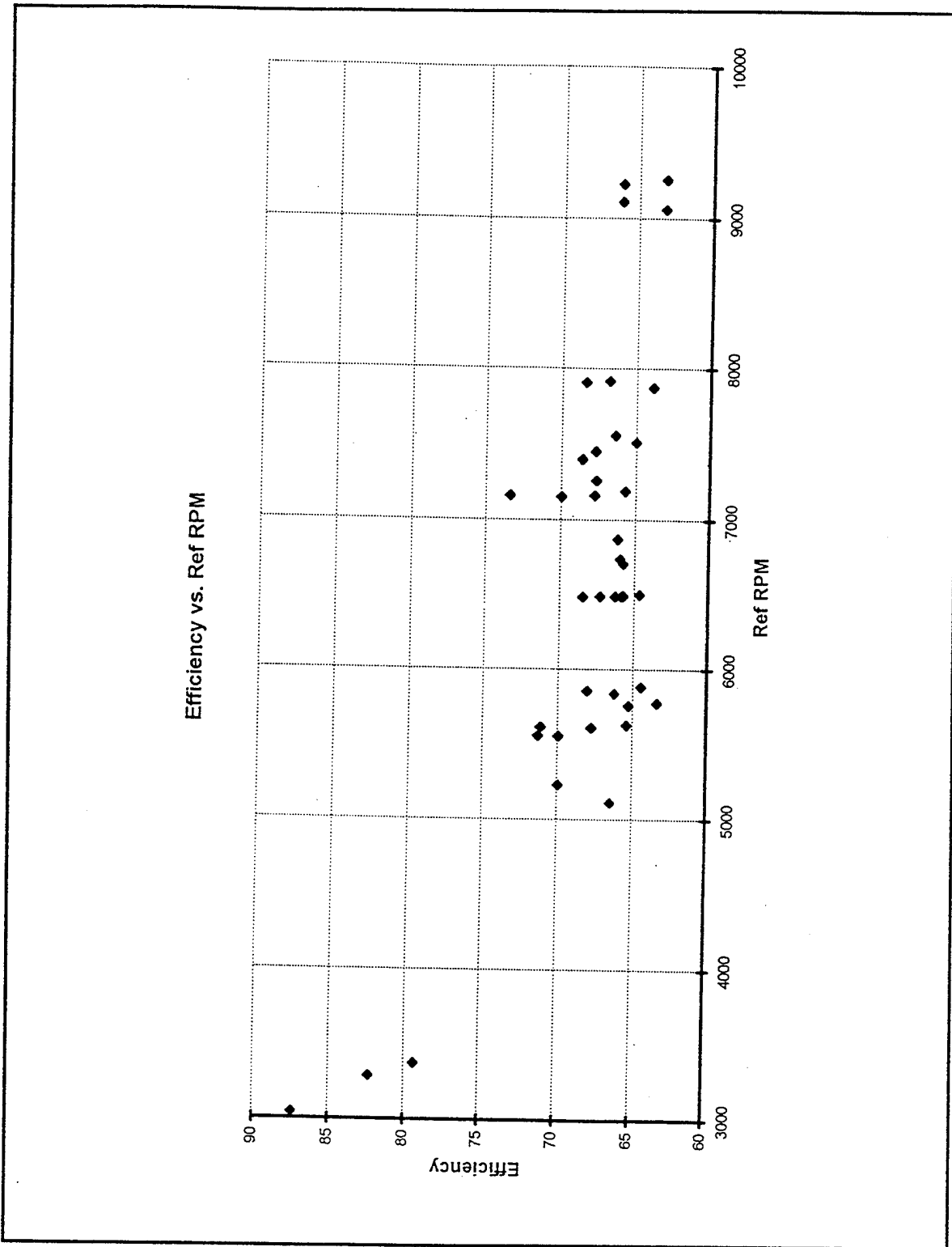


Figure 20. Efficiency vs. Referred RPM

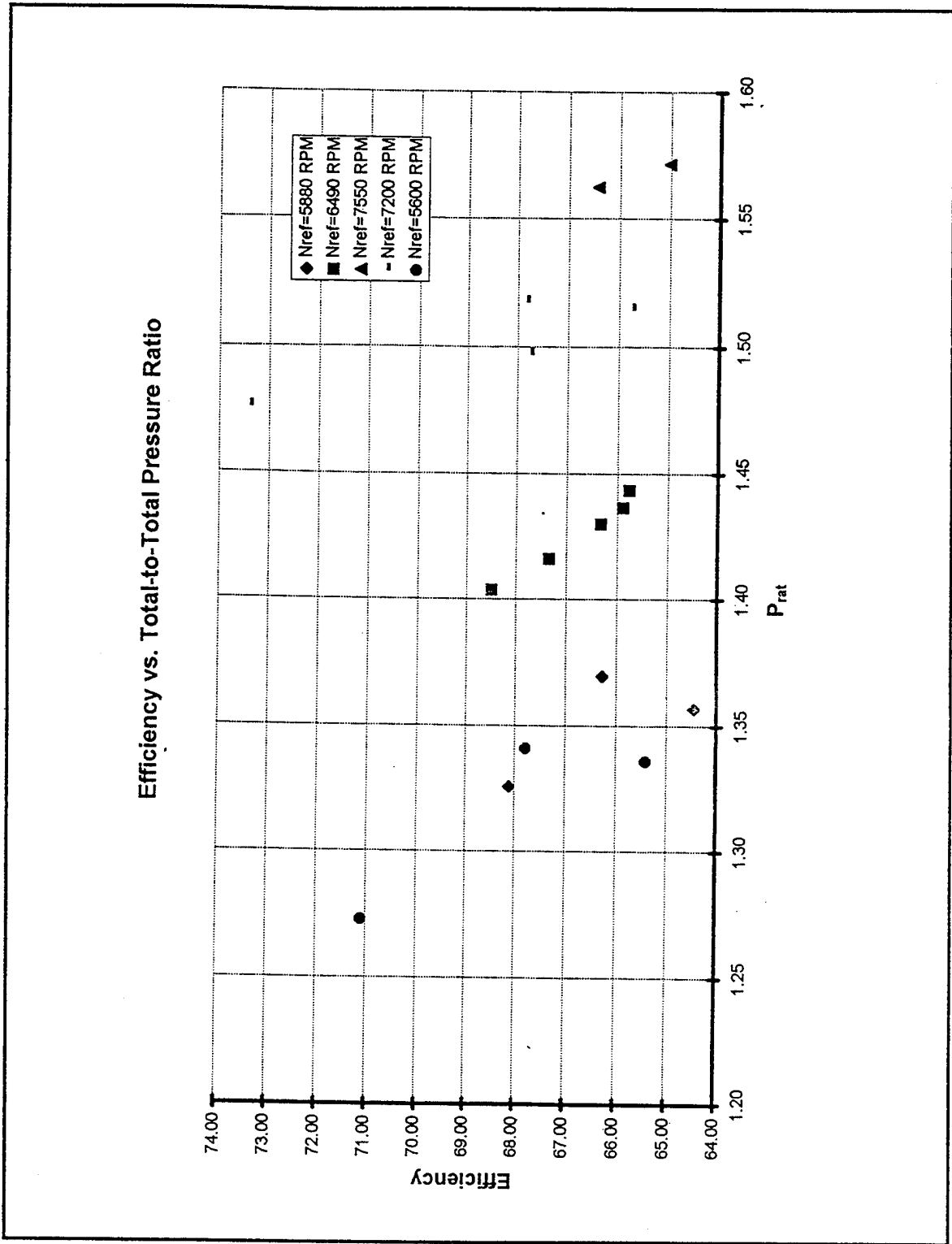


Figure 21. Efficiency vs. Total-to-Total Pressure Ratio

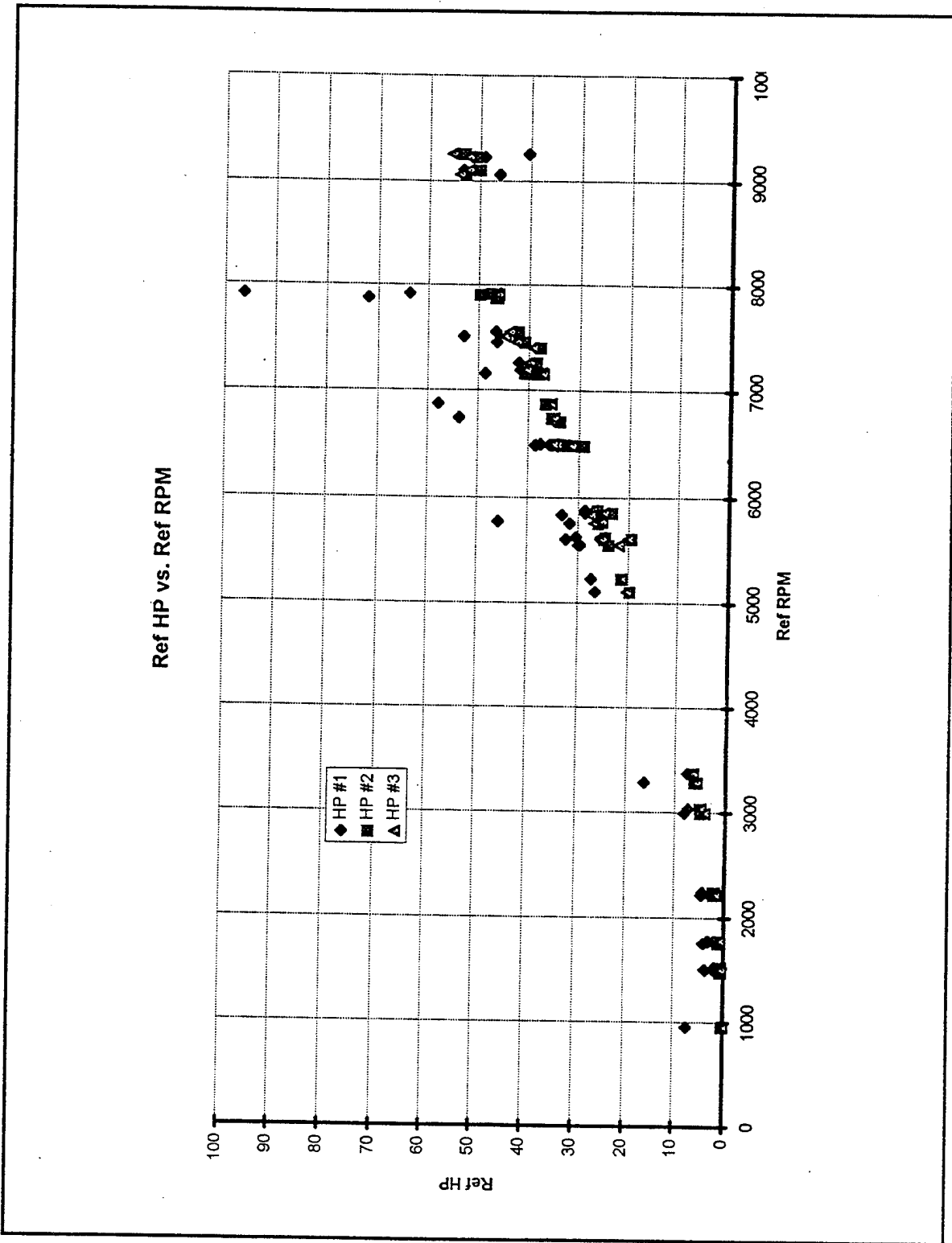


Figure 22. Referred Horsepower vs. Referred RPM

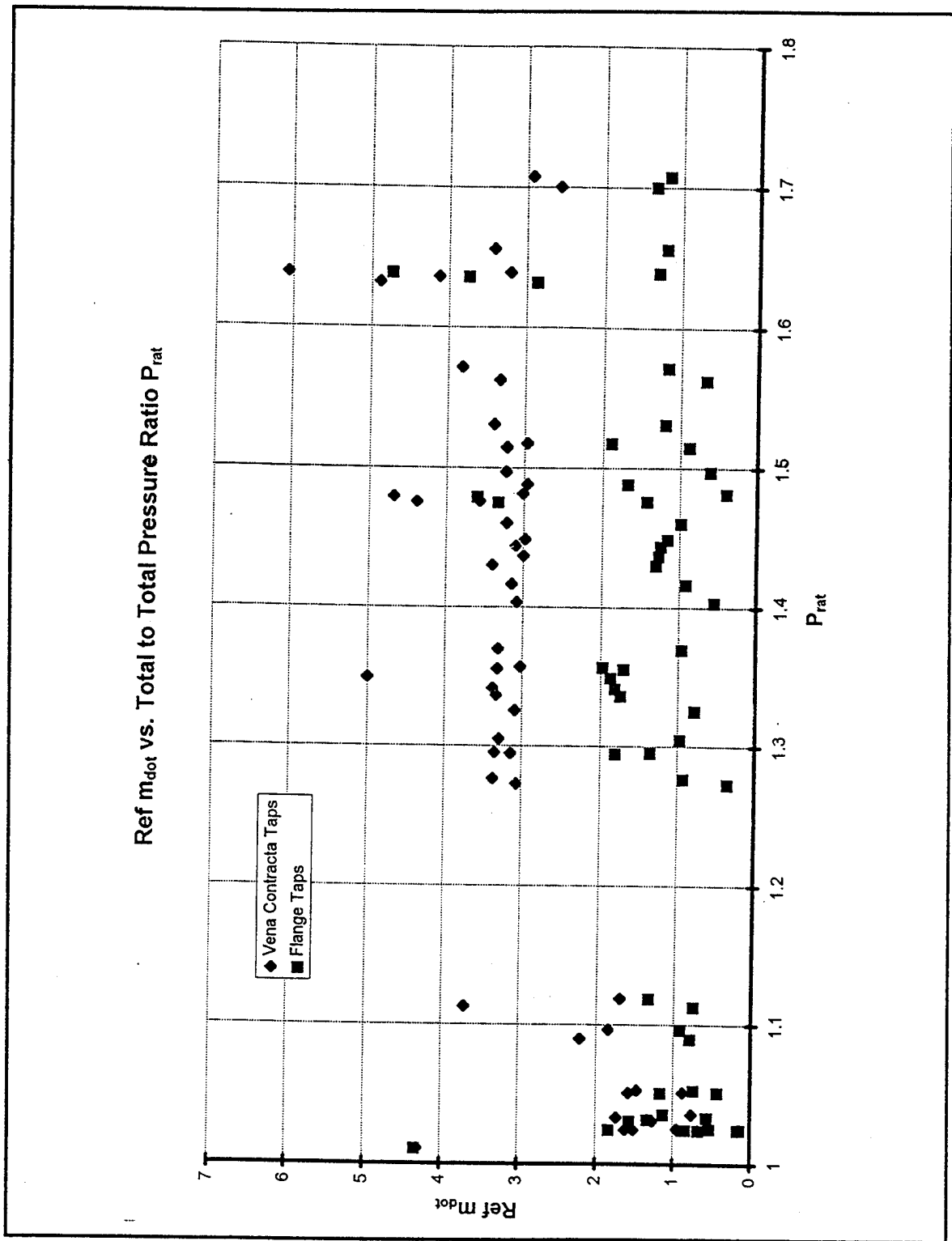


Figure 23. Referred Mass-flow vs. Total-to-Total Pressure Ratio

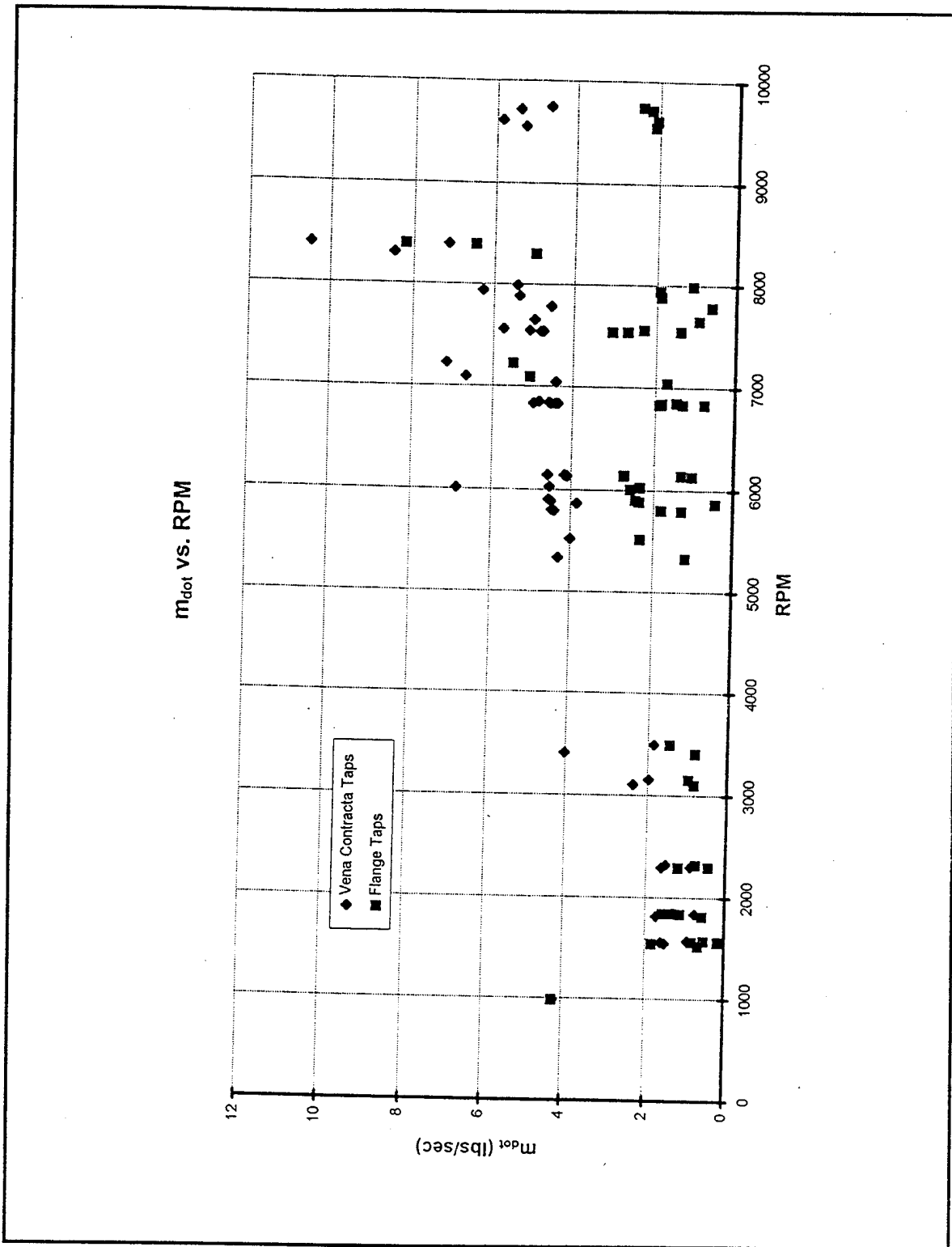


Figure 24. Mass-flow Rate vs. RPM

of turbine referred HP vs. referred RPM are shown in Figure 22. The two mechanical efficiencies HP #2 and HP #3 show good agreement throughout the RPM range.

However, the thermodynamic horsepower does not agree with the other two methods but does show the same increasing behavior with increasing RPM. The difference between the thermodynamic method and the two mechanical methods may be attributed to the mass-flow calculation. The plot of referred mass flow vs. total-to-total pressure ratio for the vena contracta and flange taps is shown in Figure 23. The mass-flow rate calculated using the flange taps showed a wide scatter and was consistently lower than the mass-flow rate calculated using the vena-contracta taps. The vena-contracta taps showed much less scatter than the flange taps. Both mass-flow characteristics showed a constant relation with pressure ratio above 1.1. This characteristic can be confused with that of a choked-flow turbine at constant RPM. This is not the case due to the fact that the data shown in Figure 23 were obtained at speeds between 3000 and 9700 RPM. Therefore, the plot of mass-flow rate (lbs/sec) vs. turbine speed (RPM) is shown in Figure 24. The two mass-flow rate calculations showed increasing behavior with increasing turbine speed.

However, the flange taps showed more scatter and consistently lower values than the vena-contracta taps. The scatter at turbine speeds of 6000 to 8500 RPM was much larger than desired. All turbine performance characteristics requiring mass-flow rate were calculated using the vena-contracta taps.

The data in Figures 25, 26, and 27 were produced over two days of testing with the turbine exit throttle valve installed on the TTR. The figures were plotted using the SSME_TTR.VI reduced data and the Excel work sheet SSME_TTR.XLS, shown in

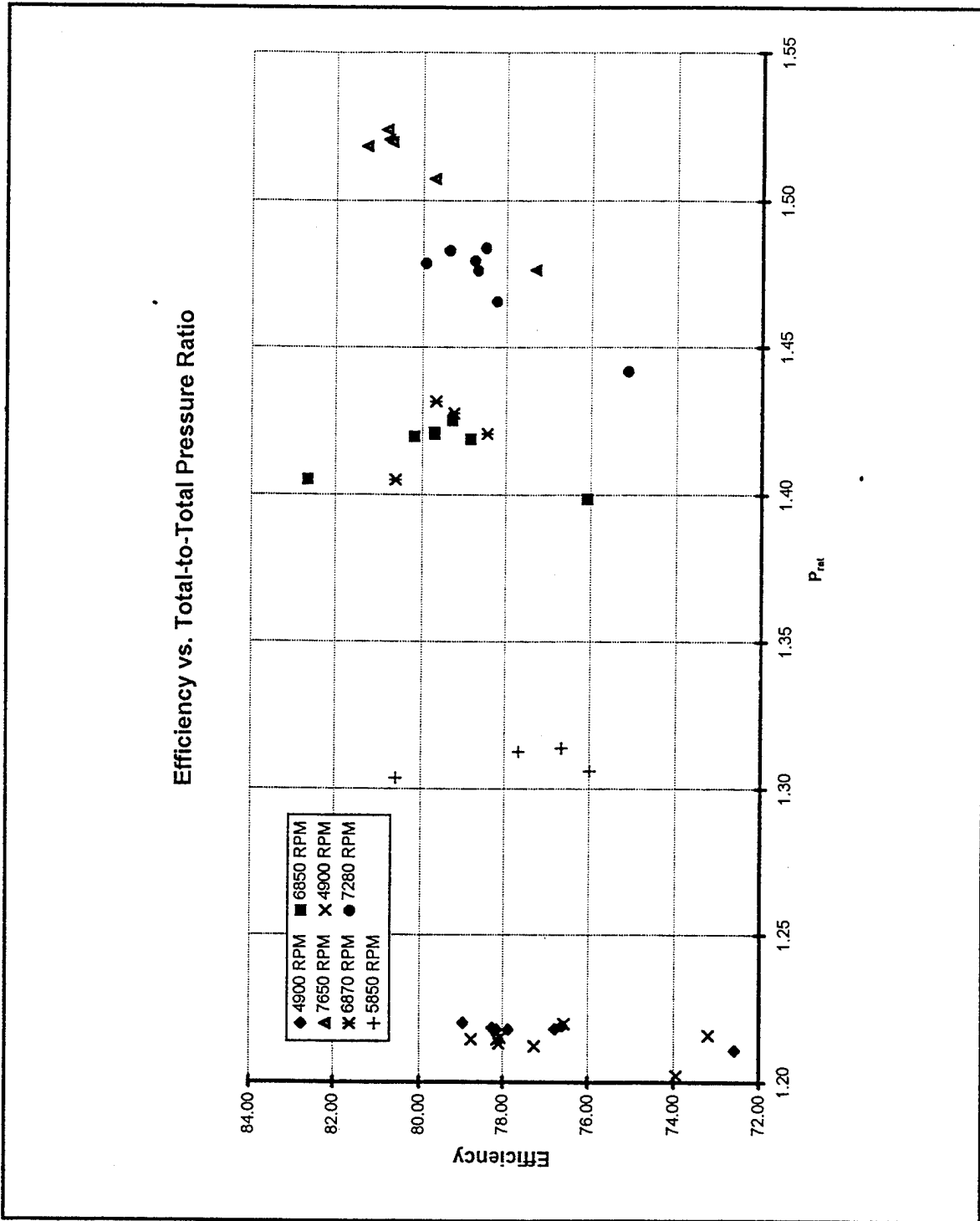


Figure 25. Efficiency vs. Total-to-Total Pressure Ratio

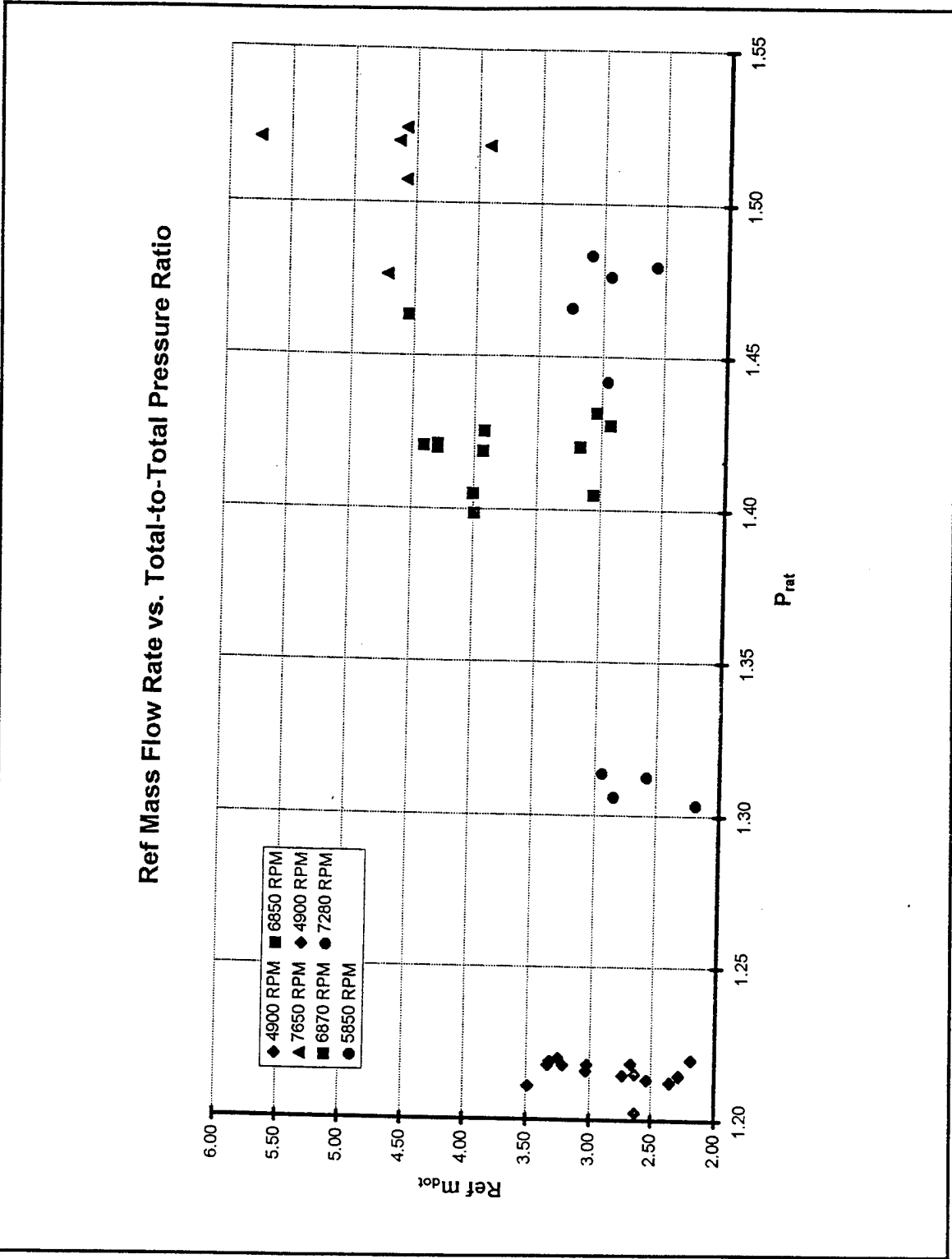


Figure 26. Referred Mass-flow Rate vs. Total-to-Total Pressure Ratio

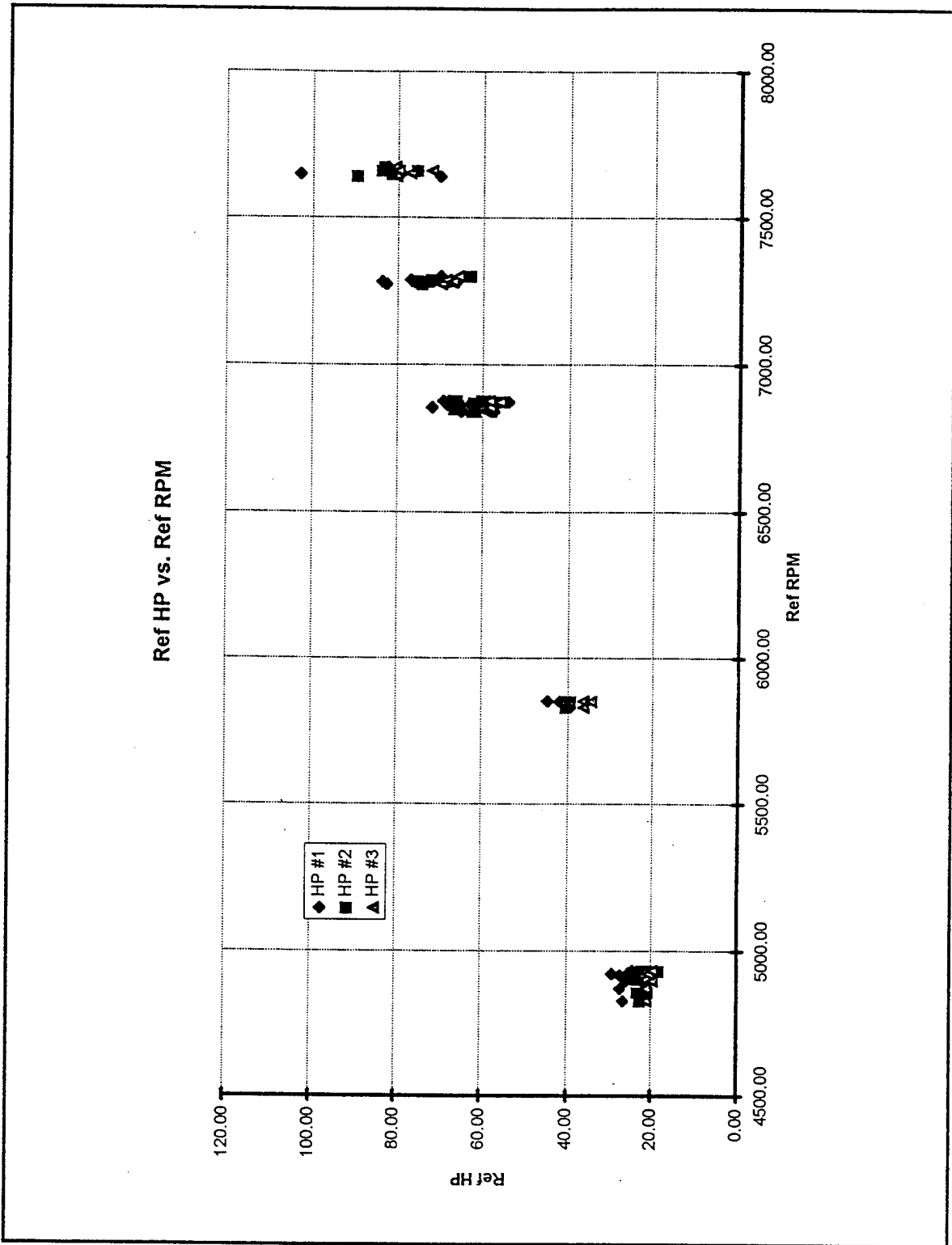


Figure 27. Referred Horsepower vs. Referred RPM

Appendix J, Figure J2. Figure 25 shows the turbine isentropic efficiency (η_t) vs. total-total pressure ratio (P_{rat}). The 4900 RPM constant speed line showed no change in P_{rat} with increase η_t . The two constant speed lines at 5850 and 6850 referred RPM showed a kink in the data and the constant speed lines at 7280 and 7650 showed an increase in P_{rat} with increased η_t . The turbine characteristics shown in Figure 25 exhibited unchoked flow behavior as illustrated in Figure 28 from [Ref. 21]. Figure 26 is a plot of referred mass-flow rate vs. P_{rat} . The constant speed line at 4900 referred RPM was repeatable and showed no change in P_{rat} with increase in referred mass-flow rate. The constant speed line at 5850 referred RPM showed a slight increase in P_{rat} as referred flow rate increased. The data at 6850 referred RPM and above were not repeatable and showed no useful pattern, due to mass-flow rate measurement errors. Figure 27 shows referred HP using the three different methods vs. referred RPM. The HP calculations using the three different methods showed good agreement at speeds below 5000 RPM. At speeds above 5000 RPM, the two mechanical HP calculations HP #2 and HP #3 showed good agreement up to 7250 RPM. The thermodynamic HP calculation, HP #1, did not show good agreement with the two mechanical HP calculations. This could be attributed to the larger error in mass-flow calculations and the dynamometer outlet valve response due to the automatic speed control commands at the higher turbine speeds.

The diagram shown in Figure 29 is a dynamometer power absorption curve drawn on a log-log scale [from Ref. 22] with SSME HPFTP ATD HP vs. speed data imposed for comparison. The horsepower capacity of the dynamometer is limited by its ability to

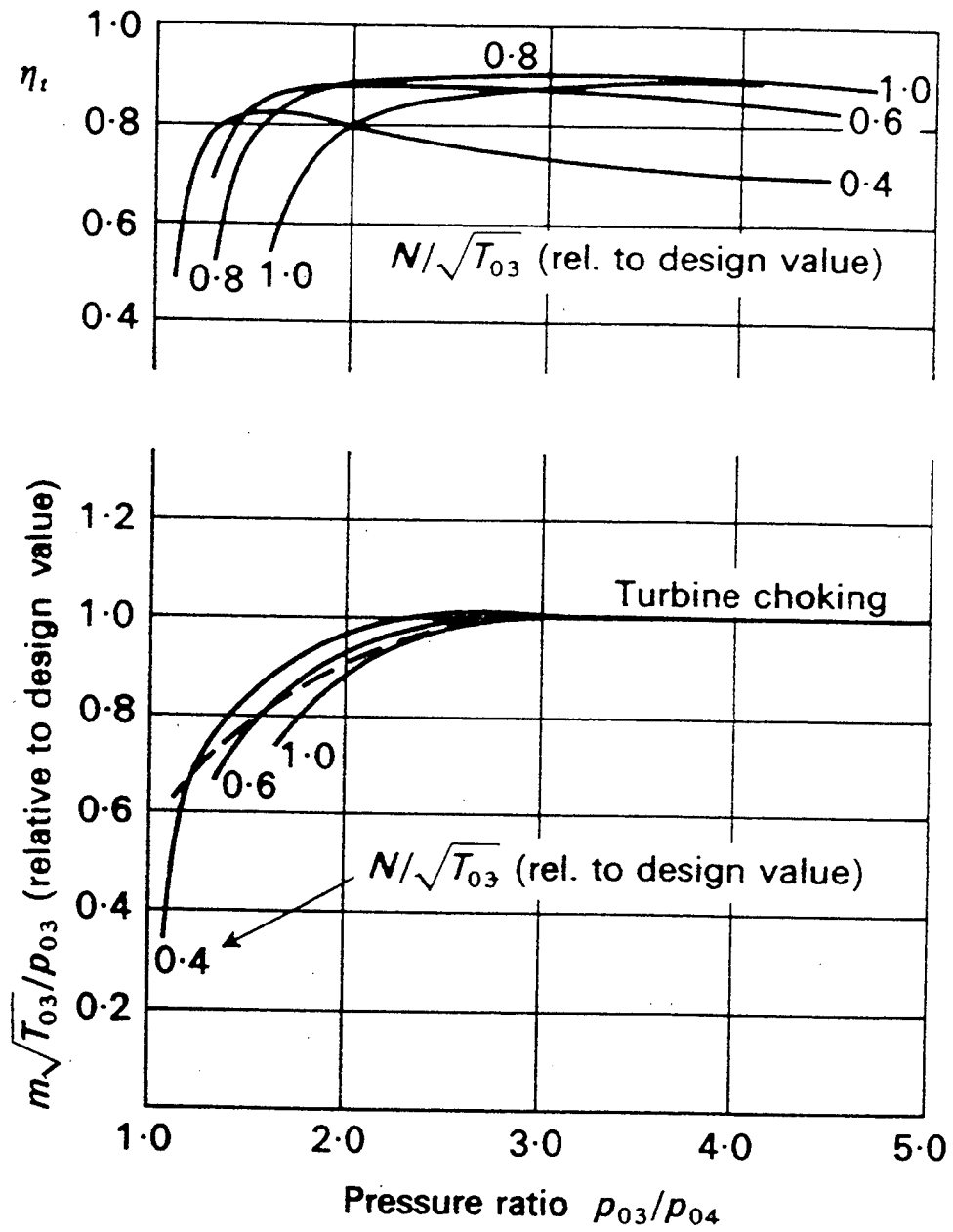


Figure 28. Turbine Characteristics

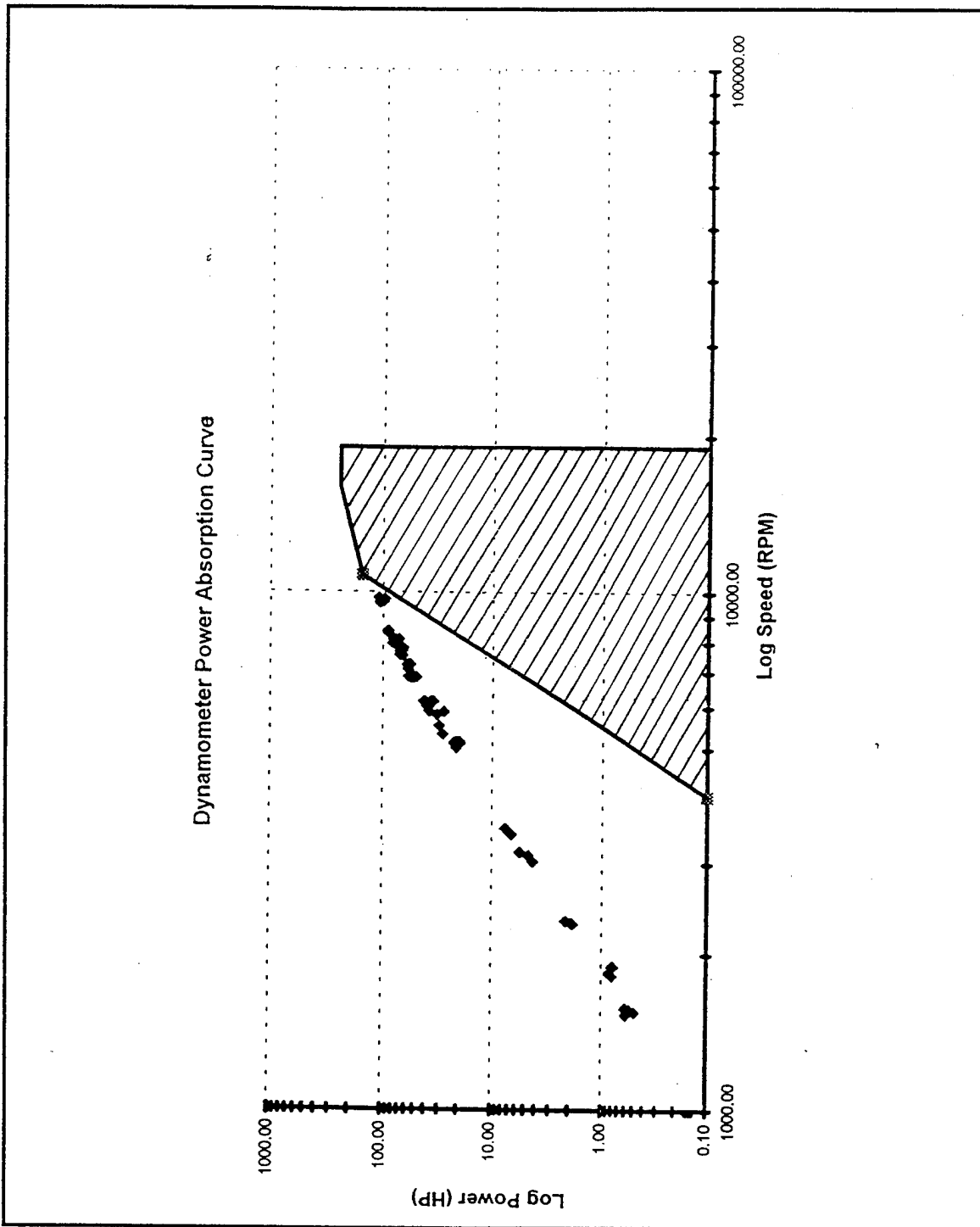


Figure 29. Dynamometer Power Absorption Curve

accept and discharge cooling water. The maximum power absorption curve depended on rotor size and rotor-stator configuration. From Figure 29, the SSME HPFTP ATD operating range was not inside the dynamometer envelope. This situation was the main reason why the SSME HPFTP ATD first stage could not be mapped in the choked-flow performance area.

The first-stage turbine-exit velocity profile with respect to the absolute frame was measured using the cobra probe setup discussed in section V.B. The absolute velocity vector is shown as V_2 in Figure 30 [from Ref. 23]. The velocity profile surveys, shown in Figures 31 and 32, were obtained by operating the TTR at referred speeds of 7250 and 7500 RPM in both the manual and automatic load-control modes. The data were obtained during approximately 12 hours of run time over the course of five days to ensure repeatability. Data obtained from the VEL_PRFL.VI were transferred to an Excel work sheet, VEL_PRFL.XLS, shown in Appendix J, Figure J3, for plotting. The turbine exit swirl angle distribution, shown in Figure 31, shows two interesting characteristics. First, an increase in flow angle started at 0.25 inches from the hub up to a peak at 0.40 inches and then decreased up to 0.60 inches, which may be attributed to secondary flow behavior. Second, an increase in flow angle started at 0.60 inches from the hub up to 0.70 and 0.80 and then decreased up to the blade tip. The swirl angle data with the throttle valve installed were repeatable. The large increase in swirl angle near 70 and 80% span may be attributed to a tip-leakage trailing vortex, (The running tip gap was 0.020 inches). The blade height vs. exit Mach number, shown in Figure 32, displays a slight Mach number

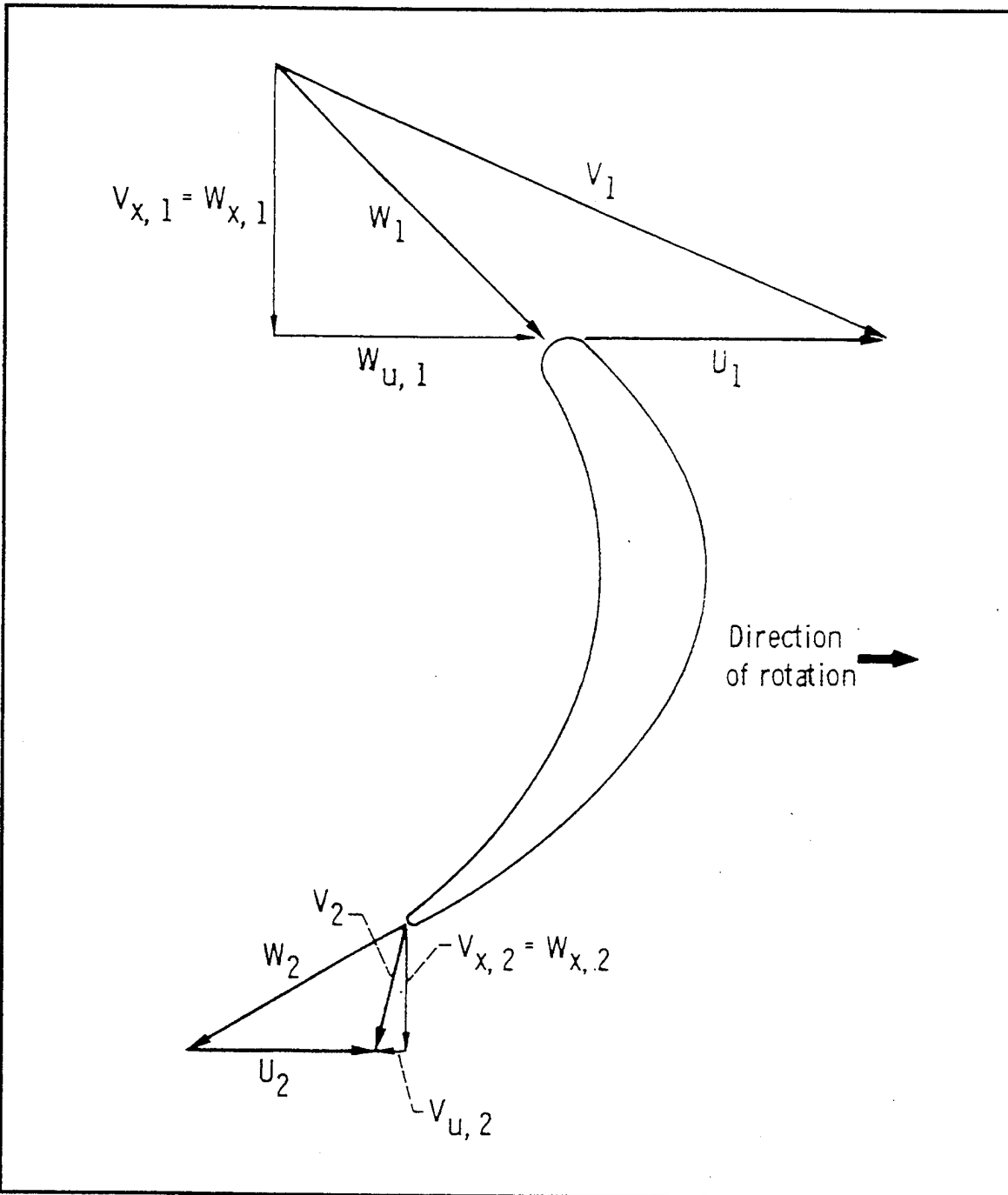


Figure 30. Absolute and Relative Velocity Vectors [from Ref. 23]

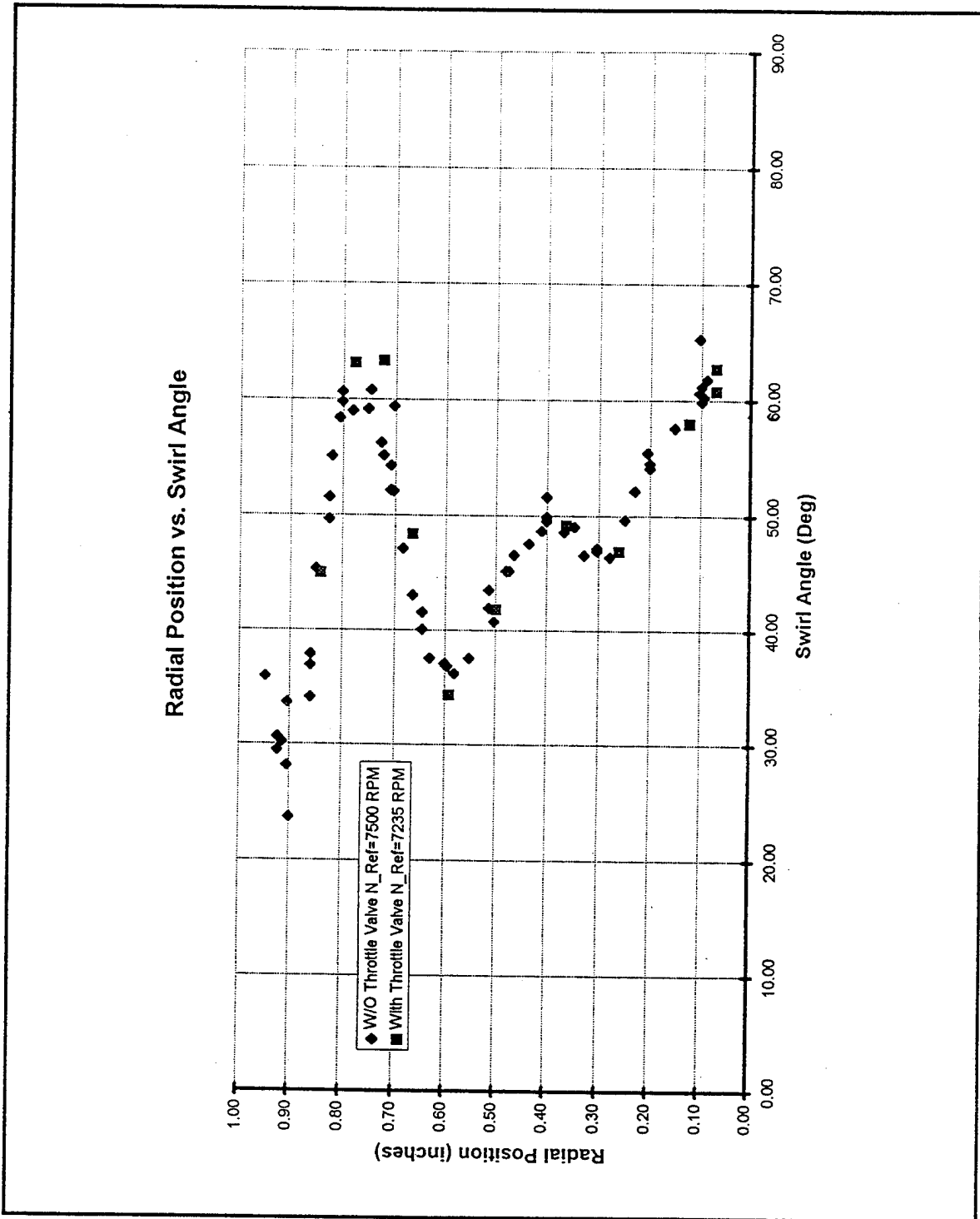


Figure 31. Radial Position vs. Swirl Angle

decrease at the mean line. Also, the data points near the tip gap show a large variation, which would indicate unsteady-flow characteristics. The Mach number with the throttle valve installed showed a constant value of 0.42 up to a blade height of 0.73 inches.

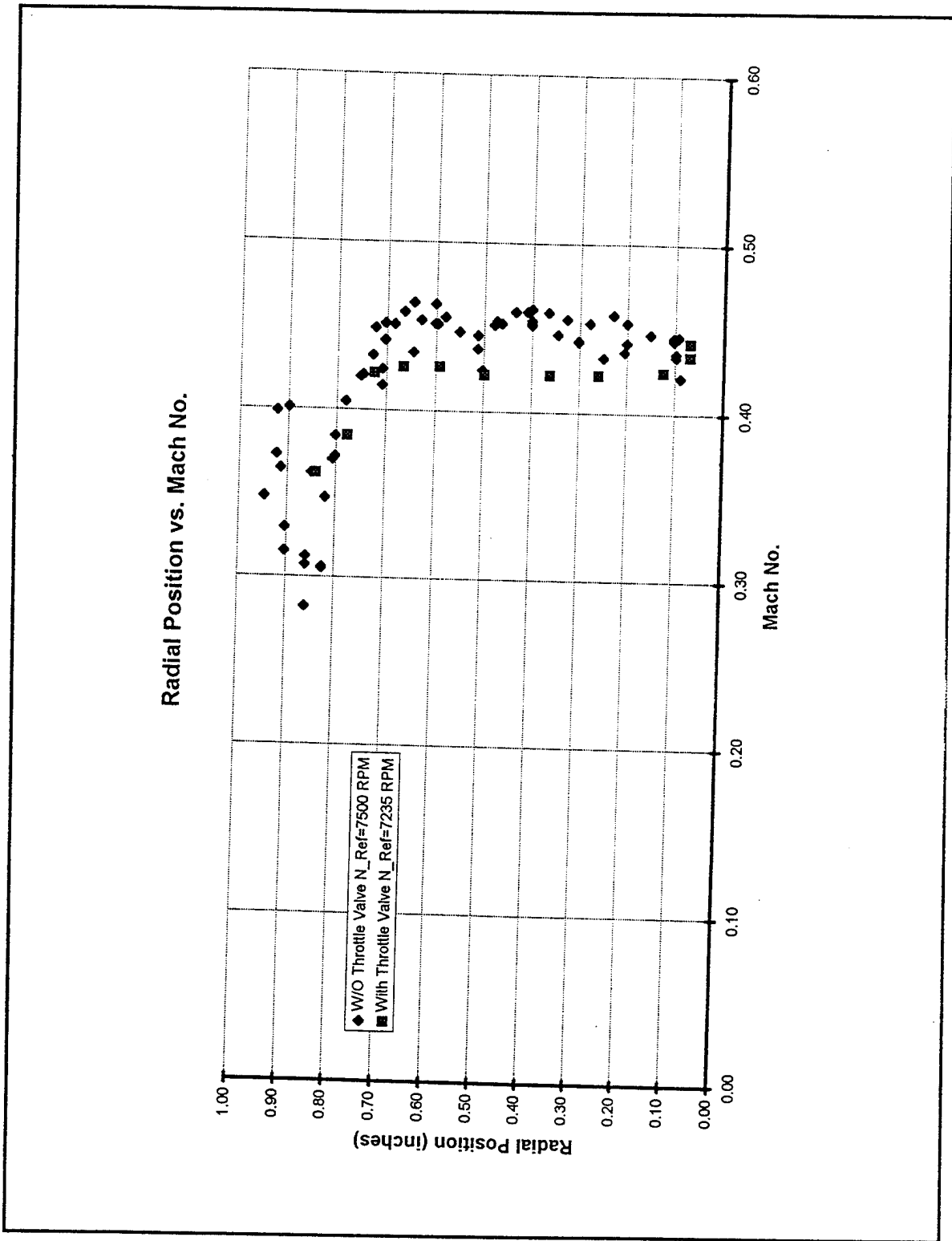


Figure 32. Radial Position vs. Mach Number

VII. NUMERICAL SIMULATION

A. INTRODUCTION

The purpose of the computational fluid dynamics (CFD) simulation was to generate a model of the SSME HPFTP ATD first stage. This consisted of generating a grid, using the stator and rotor geometry obtained from NASA Lewis Research Center in (z, theta, r) coordinates with a program called Turbomachinery C-Grid (TCGRID) [Ref. 24]. Once these grids were generated they were used as input to another program, Rotor Viscous Code 3-D (RVC3D), [Ref. 3], to simulate the flow through the first stage turbine. The solution was displayed using PLOT3D [Ref. 25]. Also, pxy.f shown in Appendix K, Figure K1 was used to display the pressure distribution along the upper and lower surface of the turbine blade, and residual history.

B. TURBINE FIRST STAGE GRID GENERATION

The hot-flow turbine geometry data for the first-stage turbine were received from NASA Lewis Research Center. Because the TTR was a cold-flow facility, a 99% thermal-shrink factor was applied to all radial and chord-wise dimensions. The thickness dimensions (theta direction) were not converted. The FORTRAN program used to accomplish this was obtained from Rutkowski [Ref. 2], which was modified to account for 5 radial blade surfaces and is presented in Appendix K, Figure K2.

Grid files were PLOT3D-compatible and were used as input to the flow solver (RVC3D) and for flow visualization once an acceptable solution was obtained. TCGRID generated grids by reading in a set of namelists and the scaled-blade geometry. The

namelists used to generate the first-stage stator and rotor grids are listed in Appendix L, Figures L1 and L2. The stator grid used by Rutkowski was modified by placing the exit plane at the 1.6 inch location (43% chord behind the trailing edge), which corresponds to the inlet rotor plane location. Also, in order to compare measured cobra probe swirl angle and Mach number data to the CFD solution, the rotor grid exit plane was placed at 0.25 inches behind the trailing edge (24% chord behind the trailing edge). This required a rotor grid size of $180 \times 25 \times 45$, which was an increase from the stator grid size as reported by Rutkowski [Ref. 2]. The 3-D stator and 2-D stator hub grids are shown in Figures 33 and 34. The 3-D rotor and 2-D rotor hub grids are shown in Figures 35 and 36.

C. FLOW SOLUTION

Once the grid was developed, it was used with the flow solver RVC3D to simulate the flow through the first-stage rotor. RVC3D is a computer code for analysis of fully three-dimensional viscous flows in turbomachinery including rotation effects. The code solves the thin-layer Navier-Stokes equations with an explicit finite difference technique. The equations are formulated in a Cartesian coordinate system with rotation about the x-axis. These equations are mapped to a general body-fitted coordinate system shown in Figure 37. Streamwise viscous terms are neglected using the thin-layer assumption, but all cross-channel viscous terms are retained. Turbulence is modeled using a three-dimensional Baldwin-Lowmax model. The equations are discretized using second-order finite-differences and solved using a multistage Runge-Kutta scheme. Mathematical formulation of RVC3D is described in [Ref. 26]. The inputs to RVC3D are

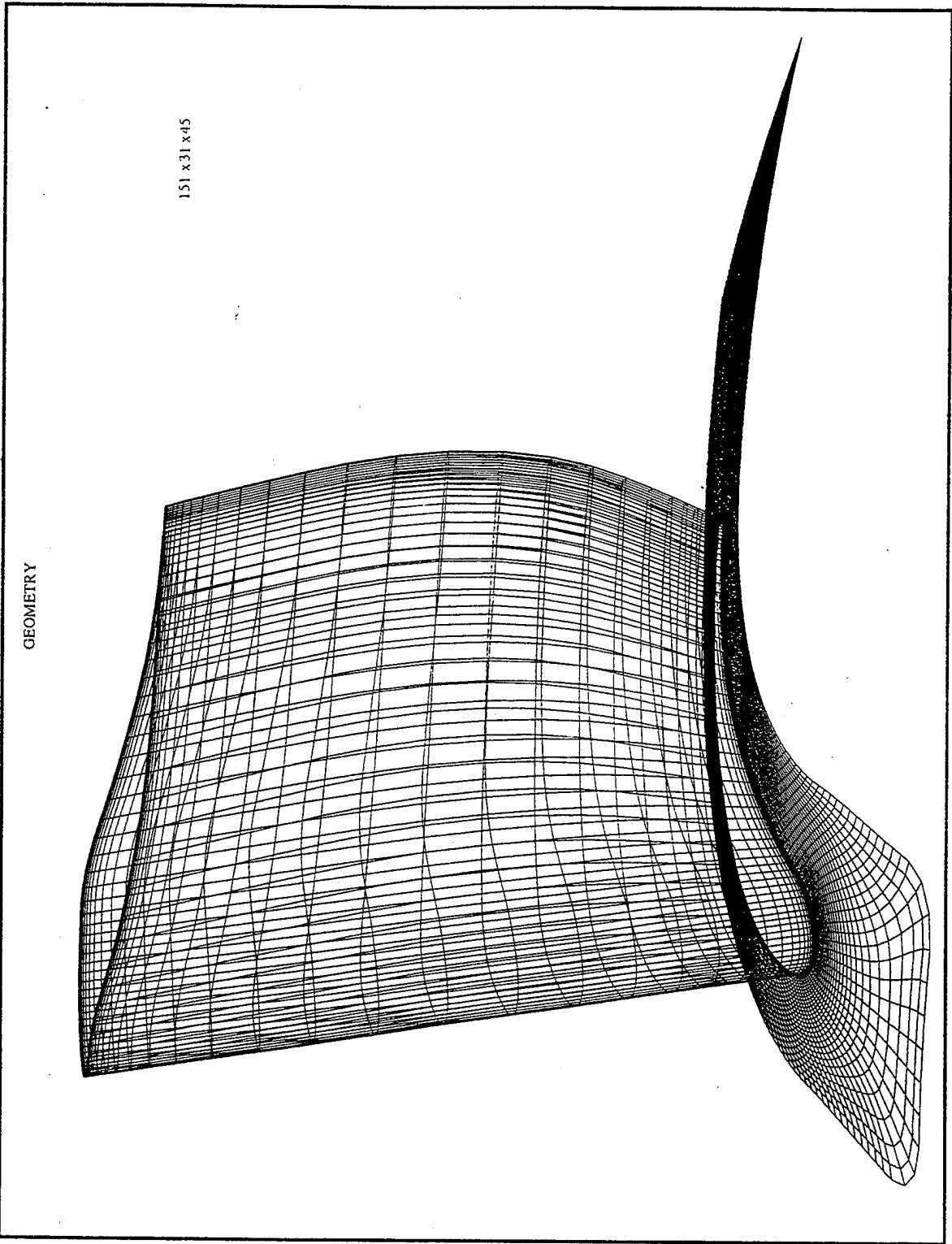


Figure 33. 3-D First Stage Stator Grid

151 x 31 x 45

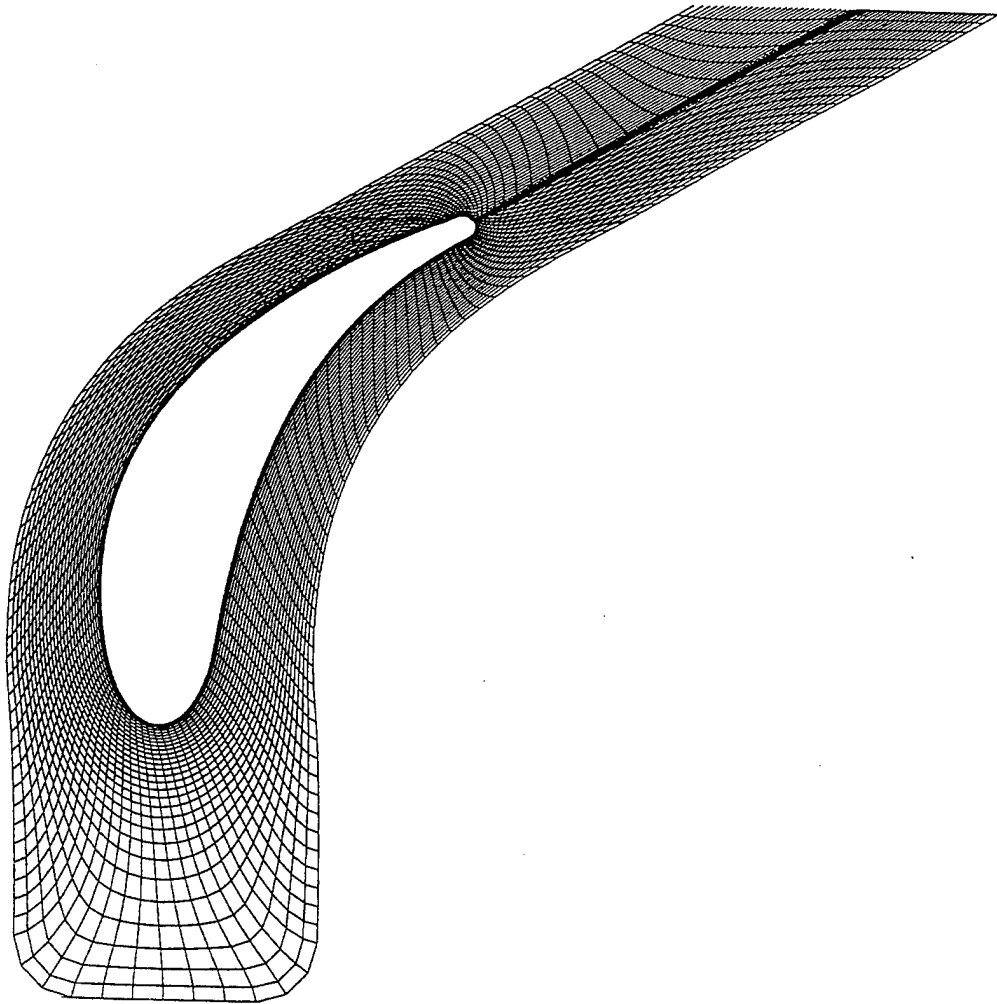


Figure 34. 2-D First Stator Hub Grid

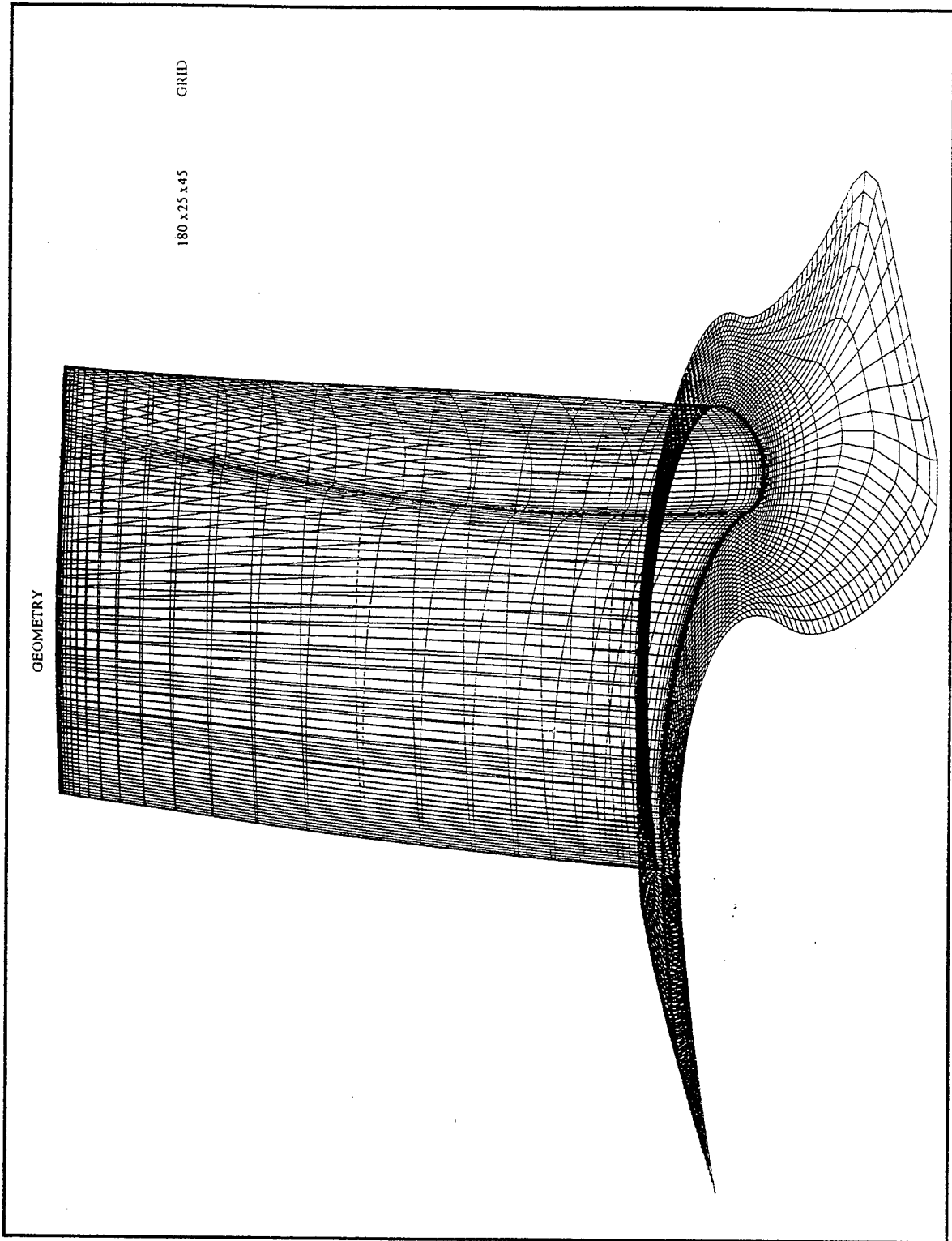


Figure 35. 3-D First Stage Rotor Grid

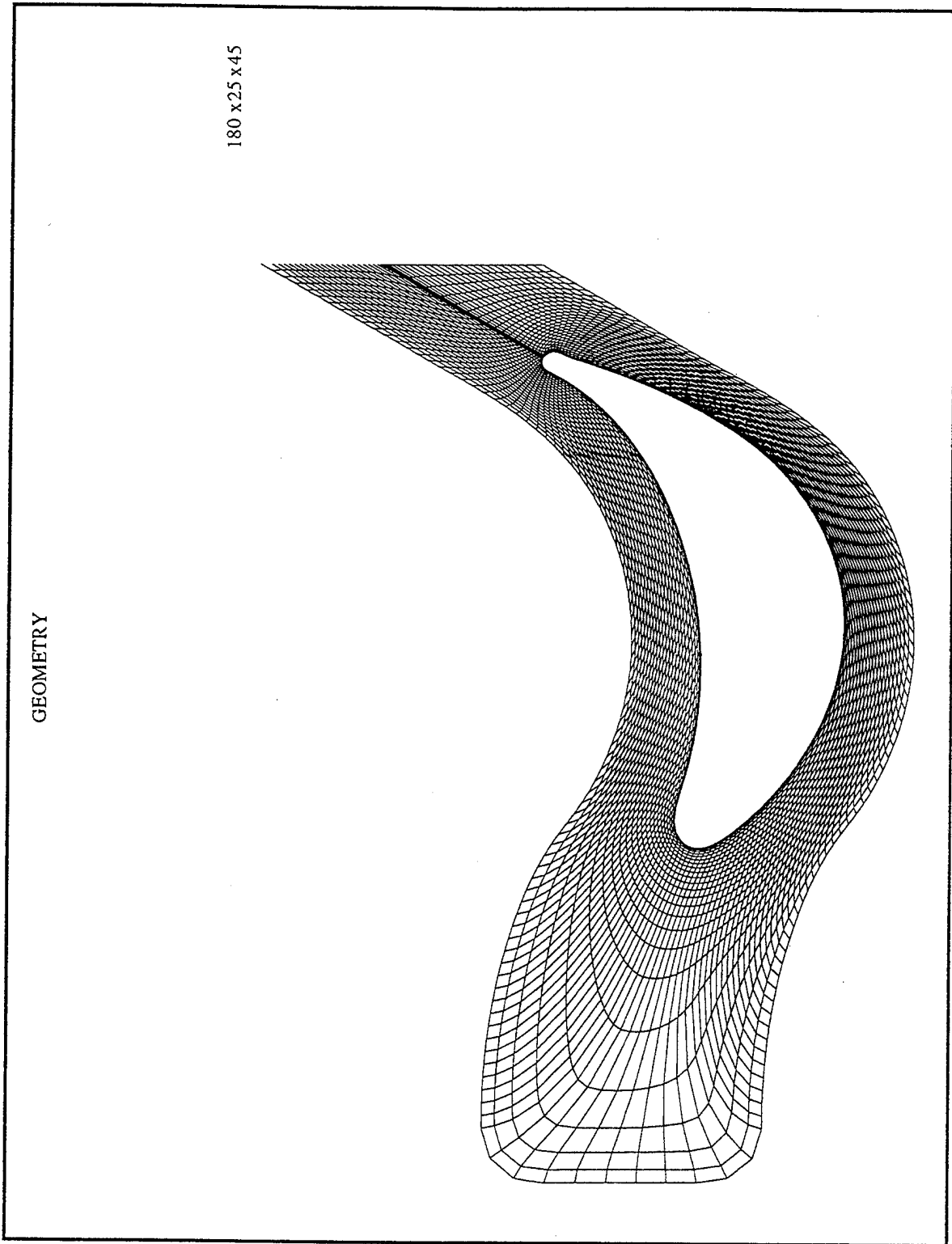


Figure 36. 2-D First Stage Rotor Hub Grid

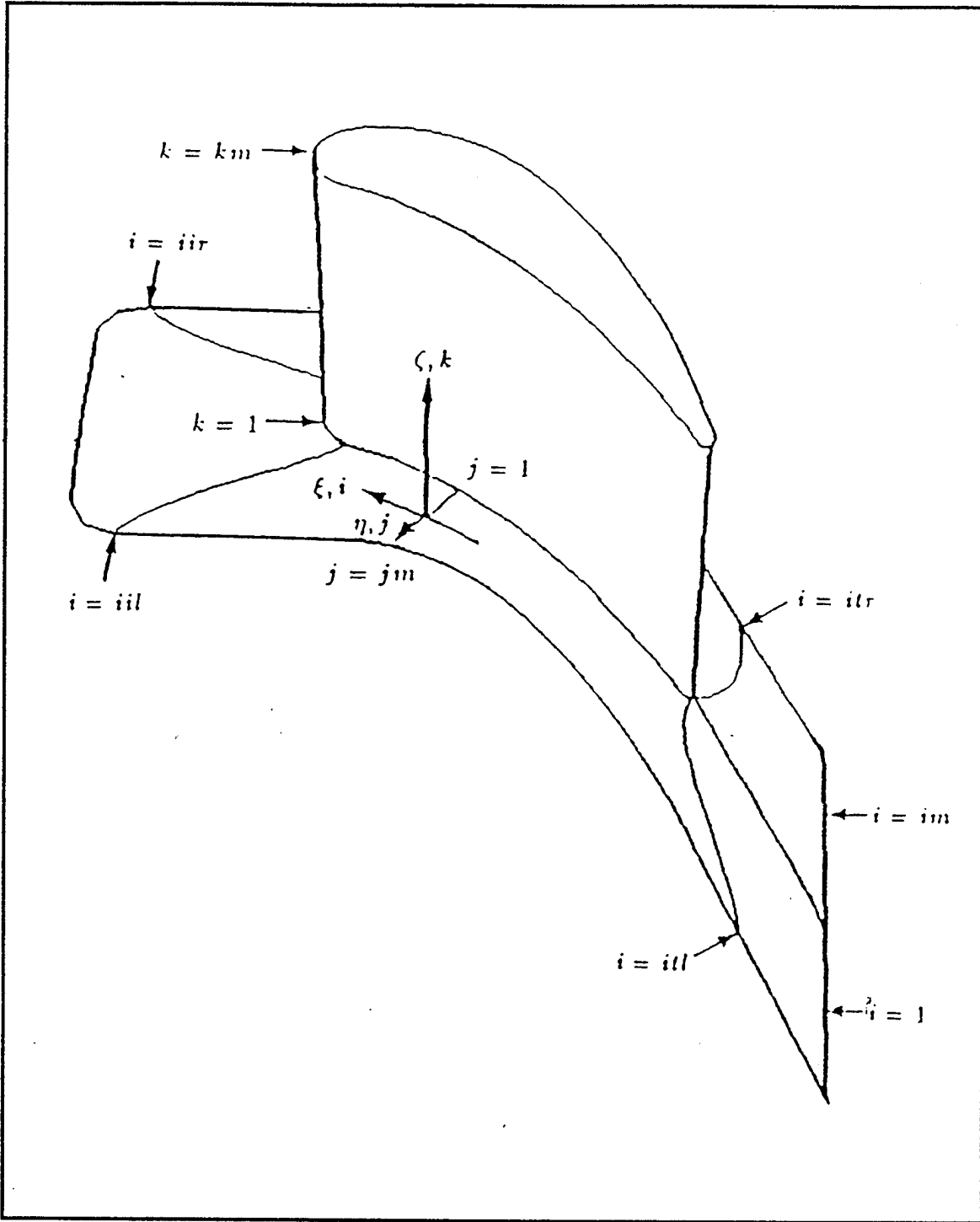


Figure 37. General Fitted Body System

strictly nondimensional, with the exception of lengths which remain in the same units as the grid. All quantities are nondimensionalized by an arbitrary reference stagnation state defined by total density ρ_0 and total sonic velocity c_0 . A reference viscosity μ_0 is defined by the stagnation temperature T_0 . FORTRAN files used and generated by RVC3D are as follows: fort.1 - grid input file generated by TCGRID; fort.2 - input restart file; fort.3 - output solution file, and fort.4 - input inlet flow profile.

RVC3D was executed on the Cray Y-MP EL-98 supercomputer using the namelist input files rvc3d.in for both the stator and rotor. The stator and rotor input files are shown in Appendix L , Figure L3. The stator and rotor solutions shown in Figures 38 and 39 and 41 and 42 were run out to 1000 iterations. The residual history for the stator and rotor are shown in Figures 40 and 43, respectively.

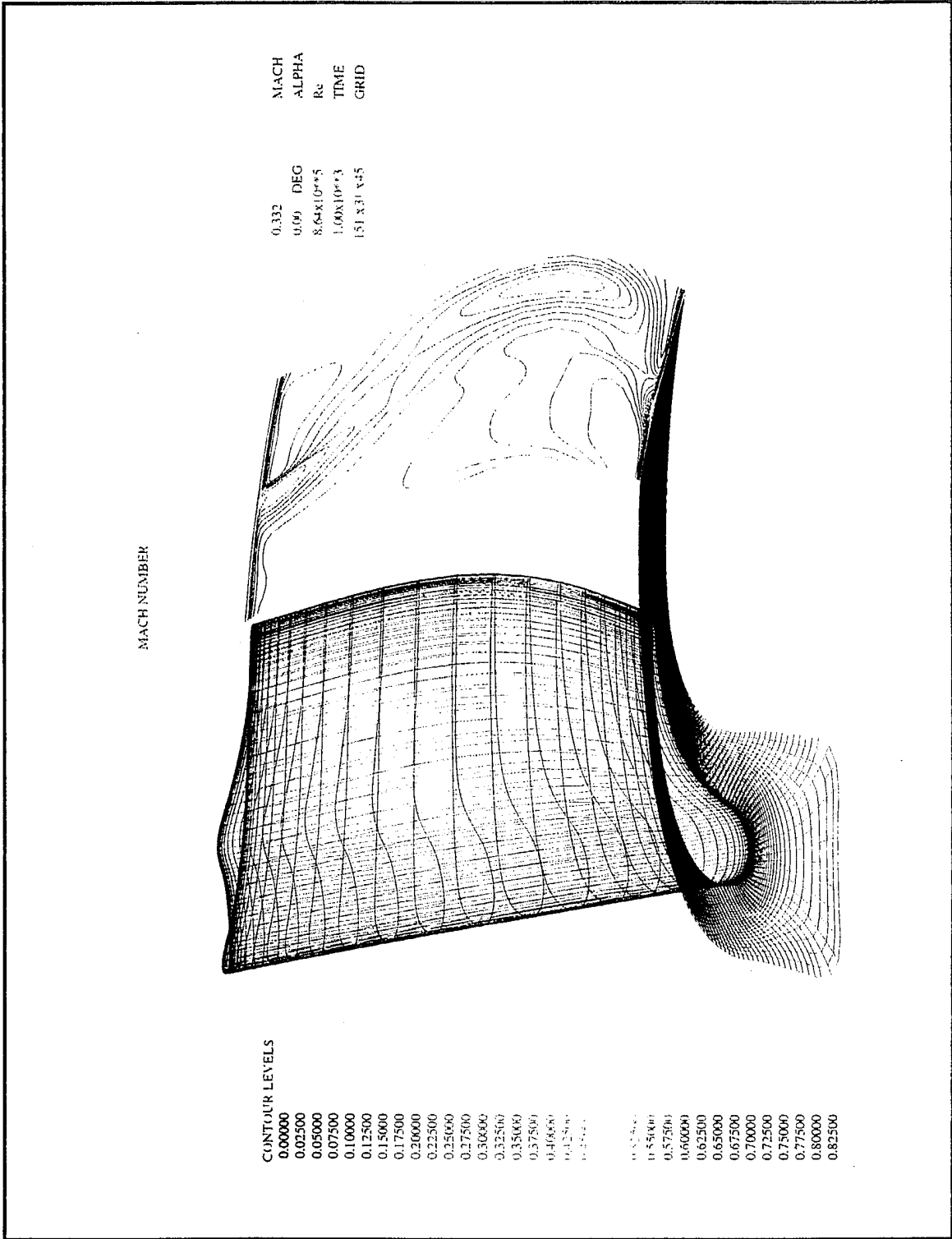


Figure 38. Stator Exit Plane Mach Number Contours

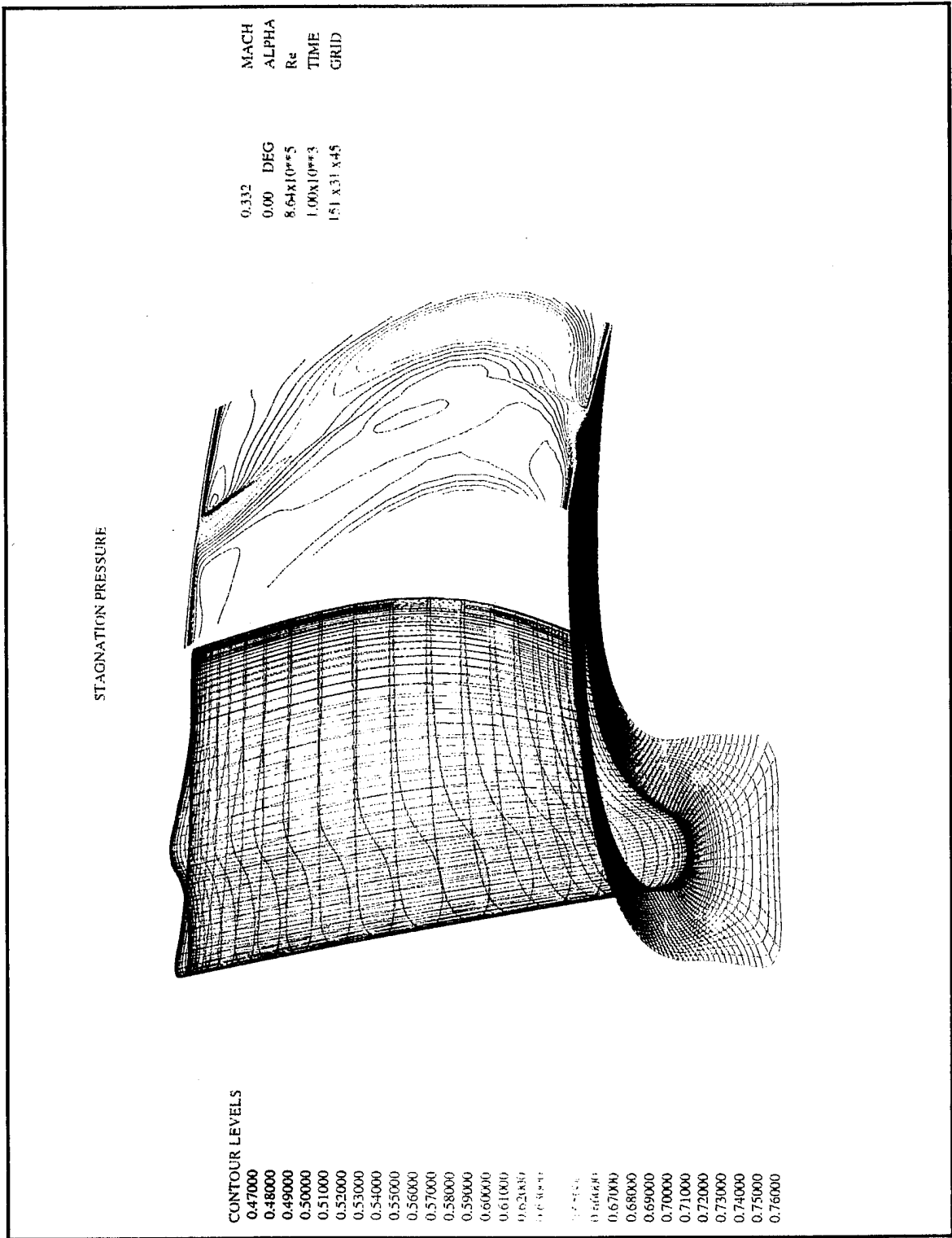


Figure 39. Stator Exit Plane Stagnation Pressure Contours

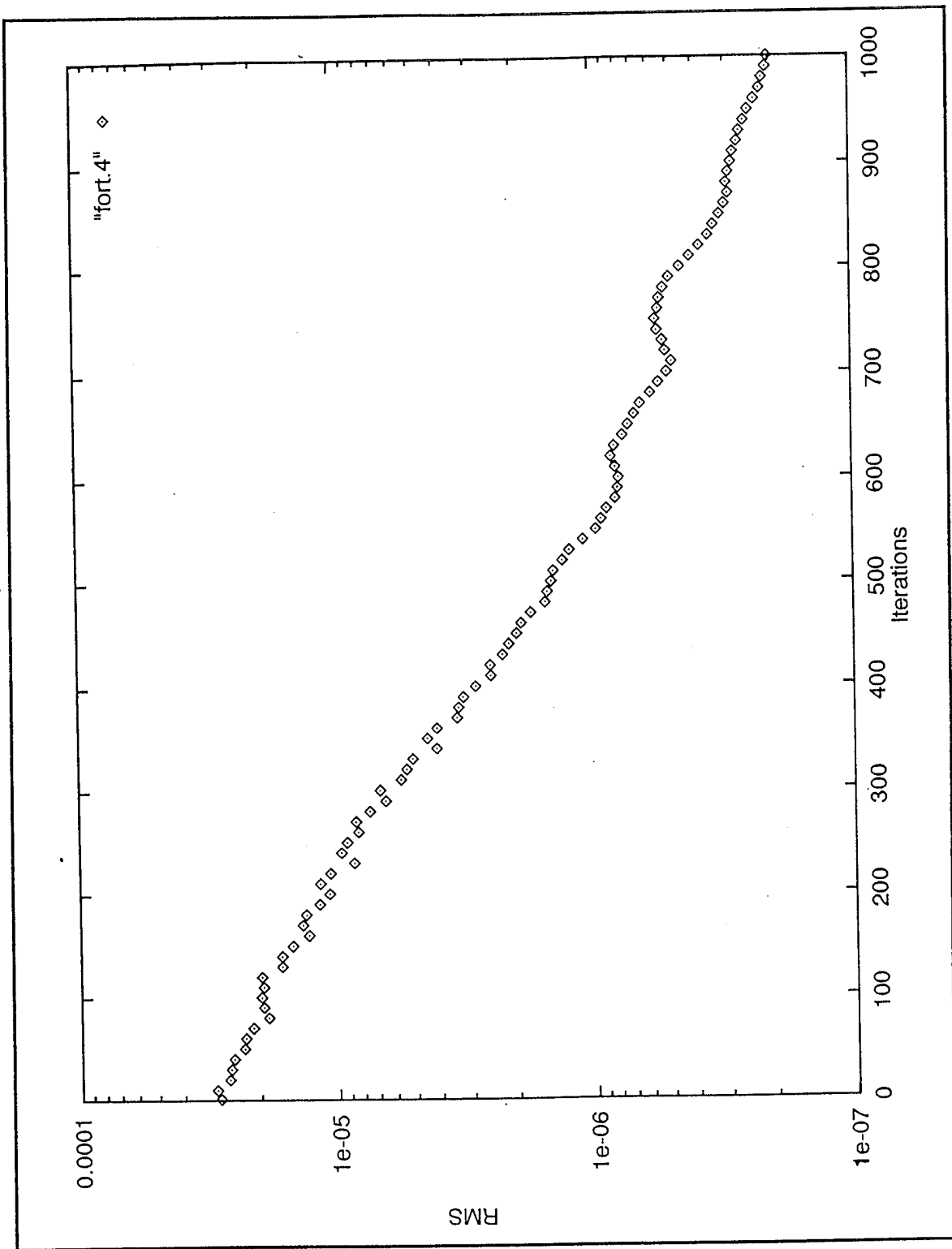


Figure 40. Stator Residual History

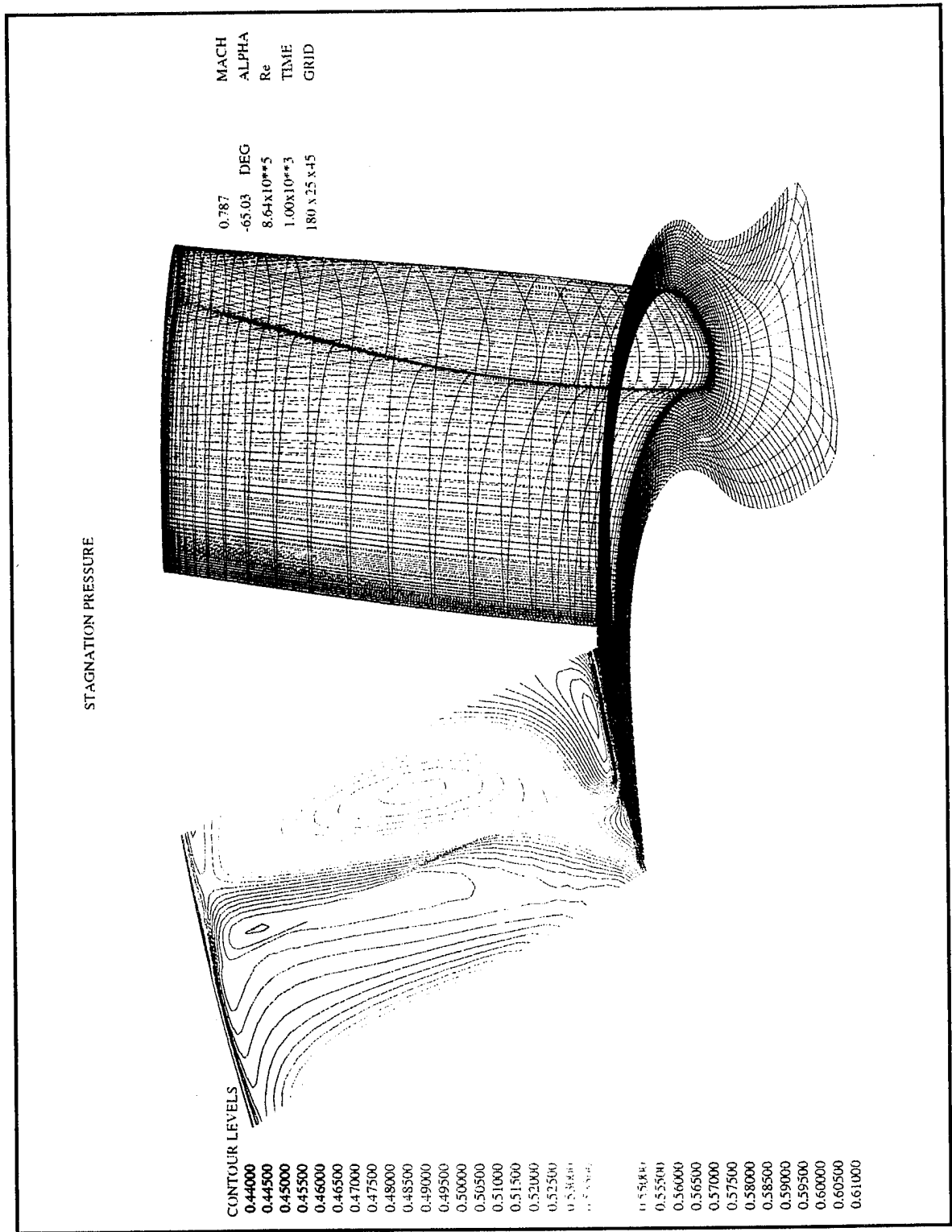


Figure 42. Rotor Exit Plane Stagnation Pressure Contours

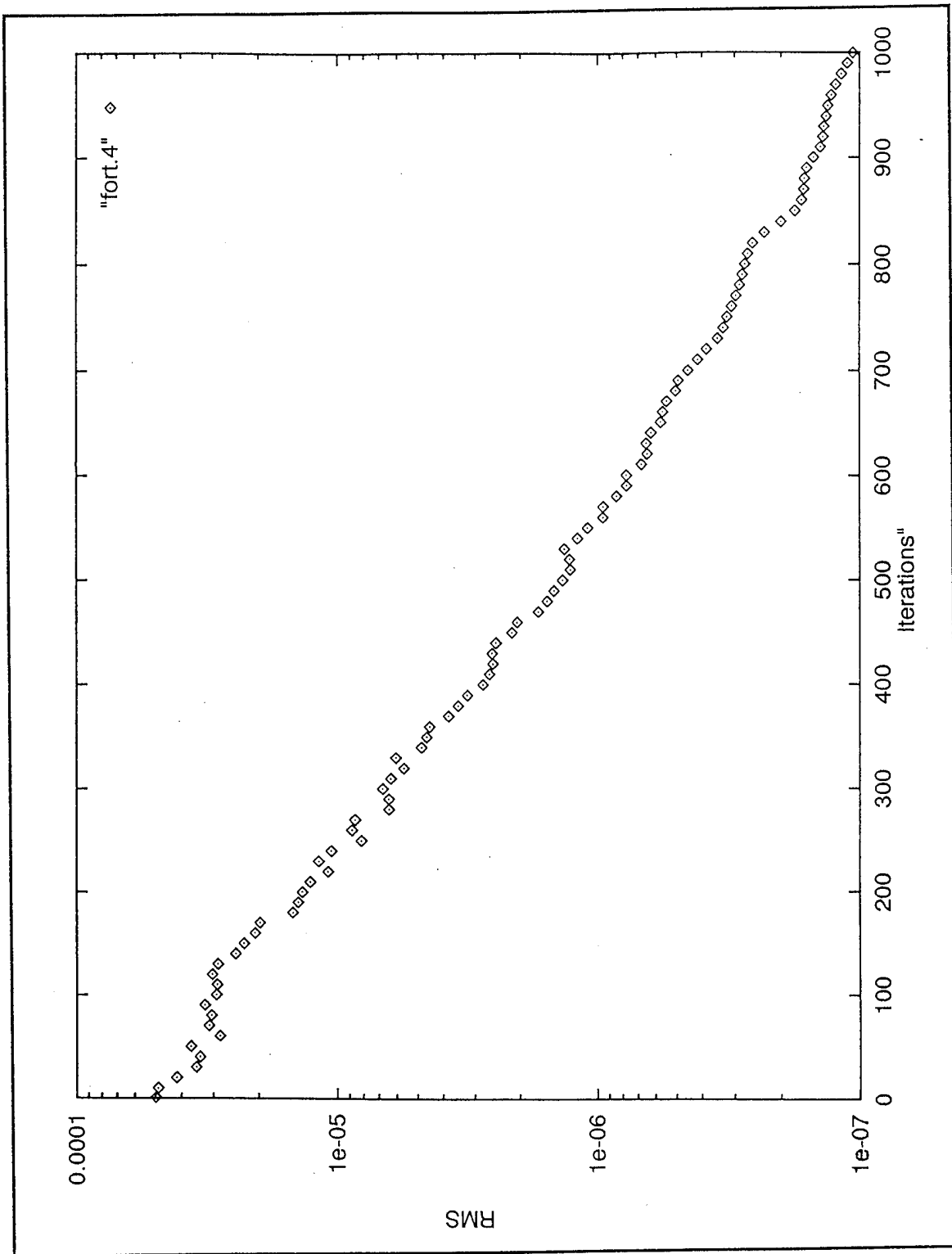


Figure 43. Rotor Residual History

VIII CONCLUSIONS AND RECOMMENDATIONS

A. EXPERIMENT AND TTR

The redesign of the TTR was completed and the rig was successfully operated. The redesign included the addition of the turbine-exit throttle valve, first- and second-stage outer casings, and cobra probe mounting brackets. An LDV optical window was made available through the first-stage outer housing and was located over the blade tips of the first-stage turbine rotor. Also, an access hole for a combination probe was attached to the second-stage outer housing for pressure and temperature measurements downstream of the first-stage turbine rotor exit.

Extensive performance measurements were made with and without the turbine throttle valve. However the dynamometer was not operating within its performance envelope. Consideration should be given to incorporating another dynamometer in order to improve the SSME HPFTP ATD operating range. For more accurate total-to-total pressure ratio and efficiency results, total pressure should be mass averaged from cobra probe radial surveys, at the first stage stator inlet and the at the rotor exit. Mass-flow measurements need to be more accurate in order to correctly calculate the thermodynamic power. An air-flow meter located at the turbine inlet should be considered.

The dynamometer water supply system as reported in [Ref. 2], should be redesigned as a closed-loop system in order to eliminate the supply pressure fluctuations at the higher turbine speeds. The dynamometer inlet water supply should be controlled by a regulator in order to maintain constant inlet pressure. The existing water tank scavenge

pump should be replaced with a variable speed pump. The water tank's level should be monitored using an electronic controller linked to the variable speed pump.

To improve the turbine speed-control response, the electronic control system should be operated as a Cascade Control described in [Ref. 19]. A cascade control system is one in which the output of a primary controller is used as a set point input to a secondary controller. The final control element is operated by the secondary controller output. In the cascade control setup, the PC-486 computer would be used as the primary controller and the Fischer & Porter electronic controller would be used as the secondary controller.

In order to traverse the turbine-exit throttle valve more smoothly, a dual actuator system should be incorporated and all guide rods installed.

The turbine-exit velocity profile was measured and successfully repeated over the course of five days of data collection. However, the large increase in swirl angle near the tip should be further investigated. Other velocity profiles should be measured at different circumferential positions in order to check for circumferential uniformity and/or flow periodicity. This may be accomplished by rotating the second-stage outer housing and cobra probe setup. The inlet velocity profile needs to be measured so that it may be used as input for flow simulation through the first-stage stator. Also, in order to obtain the required data for numerical flow simulation, the static pressure at the hub between the first-stage stator and rotor must be determined. The hub location is such that it is difficult

to drill static pressure ports due the close proximity of the rotor and the stator. An alternate position may be through the first-stage outer housing at the stator exit plane.

B. DATA ACQUISITION SYSTEM

The TTR sensors and measurement instrumentation have been interfaced to a personal computer for data acquisition. Also, software has been developed, using LabVIEW for Windows, in order to control the data acquisition system to collect TTR data via the various sensors, automatically display critical operating parameters and reduce the data for turbine performance plots.

The real-time display software should be modified to allow the data to be available to a plotter for real-time printout. Currently the program generates the real-time display on the TTR_TEST.VI's front panel only. Also, the latest version of LabVIEW for Windows and the LabVIEW PID Control Toolkit should be purchased and installed on the PC-486 computer. The updated version of LabVIEW for Windows includes additional programming icons and an advanced plotting capability. The PID Control Toolkit adds sophisticated control algorithms to LabVIEW. By combining the PID Control Toolkit with the mathematic and logic functions of LabVIEW, one can develop programs for automated control. This capability would be required to operate a dual throttle-valve actuator setup, water-tank level controller, and a cascade electronic turbine speed-control system as discussed above.

C. COMPUTATIONAL FLUID DYNAMICS

A working CFD model of the SSME HPFTP ATD first-stage stator and rotor has been developed, but more work is needed to accurately predict the flow field through the entire first-stage turbine. The measured inlet velocity profile should be used as input to RVC3D for the flow solution through the stator. The stator solution at the rotor inlet plane should then be mass averaged along each peripheral contour. The mass averaged stator solution should then be used as input to RVC3D for flow through the first stage rotor. The rotor solution at the cobra probe exit plane should then be mass averaged in the same manner as the stator solution. Also, in order to account for the increased swirl angles near the rotor tip, the tip gap needs to be included in the computational model for the rotor. The final solution at the turbine exit plane must then be converted to absolute quantities so that they can be compared to the measured results shown previously.

APPENDIX A. ENGINEERING DRAWINGS

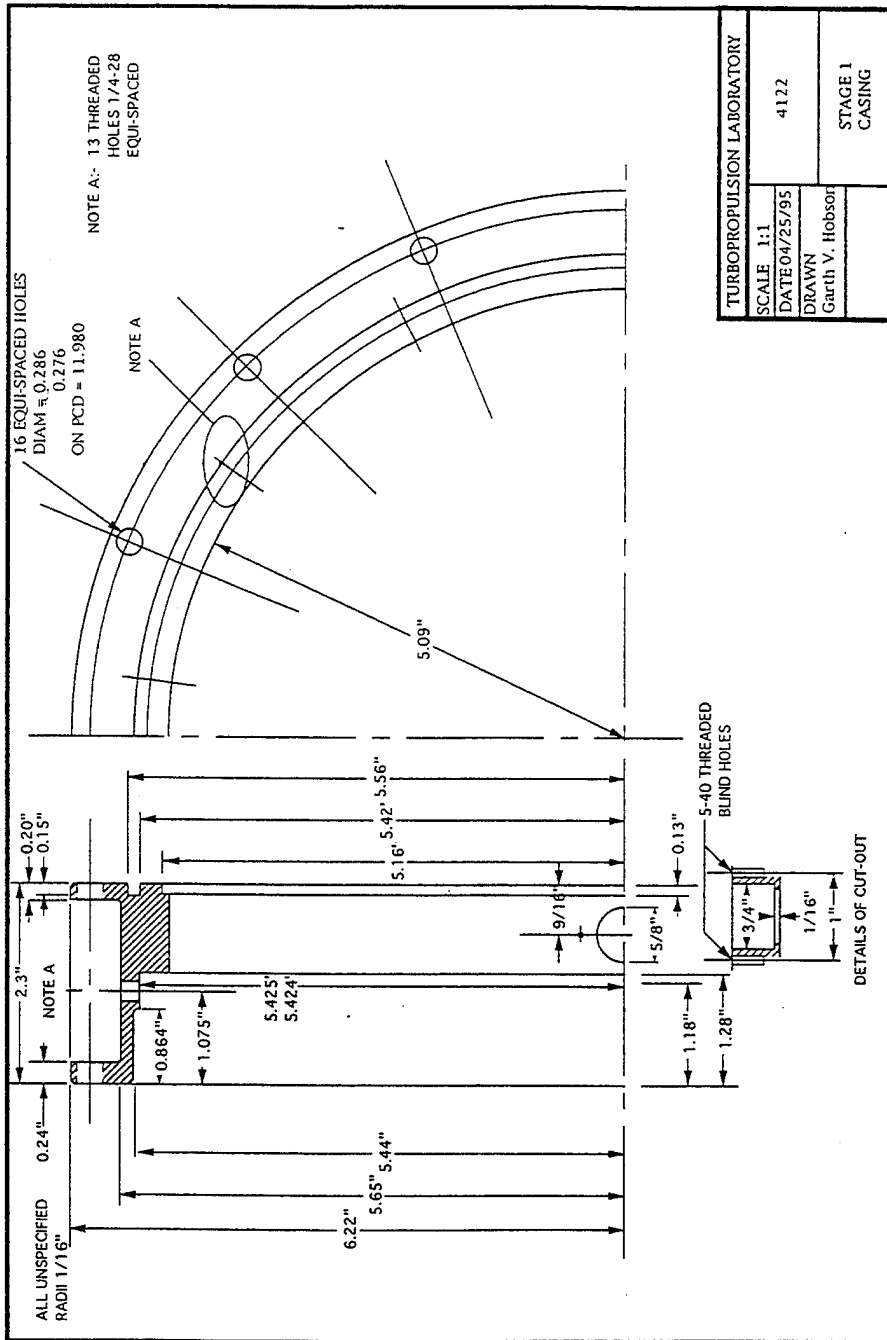


Figure A 1. Stage 1 Casing

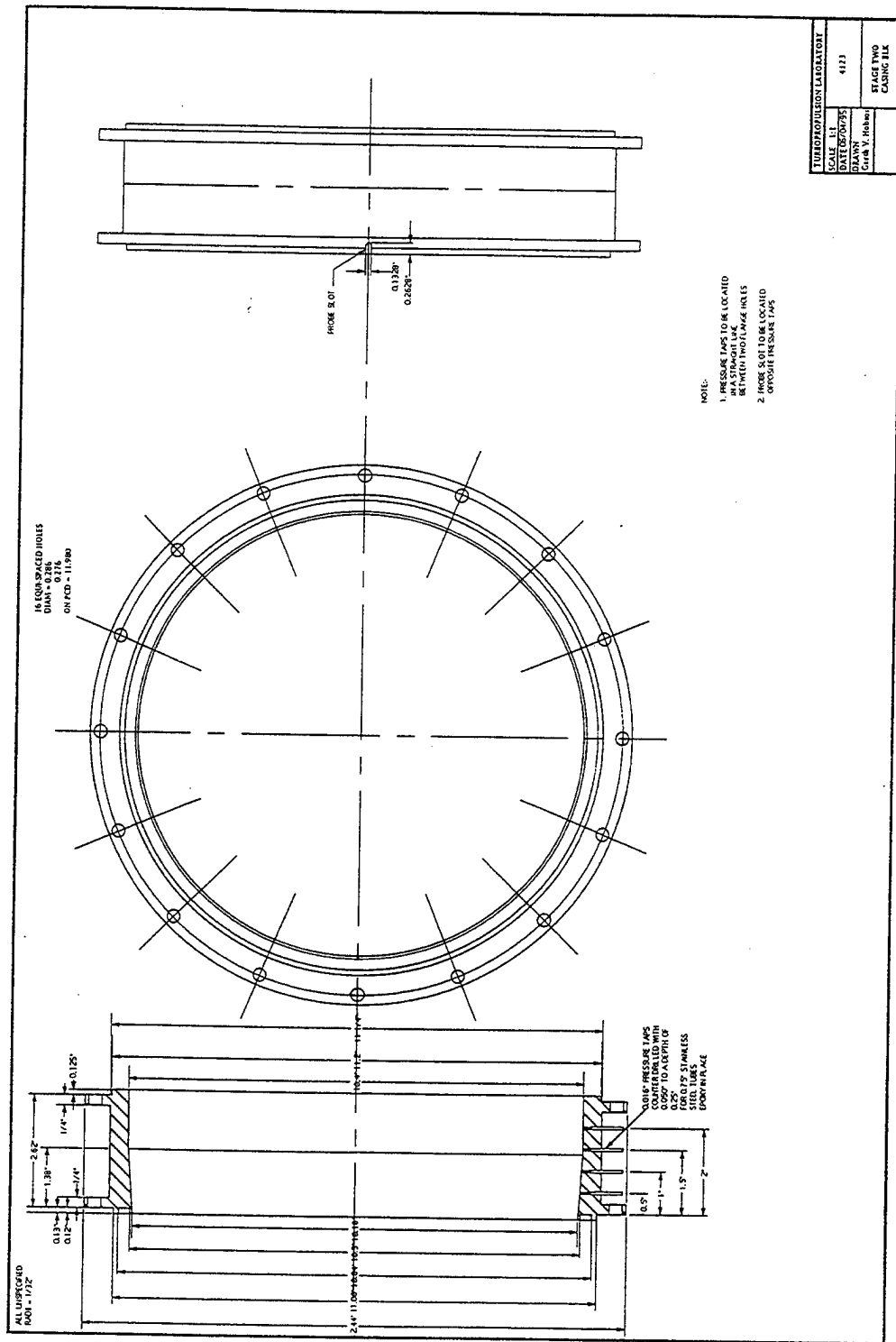


Figure A 2. Stage 2 Casing

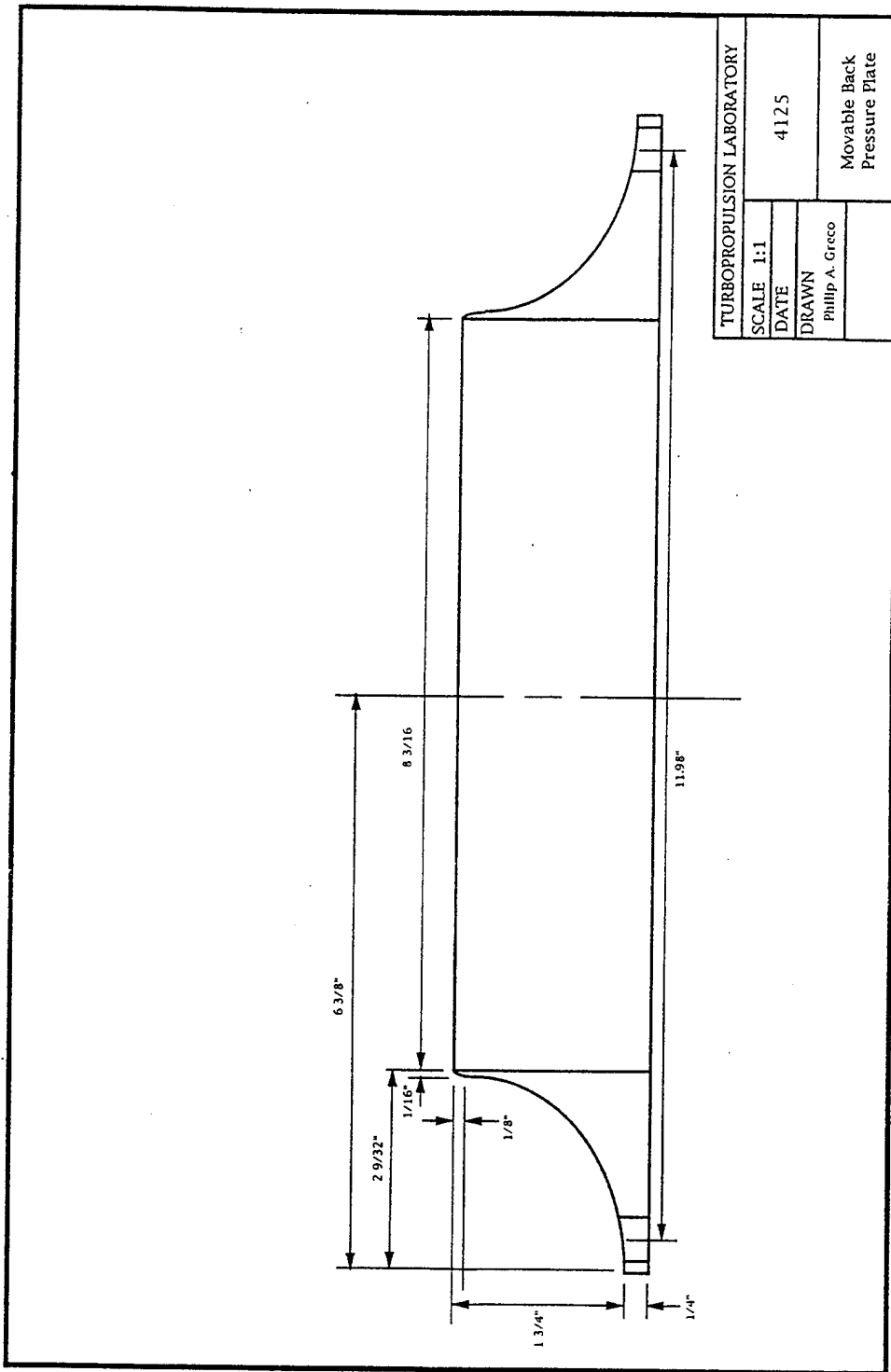


Figure A 4. Movable Back-Pressure Plate

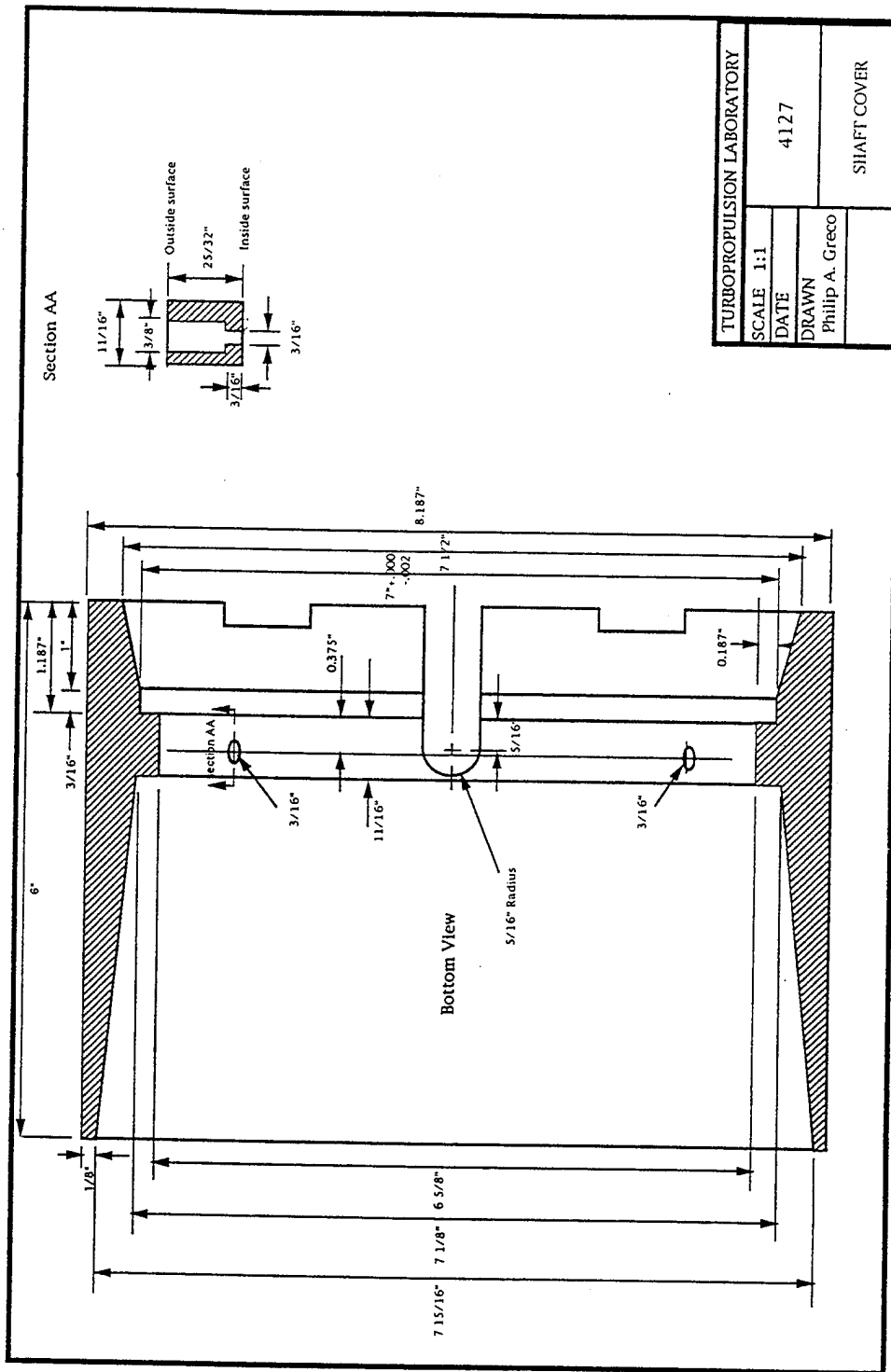
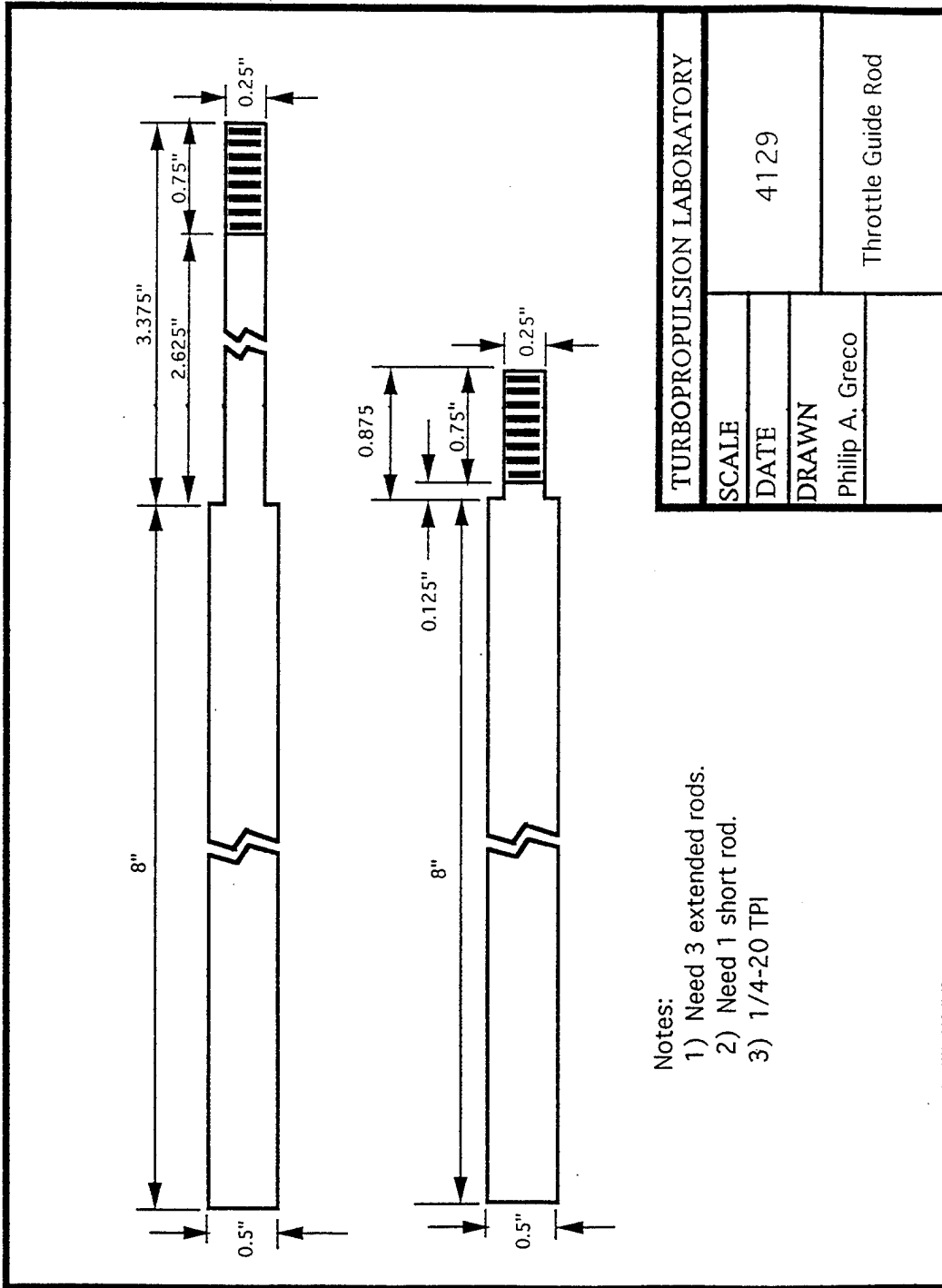


Figure A 5. Shaft Cover



- Notes:
- 1) Need 3 extended rods.
 - 2) Need 1 short rod.
 - 3) 1/4-20 TPI

Figure A 6. Throttle Guide Rod

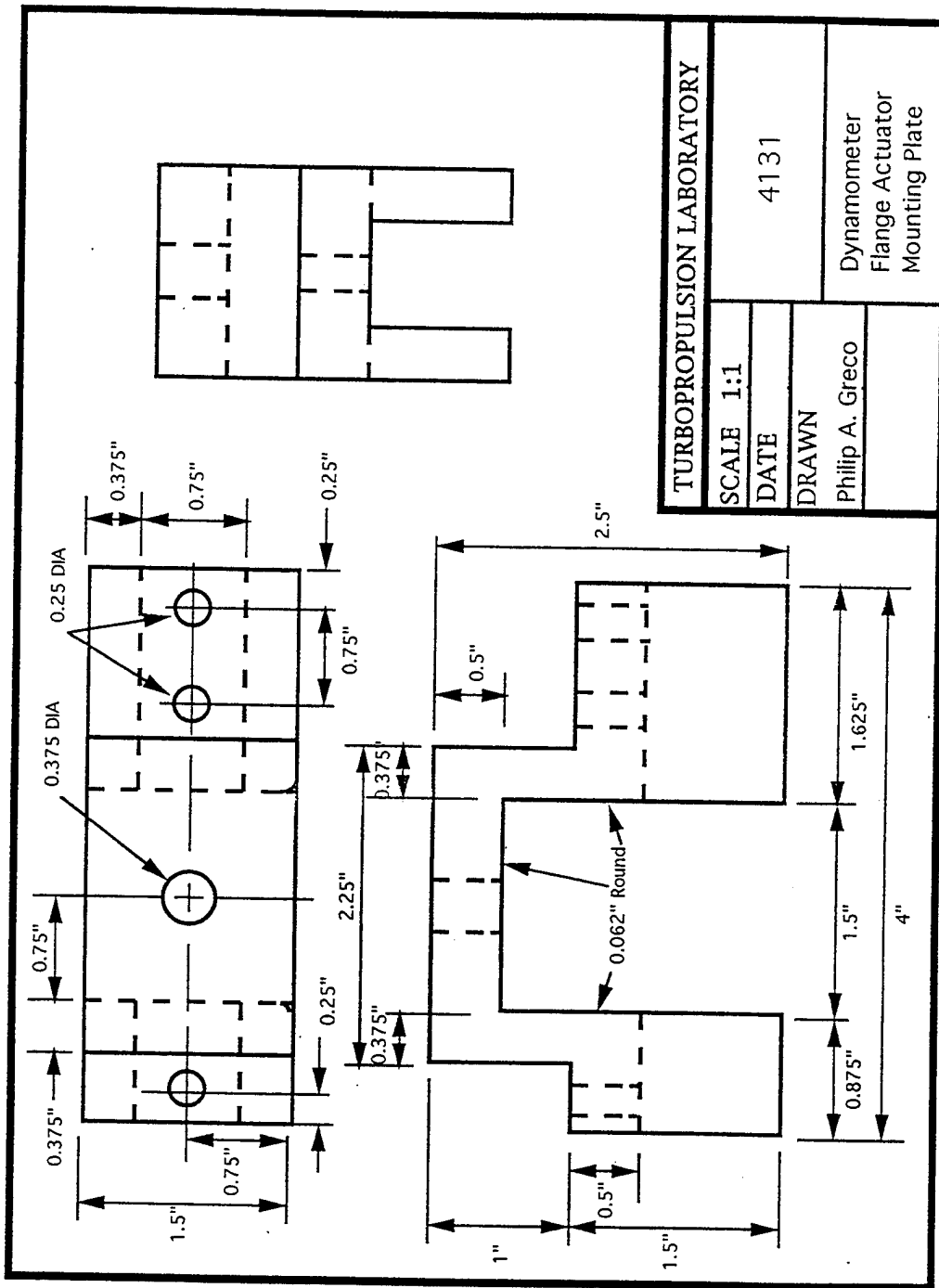


Figure A 7. Dynamometer Flange Actuator Mounting Plate

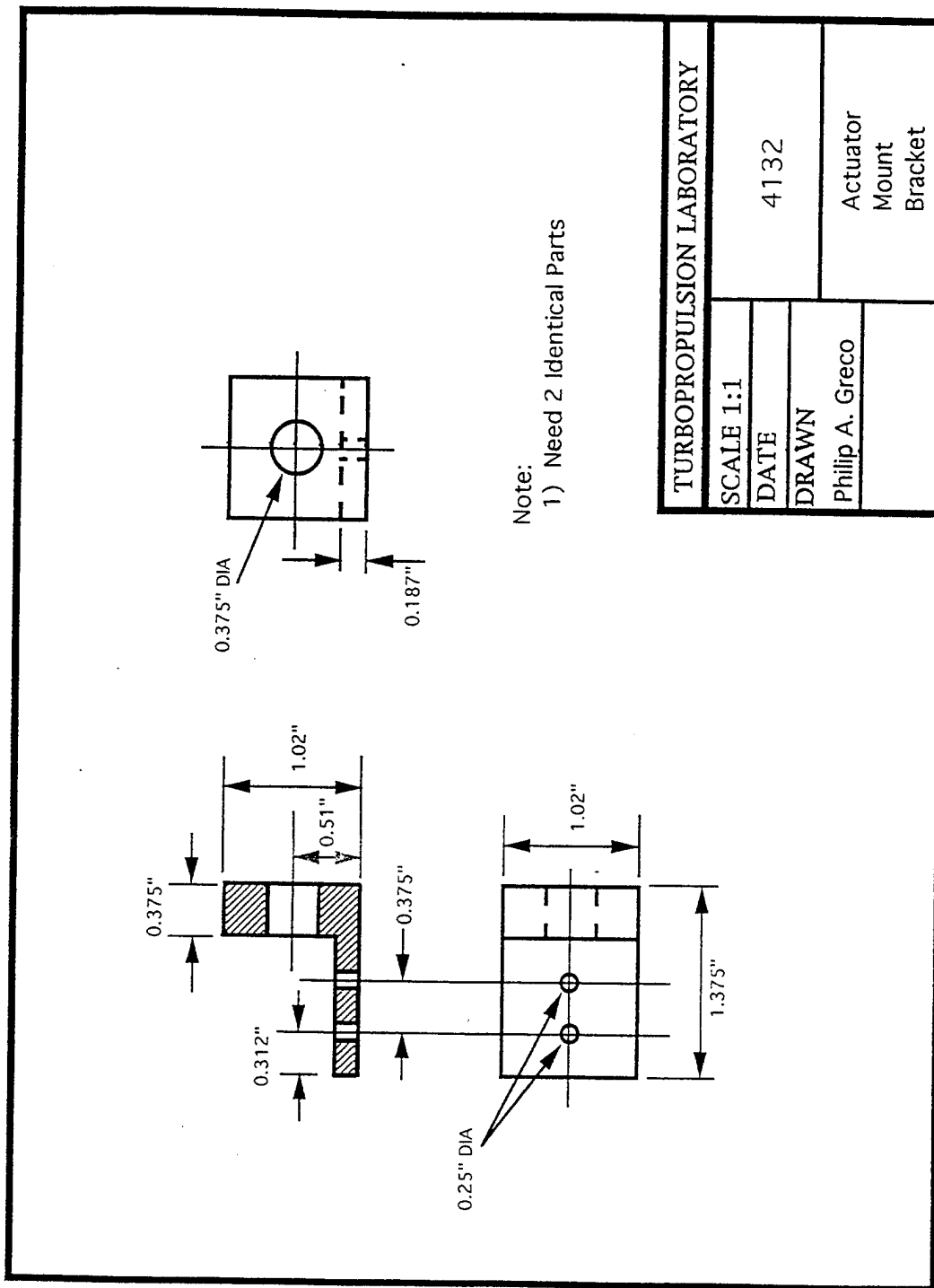


Figure A 8. Actuator Mounting Bracket

APPENDIX B. WIRING DIAGRAMS

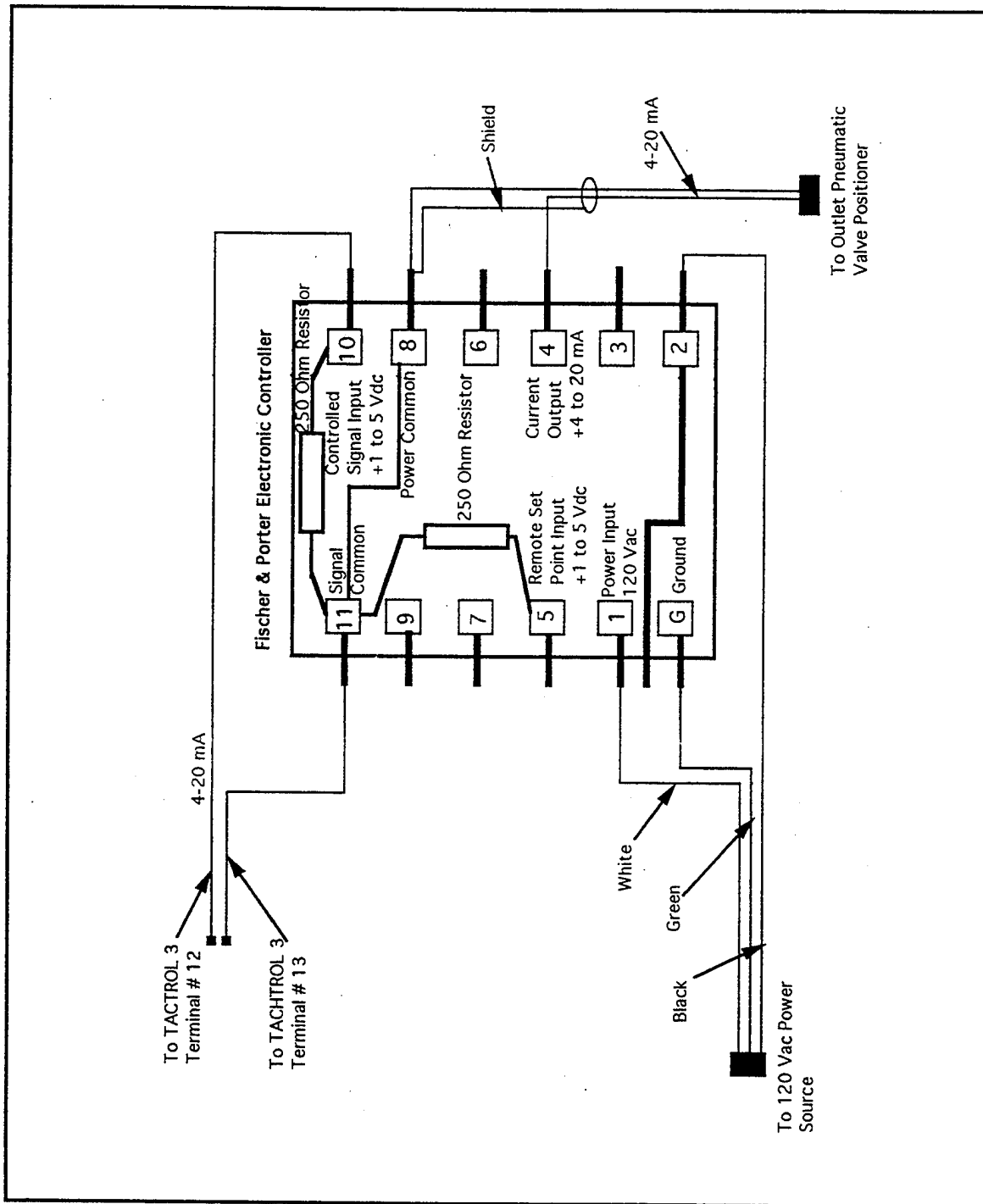


Figure B 1. Automatic Load-Control System Wiring Diagram

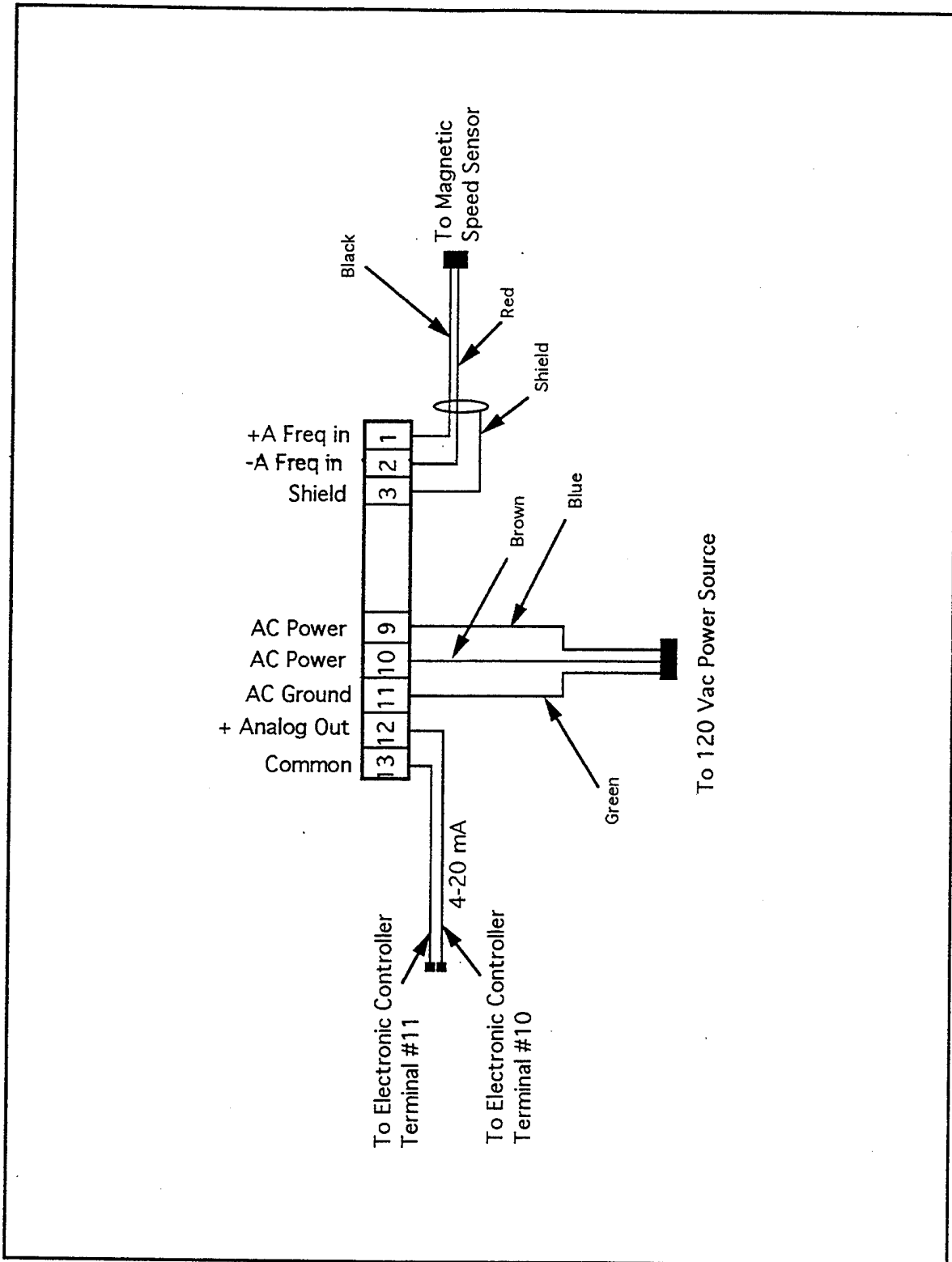


Figure B 2. AIRPAX TACHTROL 3 Terminal Bus Connections

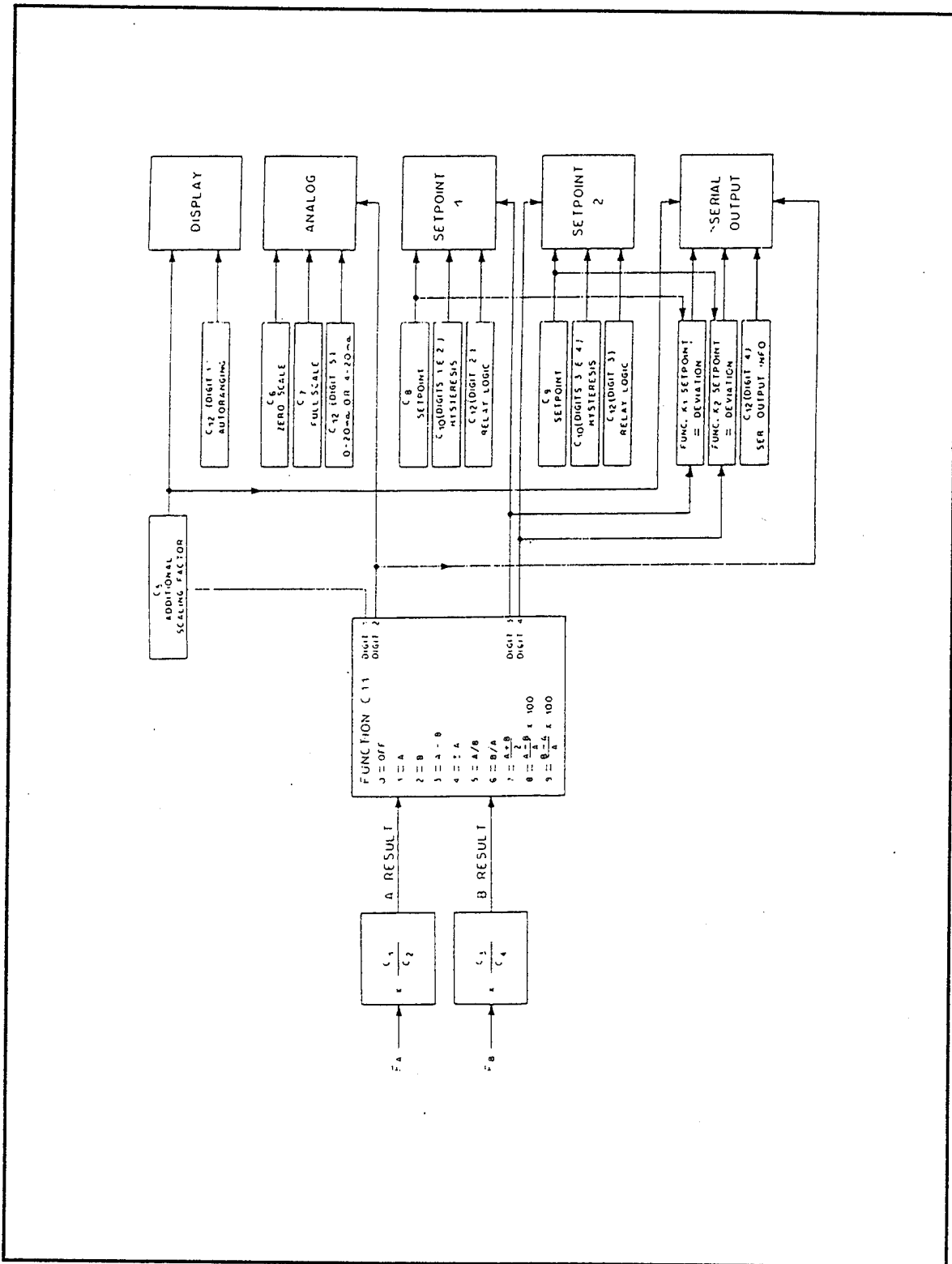


Figure B 4. AIRPAX TACHTROL 3 Flow Diagram

**APPENDIX C. SOFTWARE PROGRAMMING CODES & HARDWARE
DIP SWITCH SETTINGS**

Table C1. Address Settings

Device	Dip Switch (Binary Code)	Address
AT-GPIB/TNT	0 1 1 1 0	14
PC-DIO-24	0 1 0 0 0 1	34
PC-LPM-24	1 0 1 1 1	25
Scanner #1	1 0 0 0 0	1
Scanner #2	0 0 0 1 0	8
Universal Counter	1 0 1 0 0	5
Digital Voltmeter	0 1 1 0 1	22
SDIU	0 1 0 1 0	10

Table C2. AT-GPIB/TNT Board Settings

GPIB Board Setting	Dip Switch Setting
I/O Address	0 1 1 1 0
DMA Channel	5
Interrupt Line (IRQ)	11

Table C3. PC-DIO-24 Board Settings

DIO Board Setting	Dip Switch Setting
I/O Address	U2: 34
Interrupt Line	W1: PC4
Interrupt Level (IRQ)	W2: 4

Table C4. PC-LPM-16 Board Settings

Analog Board Setting	Dip Switch Setting
I/O address	U34: 1 1 0 0 1
Interrupt Level	W3: 5
Analog Input $\pm 5V$	W1: B:C W2: B:C

Table C5. HP 3456A DVM Program Codes

Parameter	Control	Program Code	VI Icon Code
Function	Shift Function Off	S0	-
	Shift Function On	S1	-
	DCV	SOF1	0
	ACV	SOF2	1
	ACV+DVC	SOF3	2
	2 Wire K Ohms	SOF4	3
	4 Wire K Ohms	SOF5	4
	DCV/DCV Ratio	S1F1	5
	ACV/DCV Ratio	S1F2	6
	ACV+DCV/DCV Ratio	S1F3	7
	O.C. 2 Wire K Ohms	S1F4	8
	O.C. 4 Wire K Ohms	S1F5	9
RANGE	Auto	R1	0
	100 mV or .1 K Ohms	R2	1
	1000 mV or 1 K Ohms	R3	2
	10 V or 10 K Ohms	R4	3
	100 V or 100 K Ohms	R5	4
	1000 V or 1 M Ohms	R6	5
	10 M Ohms	R7	6
	100 M Ohms	R8	7
	1000 M Ohms	R9	8

Table C6. HP Universal Counter Device Commands

Parameter	Control	Program Code	VI Icon Code
Statistic	Disable Mean	SM0	False
	Enable Mean	SM1	True
Input Slope A	Slope A Positive	AS0	True
	Slope A Negative	AS1	False
Input Slope B	Slope B Positive	BS0	True
	Slope B Negative	BS1	False
Filter	Filter A Off	AF0	False
	Filter A On	AF1	True
	Filter B Off	BF0	False
	Filter B On	BF1	True
AC	Set A to DC	AA0	False
	Set A to AC	AA1	True
	Set B to DC	BA0	False
	Set B to AC	BA1	True
Z=50Ω	Set A Z to 1MΩ	AZ0	False
	Set A Z to 50Ω	AZ1	True
	Set B Z to 1MΩ	BZ0	False
	Set B Z to 50Ω	BZ1	True
X10 ATTN	Set ATTN A to X1	AX0	False
	Set ATTN A to X10	AX1	True
	Set ATTN B to X1	BX0	False
	Set ATTN B to X10	BX1	True
COM A	Set COM A Off	CO0	False
	Set COM A On	CO1	True
Function	FREQ A	FN1	0
	TIME A→B	FN2	1
	RATIO A/B	FN4	2
	FREQ C	FN5	3
	1/TIME A→B	FN6	4
	PULSE A	FN7	5
	RATIO C/A	FN8	6
	PER A	FN9	7
	RISE/FALL A	FN10	8
	DUTY CY A	FN12	9
	FREQ B	FN17	10

Table C7. SDIU Commands

Definition	Description	Format/Result	Available Value's
Data Acquisition:		AD Rate,Port,Count	AD
Rate	Acquisition Rate	Ports/sec	1,2,3,4,5,6, or 7
Port	Scanivalve Port Commands	Step Advance Home	-1 Scanivalve Port # 0
Count	Data Acquisition Commands	Continuous Data Collection Stop Data Collection Number of Samples	-1 0 1,2, or 3
Output single Channel Data		OC module	OC
module	Information Source	A/D Card #1	0
Turn Around Delay		TD delay	TD
	Time Delay	Delay	Time in ms
Enable SRQ	Request Service after each Reading		TS1
System Reset	Resets SDIU		RS
Local/Remote Mode	Puts SDIU in Remote Mode		RL1

Table C8. TACHROL 3 Constant Settings

Constant	Value	Constant	Value	Constant	Value
C1	2	C5	1	C9	9000
C2	1	C6	0	C10	00500
C3	1	C7	10000	C11	01111
C4	1	C8	0	C12	00011

Table C9. Cantilever Beam and Weight Set-up

	Moment Arm (ft)	Weight (lbs)	Torque (ft-lbs)
Cantilever Beam	2.167	2.97	6.436
Weights	3.917	14.01	54.877
Total			61.312

Table C10. Electronic Controller Settings

Perimeter	Setting
Derivative Minutes	.01
P.B.	25
Reset Minutes	.24

APPENDIX D. 50 PIN CONNECTOR ASSIGNMENTS

PC7	1	2	GND
PC6	3	4	GND
PC5	5	6	GND
PC4	7	8	GND
PC3	9	10	GND
PC2	11	12	GND
PC1	13	14	GND
PC0	15	16	GND
PB7	17	18	GND
PB6	19	20	GND
PB5	21	22	GND
PB4	23	24	GND
PB3	25	26	GND
PB2	27	28	GND
PB1	29	30	GND
PB0	31	32	GND
PA7	33	34	GND
PA6	35	36	GND
PA5	37	38	GND
PA4	39	40	GND
PA3	41	42	GND
PA2	43	44	GND
PA1	45	46	GND
PA0	47	48	GND
+5V	49	50	GND

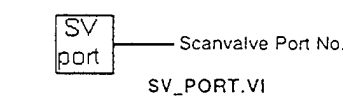
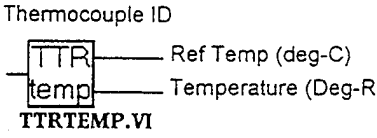
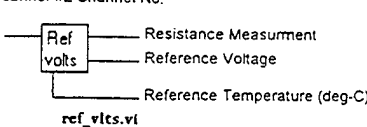
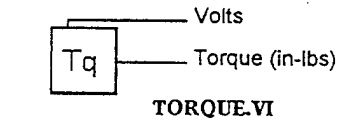
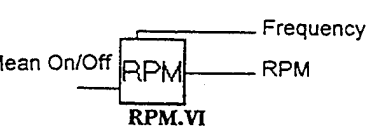
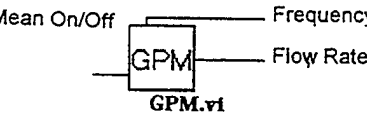
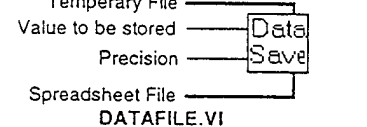
Figure D 1. PC-DIO-24 50 Pin Connector Assignments

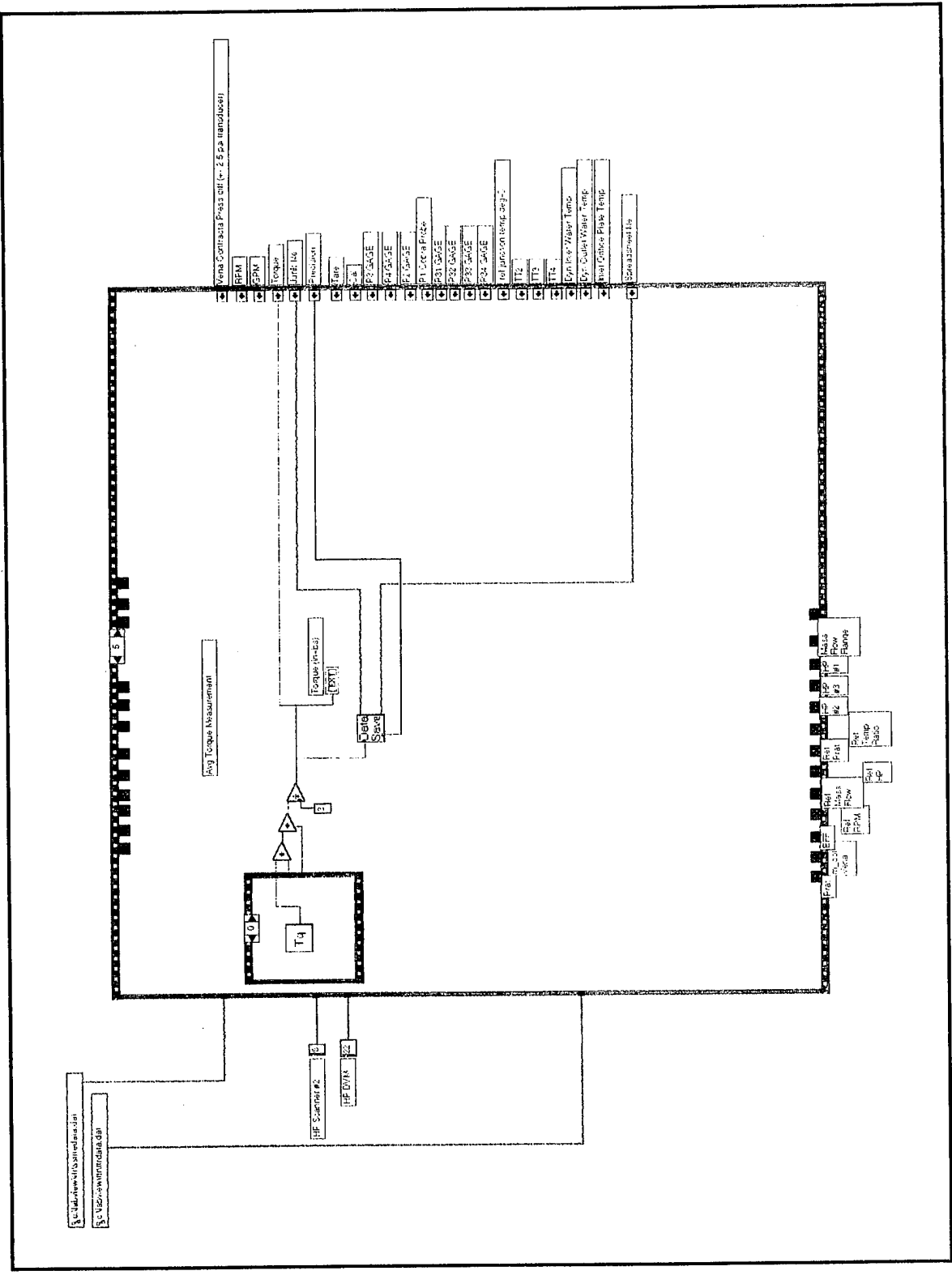
AIGND	1	2	AIGND
ACH0	3	4	ACH8
ACH1	5	6	ACH9
ACH2	7	8	ACH10
ACH3	9	10	ACH11
ACH4	11	12	ACH12
ACH5	13	14	ACH13
ACH6	15	16	ACH14
ACH7	17	18	ACH15
DGND	19	20	-12 V
+12 V	21	22	DIN0
DIN1	23	24	DIN2
DIN3	25	26	DIN4
DIN5	27	28	DIN6
DIN7	29	30	DOUT0
DOUT1	31	32	DOUT2
DOUT3	33	34	DOUT4
DOUT5	35	36	DOUT6
DOUT7	37	38	OUT1*
EXTINT*	39	40	EXTCONV*
OUT0	41	42	GATE0
OUT1	43	44	GATE1
CLK1	45	46	OUT2
GATE2	47	48	CLK2
+5 V	49	50	DGND

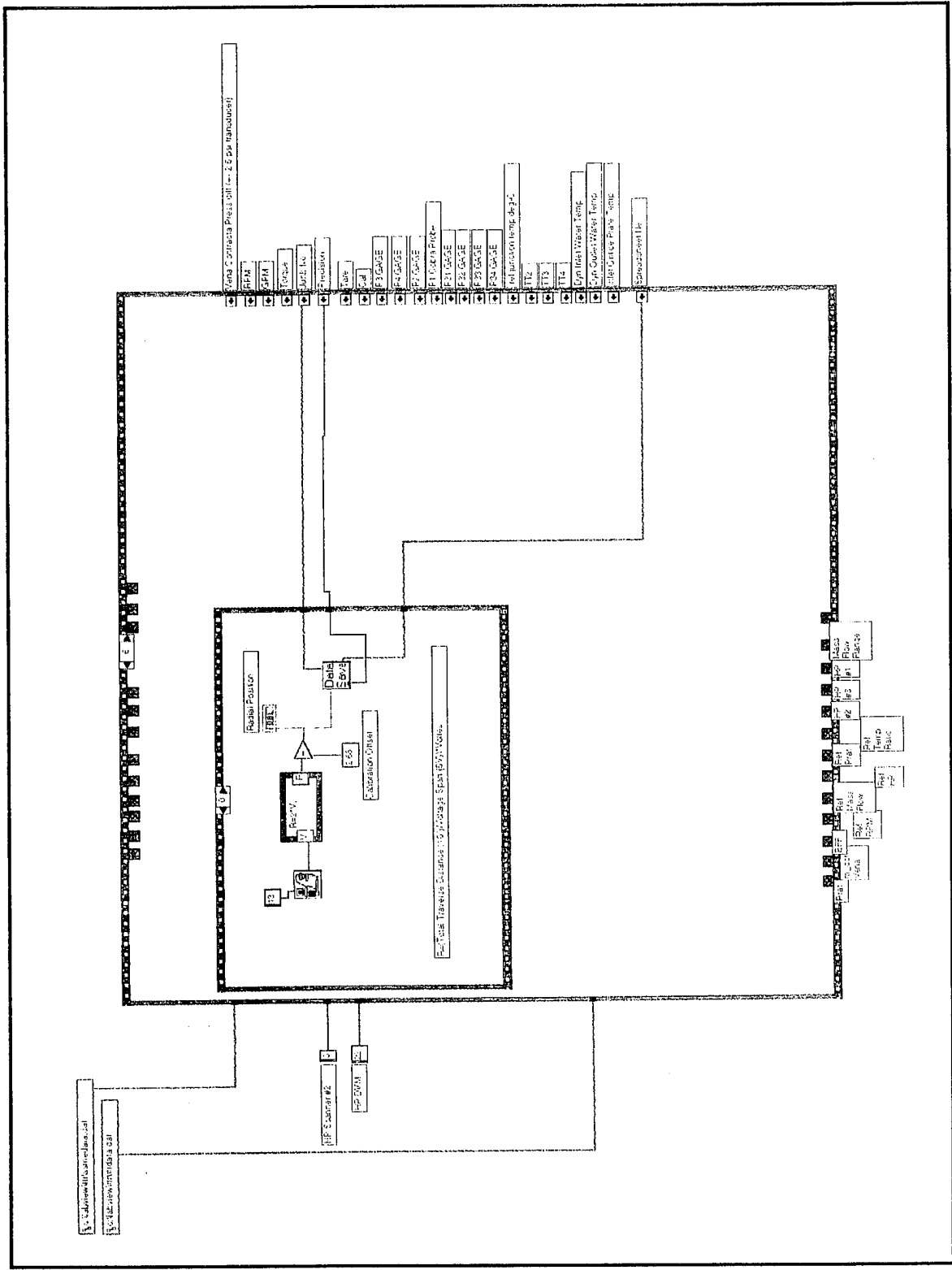
Figure D 2. PC-LPM-16 50 Pin Connector Assignments

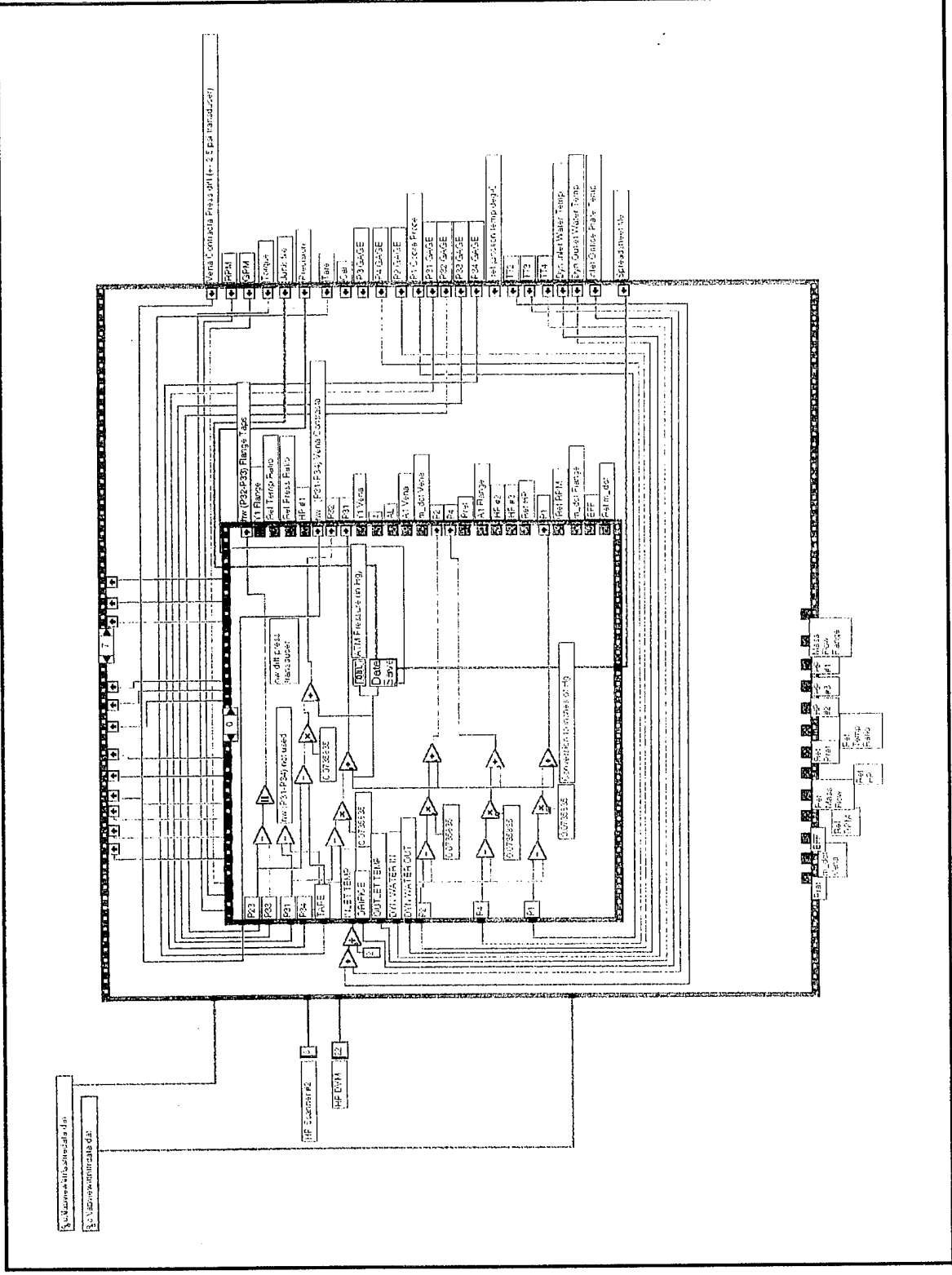
APPENDIX E. LabVIEW VISUAL INSTRUMENT FUNCTIONS

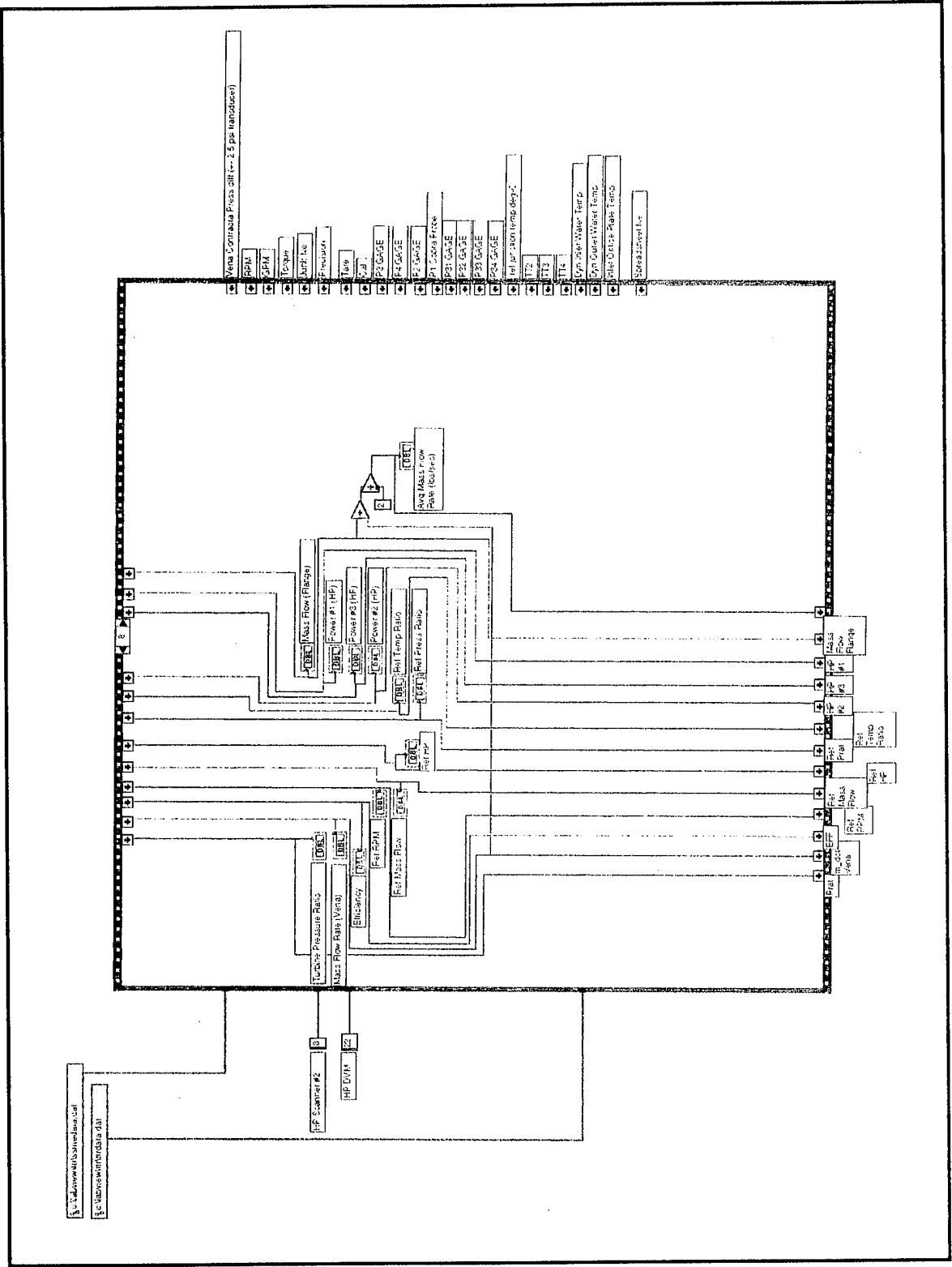
Table E 1. Description of Sub_VI's

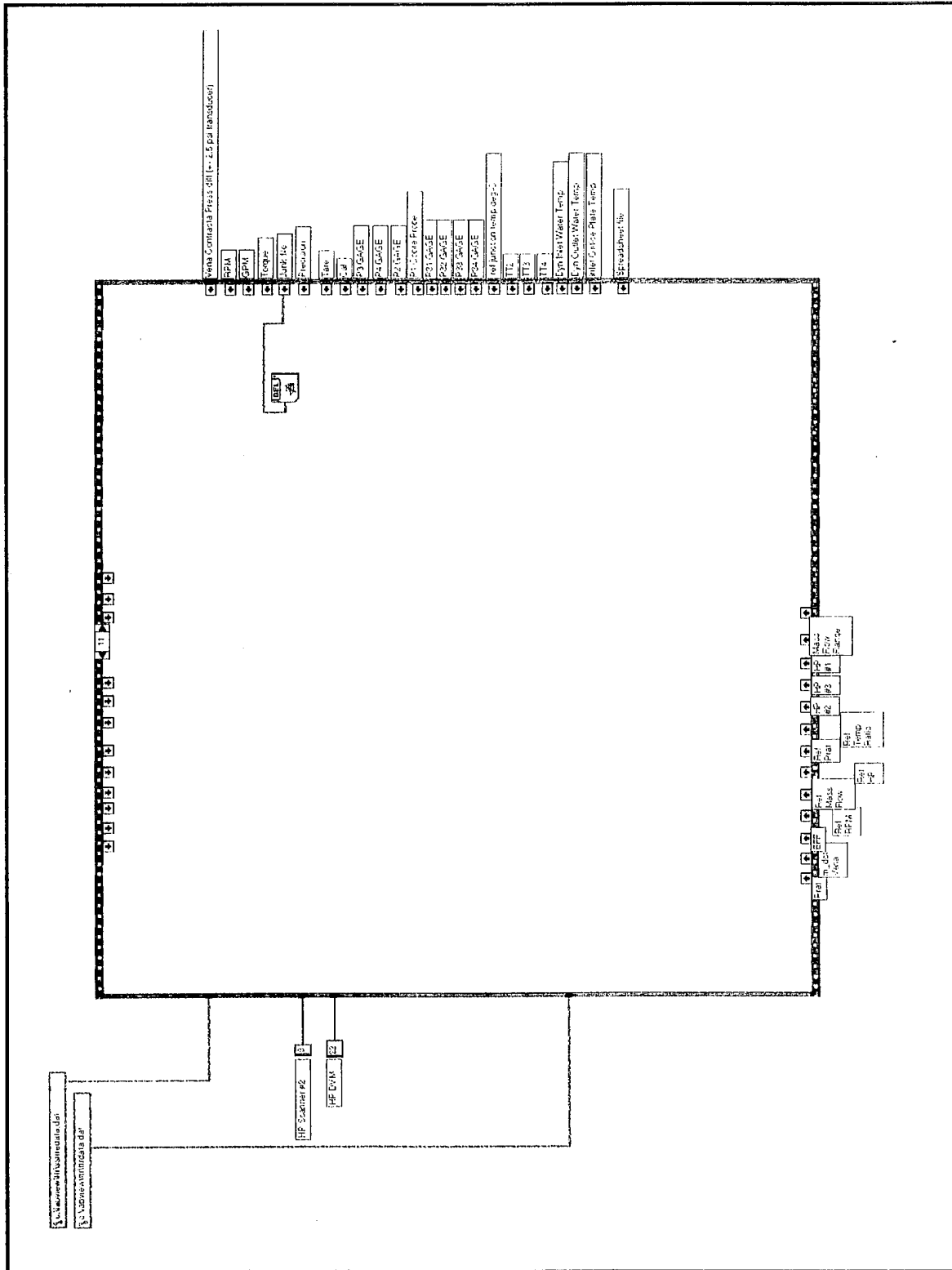
VI Name	VI Icon/Connector	Description/Function
SV_PORT.VI		<p>This VI is used to at the beginning of the pressure data collection in Frame 0 of SSME_TTR.VI. The function of SV_PORT.VI is to determine if the Scanivalve is on port #1, if it is, data collection is started at port #1. If it is not, the Scanivalve is advanced to port #1 where data collection begins.</p>
TTRTEMP.VI		<p>This VI is used in Frame #2 of SSME_TTR.VI to connect scanner #2 channels 60-66 to the DVM for reference temperature and thermocouple voltage measurements. The voltage measurements are then converted to stagnation temperature in $^{\circ}R$ using the procedure outlined in section V.A.</p>
REF_VLTS.VI		<p>This VI is used in TTRTEMP.VI as a sub_VI. The VI's function is to determine the resistance at the reference junction (channel 60) in order to calculate the reference junction temperature using Equation 1 listed in section V.A.</p>
TORQUE.VI		<p>This VI is used in Frame 5 to connect scanner #2 channel #33 to the DVM for voltage measurement from the Lebow Load Cell. The voltage information is then converted to torque using the calibration curve fit equation shown in Figure 16.</p>
RPM.VI		<p>This VI is used in Frame 3 to measure the frequency signal from the magnetic speed pick-up which is located over a 30 toothed gear. The sensor is connected to the HP universal counters front panel channel A. The frequency information is multiplied by 2 to convert it to RPM.</p>
GPM.VI		<p>This VI is used in Frame 4 to measure the frequency signal from the Cox flowmeter which is connected to the HP universal counters front panel channel B. The frequency information is then converted to GPM using the calibration equation shown in Figure 17.</p>
POSITION.VI		<p>This VI is used in ACTUATOR.VI as a sub_VI and in Frame #6 of SSME_TTR.VI. POSITION.VI measures the linear potentiometer voltages from channels 13, 14, and 15 via the PC-LPM-16 A/D board.</p>
DATAFILE.VI		<p>This VI is used to store TTR measured and reduced data to two different files. One file is in spreadsheet form which is use in M.S. Excel for plotting. The other file is a temporary file which is deleted at the completion of data collection and reduction.</p>











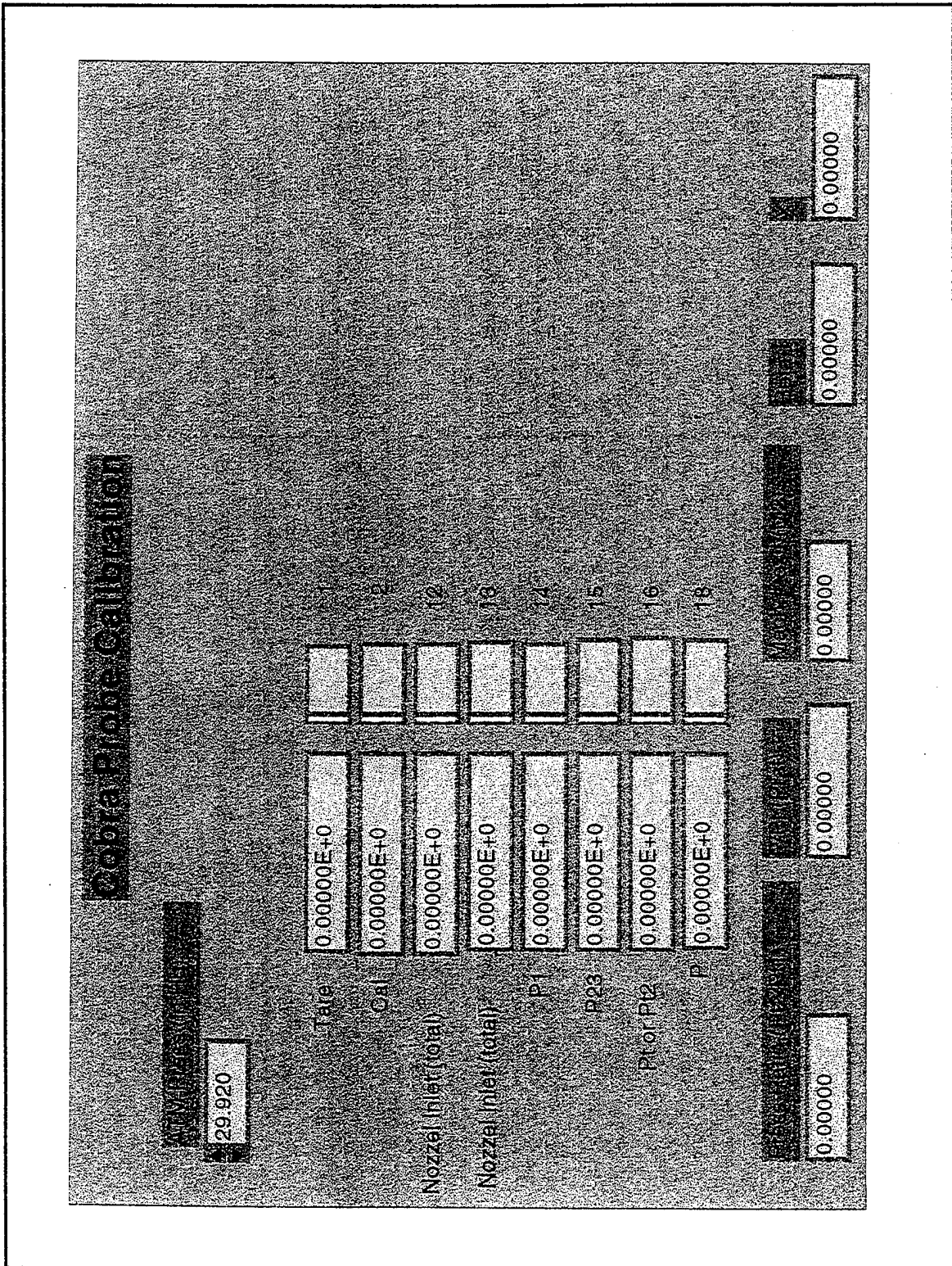


Figure F 2. COBR_CAL.VI Front Panel

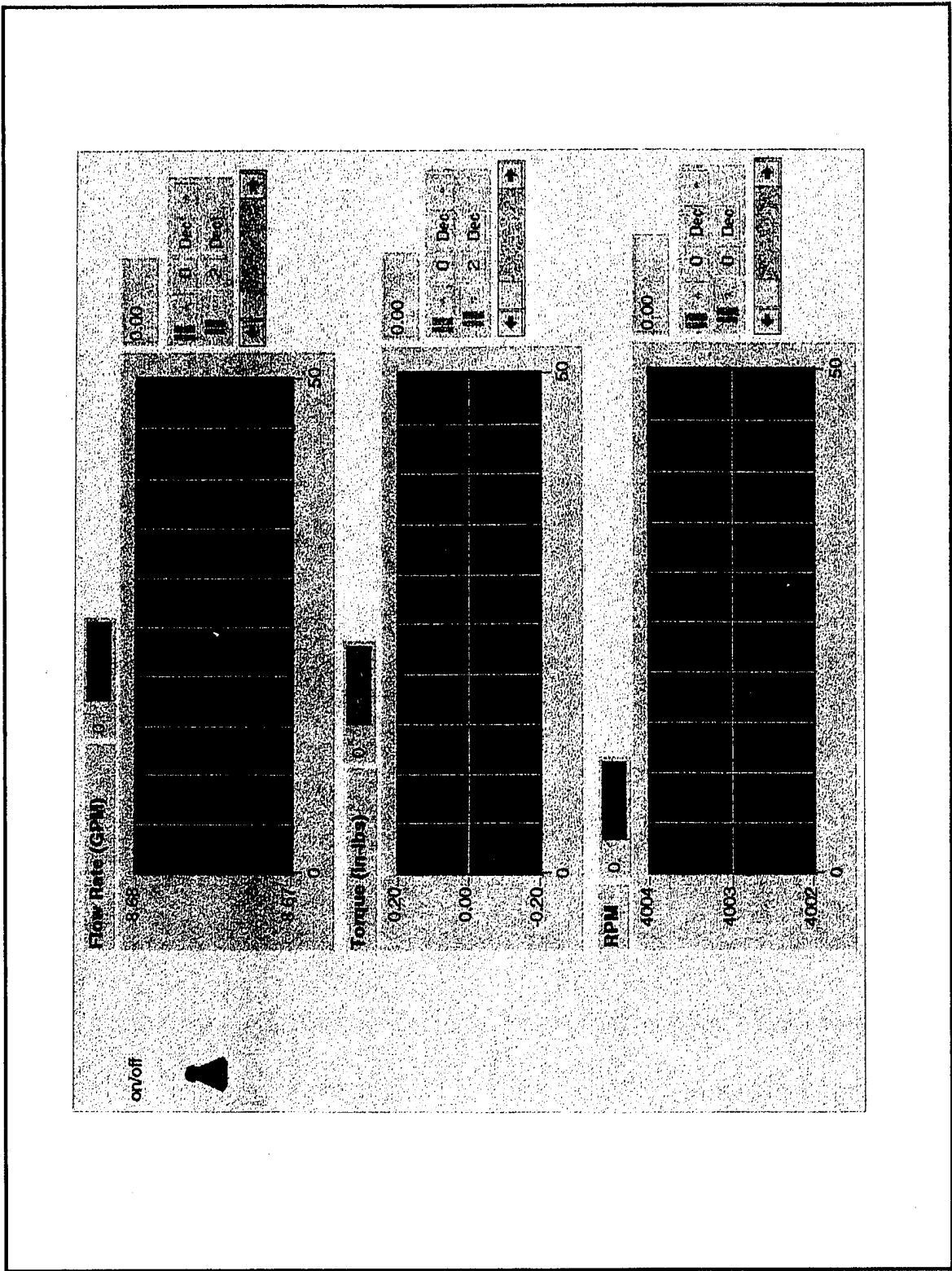
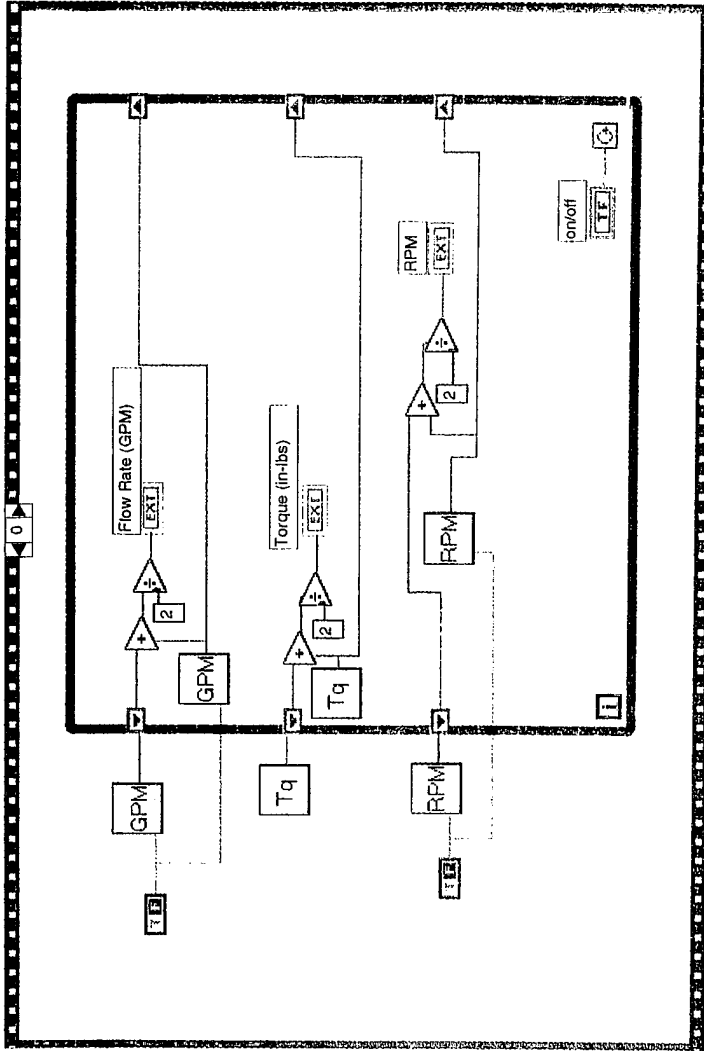
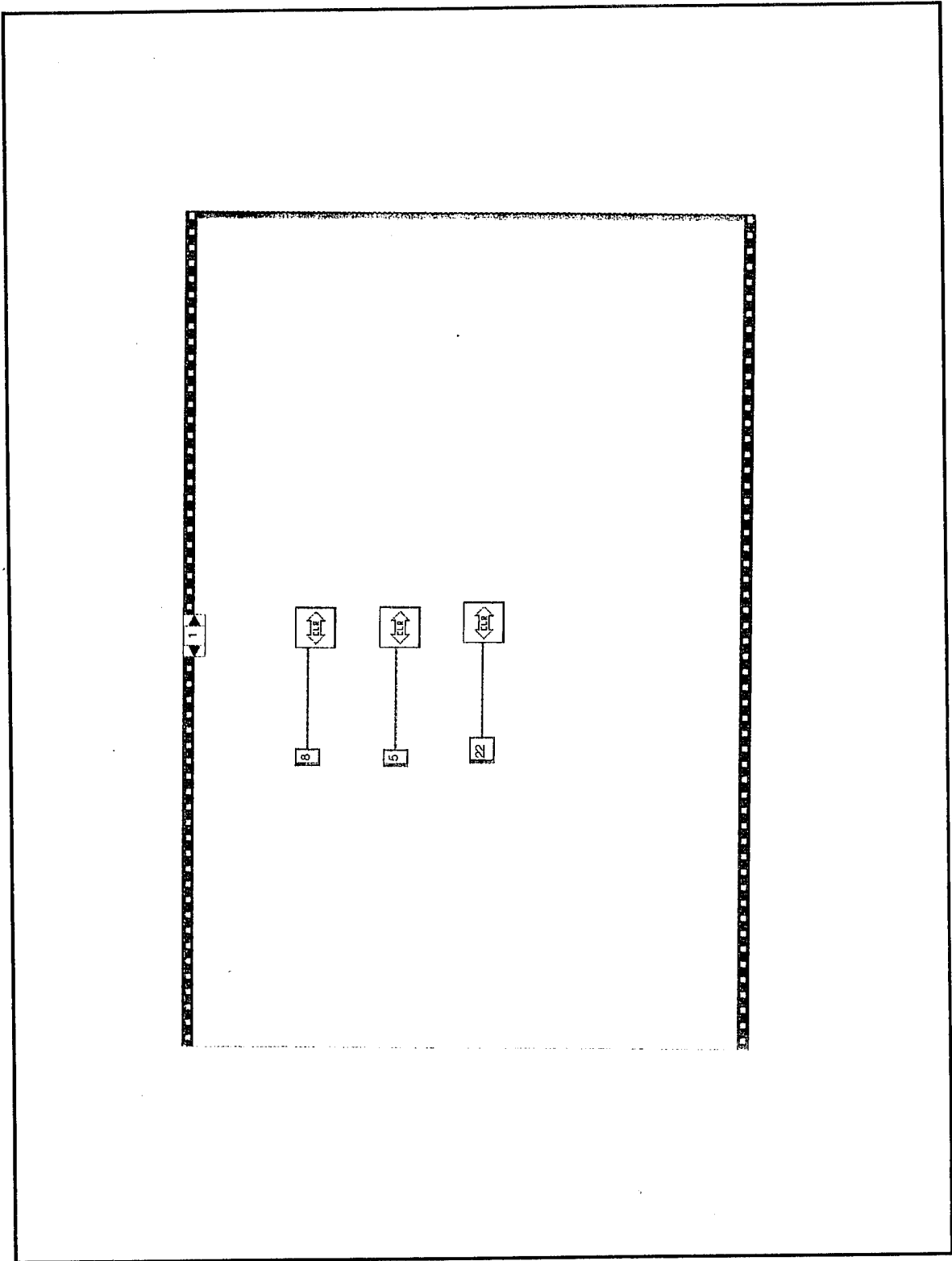


Figure F 3. TTR_TEST.VI Front Panel and Block Diagram





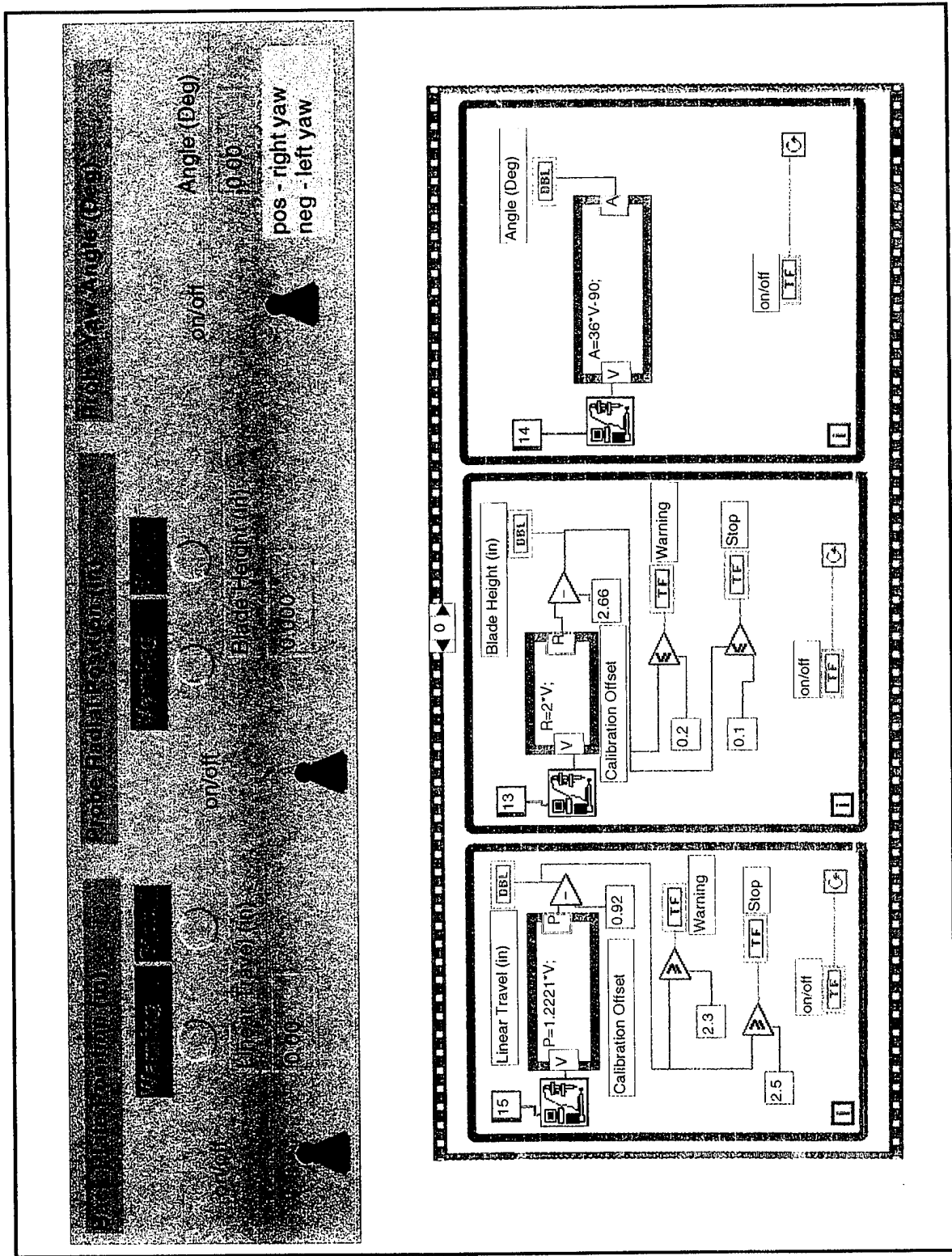


Figure F 4. ACTUATOR.VI Front Panel and Block Diagram

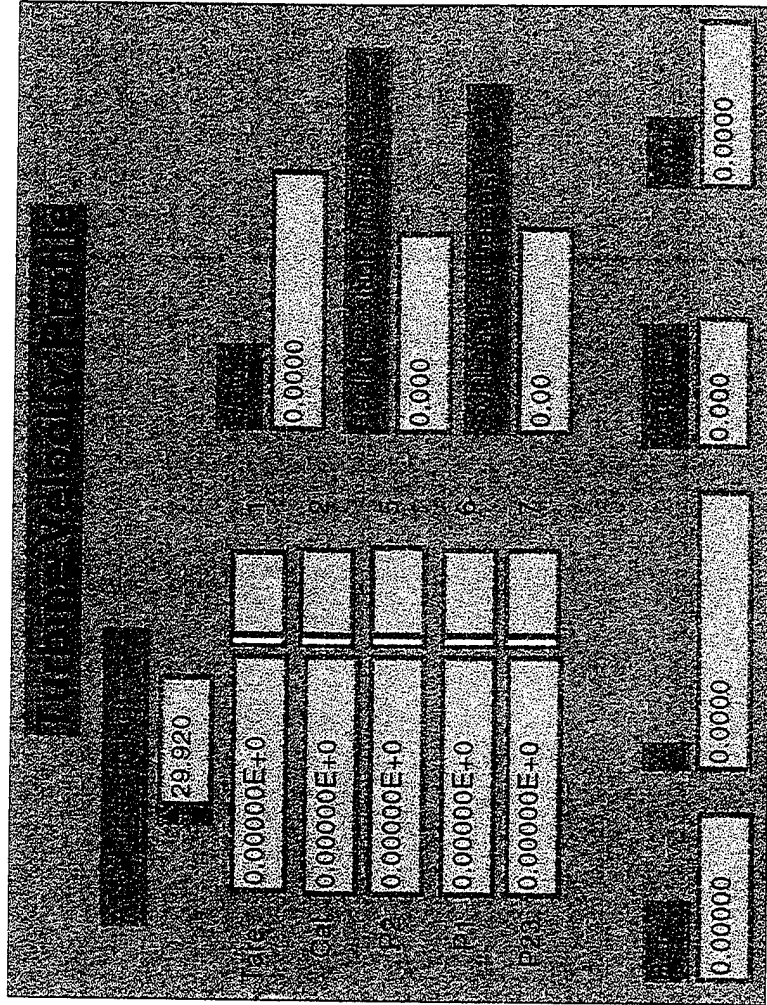


Figure F 5. VEL_PRFL.VI Front Panel

APPENDIX G. COBRA PROBE CALIBRATION

The following set of equations from [Ref. 18] were used in the cobra probe calibration data acquisition program PROBE CAL.VI. PROBE CAL.VI is a LabVIEW program used to collect pressure information outlined in Figure 18.

$$\frac{P}{P_t} = \left[1 + \frac{\gamma-1}{2} M^2 \right]^{-\left(\frac{\gamma}{\gamma-1}\right)}$$

The stagnation pressure (P_t) and static pressure (P) were measured from the pitot static probe connected to Scanivalve port #16 and 18, respectively. The Mach number was then determined and used to calculate the dimensionless velocity X .

$$X = \sqrt{\frac{\frac{\gamma-1}{2} M^2}{1 + \frac{\gamma-1}{2} M^2}}$$

The dimensionless pressure coefficient β was determined by measuring the cobra probe pressures P_1 and P_{23} shown in Figure 18. P_{23} was the left and right cobra probe pressure with the probe aligned in yaw ($P_2=P_3$).

$$\beta = \frac{P_1 - P_{23}}{P_1}$$

Dimensionless velocity X was plotted vs. dimensionless pressure coefficient β and is shown in Figure G1. The sixth order curve fit equation is:

$$X = a_0 + a_1\beta + a_2\beta^2 + a_3\beta^3 + a_4\beta^4 + a_5\beta^5 + a_6\beta^6$$

where:

$$a_0 = 0.0662$$

$$a_1 = 0.8443$$

$$a_2 = 83.74$$

$$a_3 = -1962$$

$$a_4 = 19342$$

$$a_5 = -87713$$

$$a_6 = 150585$$

The sixth order curve fit equation for X was used in the LabVIEW data acquisition program VELPRFL.VI. in order to determine the Mach number M .

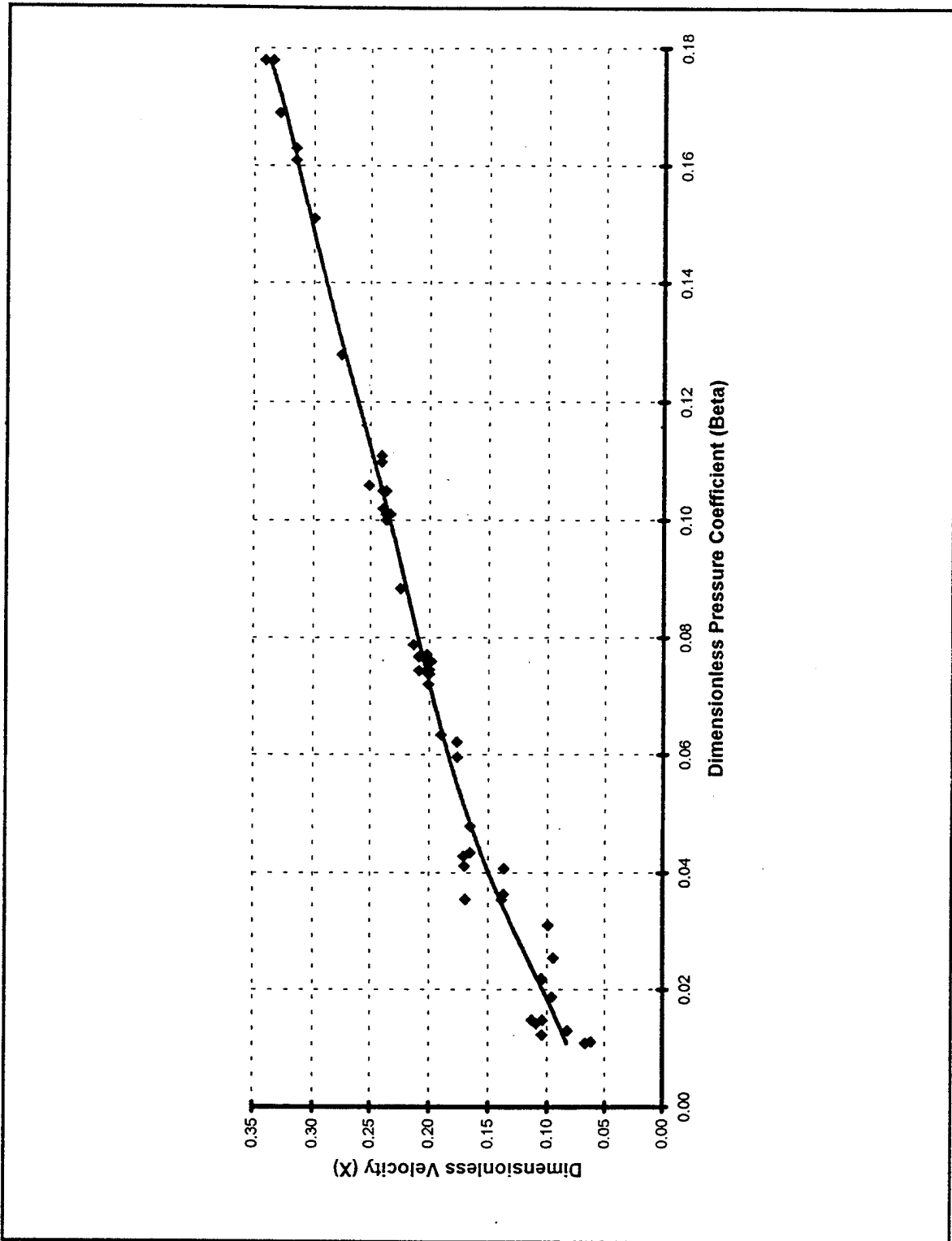


Figure G 1. Cobra Probe Calibration

**APPENDIX H. TTR PRE-OPERATIONS CHECKLIST and DATA
COLLECTION SHEET**

TTR Pre-Operation Check List

- 1) Check shop air:
 - a) compressor on
 - b) bleed off moisture in tank
 - c) check connection valve
- 2) Set air at 20 psi on inlet water valve to Dynamometer
- 3) Shop air in test cell "ON" - check Dyno inlet valve closed
- 4) Check all movable probes in the full out position
- 5) Check full traverse of throttle actuator and integrity of lock nut
- 6) Set oil mist regulator to 30 psi
- 7) Check dynamometer water seal valve full open
- 8) Open water supply in A/C room (red valve)
- 9) Outlet valve green in A/C room open to 110 psi (1/2 turn)
- 10) Scavenge pump in TTR cell "ON"
- 11) Inlet valve to Dynamometer control valve to 0 psi (down from 18 psi)
- 12) Start scavenge pump by dropping leftmost level switch and then adjust outlet green valve in A/C room to stabilize float (align black tapes). Pressure should be between 105 and 120 psi.
- 13) Check "pop-off" valve in bldg. 216
- 14) Lock outside gate
- 15) Check speed read out
- 16) Check pressure lines activated, manifold (#1 TTR, #2, 3, 4, A/C)
- 17) Check TTR outlet water temperature is reading out
- 18) Check both dump valves open
- 19) Dynamometer outlet valve to 50%
- 18) Bleed off air before plenum in TTR cell.
- 20) Open manual valve before plenum in TTR cell.
- 21) Set number 5 valve to 20% (~ 1000 rpm)
- 22) Close dump valve 2 (~ 1500 rpm - now mass flow rate measurement is good)
- 23) Set combination valve to 50% (~ 3000 rpm)

Figure H 1. TTR Pre-Operation Checklist

APPENDIX I. SSME HPFTP ATD PERFORMANCE EQUATIONS

The first stage thermodynamic turbine efficiency was calculated using Equation 5 from [Ref. 20].

$$\eta_t = \left(\frac{T_{t3} - T_{t4}}{T_{t3}} \right) \left[\frac{1}{1 - \left(\frac{1}{P_{rat}^{\frac{\gamma-1}{\gamma}}} \right)} \right]$$

where:

- T_{t3} = Turbine Inlet Total Temperature
- T_{t4} = Turbine Outlet Total Temperature
- P_{rat} = Total-to-Total Pressure Ratio

The horsepower developed by the SSME HPFTP ATD was calculated using three different methods. The first method used the measured and calculated thermodynamic parameters.

$$HP\#1 = \frac{\left(\frac{778.2}{550} \right) (\dot{m}) (C_p) (\eta_t) (T_{t3}) \left[P_{rat}^{\left(\frac{\gamma-1}{\gamma} \right)} - 1 \right]}{P_{rat}^{\left(\frac{\gamma-1}{\gamma} \right)}}$$

The second method was determined from the power absorbed from the dynamometer. The equation was given in [Ref. 22]. The flow rate was determined from the Cox flow meter using the calibration data in Figure 17.

$$HP\#2 = \frac{Q(T_2 - T_1)}{5.09}$$

where:

- Q = Water Flow Rate in GPM
- T_1 = Water Inlet Temperature in °F
- T_2 = Water Outlet Temperature in °F

The third method used the mechanical measured quantities of torque and rotational speed. The torque was determined by measuring the voltage using the Lebow load cell

shown in Figures 1 and 2, then calculating the torque from the calibration curve shown in Figure 16. The RPM was determined from the frequency generated from the magnetic speed pick-up and the 30 toothed gear. The frequency signal was multiplied by 2 to convert it to units of RPM.

$$HP\#3 = \frac{T_q \times N}{63025}$$

where:

T_q = Torque in (in-lbs)

N = Rotational Speed (RPM)

The referred quantities of speed, horsepower, and mass-flow rate from [Ref. 27] were with respect to standard atmosphere ($P_{ref}=29.92$ in Hg and $T_{ref}=519.7$ °R).

$$\text{Speed Parameter} = \frac{N}{\sqrt{\theta}}$$

$$\text{Flow Parameter} = \frac{\left(\dot{m}\right)\sqrt{\theta}}{\delta}$$

$$\text{Power Parameter} = \frac{HP}{\delta\sqrt{\theta}}$$

where:

$$\theta = \frac{T_{t3}}{T_{ref}}$$

$$\delta = \frac{P_{t3}}{P_{ref}}$$

BB	APM	T	U	V	W	X	Y	Z	AA	AB	AC	AD	AE	AF	AG	AH	AI	AJ
90	91	92	93	94	95	96	97	98	99	100	101	102	103	104	105	106	107	108
109	110	111	112	113	114	115	116	117	118	119	120	121	122	123	124	125	126	127
128	129	130	131	132	133	134	135	136	137	138	139	140	141	142	143	144	145	146
147	148	149	150	151	152	153	154	155	156	157	158	159	160	161	162	163	164	165
166	167	168	169	170	171	172	173	174	175	176	177	178	179	180	181	182	183	184
185	186	187	188	189	190	191	192	193	194	195	196	197	198	199	200	201	202	203
204	205	206	207	208	209	210	211	212	213	214	215	216	217	218	219	220	221	222
223	224	225	226	227	228	229	230	231	232	233	234	235	236	237	238	239	240	241
242	243	244	245	246	247	248	249	250	251	252	253	254	255	256	257	258	259	260
261	262	263	264	265	266	267	268	269	270	271	272	273	274	275	276	277	278	279
280	281	282	283	284	285	286	287	288	289	290	291	292	293	294	295	296	297	298
299	300	301	302	303	304	305	306	307	308	309	310	311	312	313	314	315	316	317
318	319	320	321	322	323	324	325	326	327	328	329	330	331	332	333	334	335	336
337	338	339	340	341	342	343	344	345	346	347	348	349	350	351	352	353	354	355
356	357	358	359	360	361	362	363	364	365	366	367	368	369	370	371	372	373	374
375	376	377	378	379	380	381	382	383	384	385	386	387	388	389	390	391	392	393
394	395	396	397	398	399	400	401	402	403	404	405	406	407	408	409	410	411	412
413	414	415	416	417	418	419	420	421	422	423	424	425	426	427	428	429	430	431
432	433	434	435	436	437	438	439	440	441	442	443	444	445	446	447	448	449	450
451	452	453	454	455	456	457	458	459	460	461	462	463	464	465	466	467	468	469
470	471	472	473	474	475	476	477	478	479	480	481	482	483	484	485	486	487	488
489	490	491	492	493	494	495	496	497	498	499	500	501	502	503	504	505	506	507
508	509	510	511	512	513	514	515	516	517	518	519	520	521	522	523	524	525	526
527	528	529	530	531	532	533	534	535	536	537	538	539	540	541	542	543	544	545
546	547	548	549	550	551	552	553	554	555	556	557	558	559	560	561	562	563	564
565	566	567	568	569	570	571	572	573	574	575	576	577	578	579	580	581	582	583
584	585	586	587	588	589	590	591	592	593	594	595	596	597	598	599	600	601	602
603	604	605	606	607	608	609	610	611	612	613	614	615	616	617	618	619	620	621
622	623	624	625	626	627	628	629	630	631	632	633	634	635	636	637	638	639	640
641	642	643	644	645	646	647	648	649	650	651	652	653	654	655	656	657	658	659
660	661	662	663	664	665	666	667	668	669	670	671	672	673	674	675	676	677	678
679	680	681	682	683	684	685	686	687	688	689	690	691	692	693	694	695	696	697
698	699	700	701	702	703	704	705	706	707	708	709	710	711	712	713	714	715	716
717	718	719	720	721	722	723	724	725	726	727	728	729	730	731	732	733	734	735
736	737	738	739	740	741	742	743	744	745	746	747	748	749	750	751	752	753	754
755	756	757	758	759	760	761	762	763	764	765	766	767	768	769	770	771	772	773
774	775	776	777	778	779	780	781	782	783	784	785	786	787	788	789	790	791	792
793	794	795	796	797	798	799	800	801	802	803	804	805	806	807	808	809	810	811
812	813	814	815	816	817	818	819	820	821	822	823	824	825	826	827	828	829	830
831	832	833	834	835	836	837	838	839	840	841	842	843	844	845	846	847	848	849
850	851	852	853	854	855	856	857	858	859	860	861	862	863	864	865	866	867	868
869	870	871	872	873	874	875	876	877	878	879	880	881	882	883	884	885	886	887
888	889	890	891	892	893	894	895	896	897	898	899	900	901	902	903	904	905	906
907	908	909	910	911	912	913	914	915	916	917	918	919	920	921	922	923	924	925
926	927	928	929	930	931	932	933	934	935	936	937	938	939	940	941	942	943	944
945	946	947	948	949	950	951	952	953	954	955	956	957	958	959	960	961	962	963
964	965	966	967	968	969	970	971	972	973	974	975	976	977	978	979	980	981	982
983	984	985	986	987	988	989	990	991	992	993	994	995	996	997	998	999	1000	1001
1.477E+00	1.455E+00	1.433E+00	1.411E+00	1.389E+00	1.367E+00	1.345E+00	1.323E+00	1.301E+00	1.279E+00	1.257E+00	1.235E+00	1.213E+00	1.191E+00	1.169E+00	1.147E+00	1.125E+00	1.103E+00	1.081E+00
2.420E+00	2.398E+00	2.376E+00	2.354E+00	2.332E+00	2.310E+00	2.288E+00	2.266E+00	2.244E+00	2.222E+00	2.200E+00	2.178E+00	2.156E+00	2.134E+00	2.112E+00	2.090E+00	2.068E+00	2.046E+00	2.024E+00
3.363E+00	3.341E+00	3.319E+00	3.297E+00	3.275E+00	3.253E+00	3.231E+00	3.209E+00	3.187E+00	3.165E+00	3.143E+00	3.121E+00	3.099E+00	3.077E+00	3.055E+00	3.033E+00	3.011E+00	2.989E+00	2.967E+00
4.306E+00	4.284E+00	4.262E+00	4.240E+00	4.218E+00	4.196E+00	4.174E+00	4.152E+00	4.130E+00	4.108E+00	4.086E+00	4.064E+00	4.042E+00	4.020E+00	3.998E+00	3.976E+00	3.954E+00	3.932E+00	3.910E+00
5.249E+00	5.227E+00	5.205E+00	5.183E+00	5.161E+00	5.139E+00	5.117E+00	5.095E+00	5.073E+00	5.051E+00	5.029E+00	5.007E+00	4.985E+00	4.963E+00	4.941E+00	4.919E+00	4.897E+00	4.875E+00	4.853E+00
6.192E+00	6.170E+00	6.148E+00	6.126E+00	6.104E+00	6.082E+00	6.060E+00	6.038E+00	6.016E+00	5.994E+00	5.972E+00	5.950E+00	5.928E+00	5.906E+00	5.884E+00	5.862E+00	5.840E+00	5.818E+00	5.796E+00
7.135E+00	7.113E+00	7.091E+00	7.069E+00	7.047E+00	7.025E+00	7.003E+00	6.981E+00	6.959E+00	6.937E+00	6.915E+00	6.893E+00	6.871E+00	6.849E+00	6.827E+00	6.805E+00	6.783E+00	6.761E+00	6.739E+00
8.078E+00	8.056E+00	8.034E+00	8.012E+00	7.990E+00	7.968E+00	7.946E+00	7.924E+00	7.902E+00	7.880E+00	7.858E+00	7.836E+00	7.814E+00	7.792E+00	7.770E+00	7.748E+00	7.726E+00	7.704E+00	7.682E+00
9.021E+00	8.999E+00	8.977E+00	8.955E+00	8.933E+00	8.911E+00	8.889E+00	8.867E+00	8.845E+00	8.823E+00	8.801E+00	8.779E+00	8.757E+00	8.735E+00	8.713E+00	8.691E+00	8.669E+00	8.647E+00	8.625E+00
9.964E+00	9.942E+00	9.920E+00	9.898E+00	9.876E+00	9.854E+00	9.832E+00	9.810E+00	9.788E+00	9.766E+00	9.744E+00	9.722E+00	9.700E+00	9.678E+00	9.656E+00	9.634E+00	9.612E+00	9.590E+00	9.568E+00
10.907E+00	10.885E+00	10.863E+00	10.841E+00	10.819E+00	10.797E+00	10.775E+00	10.753E+00	10.731E+00	10.709E+00	10.687E+00	10.665E+00	10.643E+00	10.621E+00	10.599E+00	10.577E+00	10.555E+00	10.533E+00	10.511E+00
11.850E+00	11.828E+00	11.806E+00	11.784E+00	11.762E+00	11.740E+00	11.718E+00	11.696E+00	11.674E+00	11.652E+00	11.630E+00	11.608E+00	11.586E+00	11.564E+00	11.542E+00	11.520E+00	11.498E+00	11.476E+00	11.454E+00
12.793E+00	12.771E+00	12.749E+00	12.727E+00	12.705E+00	12.683E+00	12.661E+00	12.639E+00	12.617E+00	12.595E+00	12.573E+00	12.551E+00	12.529E+00	12.507E+00	12.485E+00	12.463E+00	12.441E+00	12.419E+00	12.397E+00
13.736E+00	13.714E+00	13.692E+00	13.670E+00	13.648E+00	13.62													

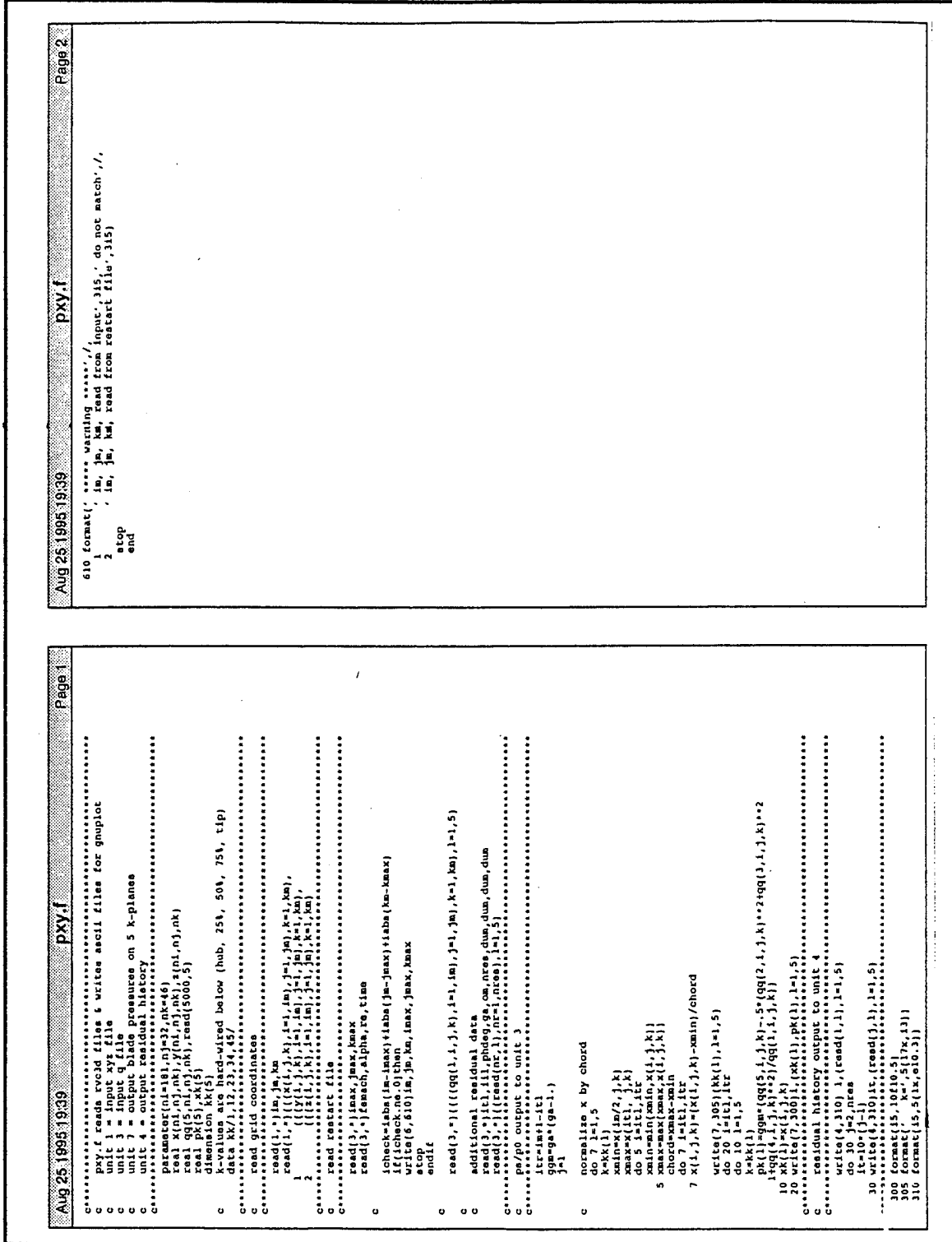
A	B	C	D	E	F	G	H	I	J	K	L	M	N	O	P	Q	R	S	T
ATM																			
1	2	3	4	5	6	7	8	9	10	11	12	13	14	15	16	17	18	19	20
1	2	3	4	5	6	7	8	9	10	11	12	13	14	15	16	17	18	19	20
...

Figure J 2. SSME_TTR Excel Reduced Data Collection Worksheet

A	B	C	D	E	F	G	H	I	J	K	L	M	N
46	8/24/95	1.03135E+00	1.4781E+00	7.6728E+01	2.9289E+03	3.7470E+00	1.1032E+00	1.0323E+00	4.9497E+00	4.2710E+00	4.7100E+00	1.0614E+00	1.2710E+00
47		1.21897E+00	3.3238E+00	7.6593E+01	4.8282E+03	1.5693E+01	1.2931E+00	1.0388E+00	2.9304E+01	2.2013E+01	2.6615E+01	1.5092E+01	2.4165E+00
48		1.2007E+00	3.2545E+00	7.8916E+01	4.9135E+03	1.6127E+01	1.3039E+00	1.0428E+00	2.3154E+01	2.1898E+01	2.1717E+01	2.0147E+00	2.6648E+00
49		1.2170E+00	3.2166E+00	7.8153E+01	4.9099E+03	1.5933E+01	1.3033E+00	1.0417E+00	2.4166E+01	2.1642E+01	2.1755E+01	2.1762E+00	2.6959E+00
50		1.2183E+00	3.2693E+00	7.8272E+01	4.9057E+03	1.6168E+01	1.3032E+00	1.0431E+00	2.3712E+01	2.1761E+01	2.1925E+01	2.1735E+00	2.1994E+00
51		1.2174E+00	3.3349E+00	7.8750E+01	4.9104E+03	1.6168E+01	1.3033E+00	1.0439E+00	2.3653E+01	2.1984E+01	2.1726E+01	1.5429E+00	2.4389E+00
52		1.2180E+00	3.0203E+00	7.6751E+01	4.9009E+03	1.5822E+01	1.3091E+00	1.0433E+00	2.3099E+01	2.1901E+01	2.1409E+01	2.2897E+00	2.6533E+00
53		1.2109E+00	3.4879E+00	7.8761E+01	4.8967E+03	1.4251E+01	1.3191E+00	1.0433E+00	2.0938E+01	1.9632E+01	2.4078E+01	1.7270E+00	2.6075E+00
54		1.4231E+00	4.2854E+00	7.9241E+01	6.9698E+03	2.5320E+00	1.6212E+00	1.0491E+00	6.6707E+01	5.8212E+01	6.7901E+01	2.4770E+00	3.1970E+00
55		1.4201E+00	4.2859E+00	8.0183E+01	6.8400E+03	3.4460E+00	1.6212E+00	1.0504E+00	6.2179E+01	5.8649E+01	6.3684E+01	1.0211E+00	2.6532E+00
56		1.4209E+00	4.3841E+00	7.9707E+01	6.8425E+03	3.4500E+00	1.6218E+00	1.0504E+00	6.2399E+01	5.9103E+01	6.5147E+01	6.7363E+01	2.4796E+00
57		1.4192E+00	3.9248E+00	7.8856E+01	6.8423E+03	3.3407E+00	1.6267E+00	1.0514E+00	6.142E+01	5.874E+01	6.5147E+01	1.5403E+00	2.9512E+00
58		1.4054E+00	3.9978E+00	7.8666E+01	6.8738E+03	2.6745E+00	1.6302E+00	1.0526E+00	6.2027E+01	5.8708E+01	6.5713E+01	5.6899E+01	2.3389E+00
59		1.3987E+00	3.9971E+00	7.8666E+01	6.8738E+03	2.6514E+00	1.6411E+00	1.0526E+00	6.2027E+01	5.8708E+01	6.5713E+01	1.3084E+00	2.4029E+00
60		1.4634E+00	4.5335E+00	7.8466E+01	6.8632E+03	2.9416E+00	1.6581E+00	1.0534E+00	6.5713E+01	5.9307E+01	6.6272E+01	8.1763E+01	2.4029E+00
61		1.5206E+00	4.5714E+00	8.0849E+01	7.6503E+03	2.1001E+00	1.7896E+00	1.0535E+00	8.1393E+01	6.635E+01	6.6272E+01	1.3084E+00	2.4007E+00
62		1.5185E+00	3.9103E+00	8.1304E+01	7.6498E+03	3.3924E+00	1.7896E+00	1.0535E+00	8.1393E+01	6.635E+01	6.6272E+01	1.3084E+00	2.4007E+00
63		1.5185E+00	3.9103E+00	8.1304E+01	7.6498E+03	3.3924E+00	1.7896E+00	1.0535E+00	8.1393E+01	6.635E+01	6.6272E+01	1.3084E+00	2.4007E+00
64		1.5185E+00	3.9103E+00	8.1304E+01	7.6498E+03	3.3924E+00	1.7896E+00	1.0535E+00	8.1393E+01	6.635E+01	6.6272E+01	1.3084E+00	2.4007E+00
65		1.5185E+00	3.9103E+00	8.1304E+01	7.6498E+03	3.3924E+00	1.7896E+00	1.0535E+00	8.1393E+01	6.635E+01	6.6272E+01	1.3084E+00	2.4007E+00
66		1.5185E+00	3.9103E+00	8.1304E+01	7.6498E+03	3.3924E+00	1.7896E+00	1.0535E+00	8.1393E+01	6.635E+01	6.6272E+01	1.3084E+00	2.4007E+00
67		1.5185E+00	3.9103E+00	8.1304E+01	7.6498E+03	3.3924E+00	1.7896E+00	1.0535E+00	8.1393E+01	6.635E+01	6.6272E+01	1.3084E+00	2.4007E+00
68		1.5185E+00	3.9103E+00	8.1304E+01	7.6498E+03	3.3924E+00	1.7896E+00	1.0535E+00	8.1393E+01	6.635E+01	6.6272E+01	1.3084E+00	2.4007E+00
69		1.5185E+00	3.9103E+00	8.1304E+01	7.6498E+03	3.3924E+00	1.7896E+00	1.0535E+00	8.1393E+01	6.635E+01	6.6272E+01	1.3084E+00	2.4007E+00
70		1.5013E+00	4.5731E+00	8.0720E+01	7.6538E+03	2.7273E+00	1.7931E+00	1.0535E+00	8.3604E+01	7.9910E+01	7.0300E+01	2.9723E+01	2.1038E+00
71		1.4764E+00	4.7169E+00	7.8729E+01	7.6538E+03	2.6901E+00	1.7931E+00	1.0535E+00	8.0219E+01	7.7123E+01	7.9262E+01	1.8962E+00	2.3248E+00
72		1.4764E+00	4.7169E+00	7.8729E+01	7.6538E+03	2.6901E+00	1.7931E+00	1.0535E+00	8.0219E+01	7.7123E+01	7.9262E+01	1.8962E+00	2.3248E+00
73	8/23/95	1.03162E+00	8.9460E+01	9.2429E+01	1.8394E+03	8.8372E+01	1.0410E+00	1.0294E+00	1.3793E+00	7.7448E+00	1.36383E+00	9.9363E+01	9.4412E+01
74		1.1968E+00	1.4047E+00	7.6532E+01	4.8575E+03	1.1240E+00	1.2973E+00	1.0371E+00	2.3129E+01	2.0931E+01	1.1249E+01	1.3269E+00	1.3666E+00
75		1.2145E+00	2.1067E+00	7.8147E+01	4.8690E+03	1.6970E+00	1.4083E+00	1.0403E+00	1.3788E+00	2.1807E+00	1.6966E+00	2.0813E+00	2.0940E+00
76		1.2145E+00	2.1067E+00	7.8147E+01	4.8690E+03	1.6970E+00	1.4083E+00	1.0403E+00	1.3788E+00	2.1807E+00	1.6966E+00	2.0813E+00	2.0940E+00
77		1.2145E+00	2.1067E+00	7.8147E+01	4.8690E+03	1.6970E+00	1.4083E+00	1.0403E+00	1.3788E+00	2.1807E+00	1.6966E+00	2.0813E+00	2.0940E+00
78		1.2145E+00	2.1067E+00	7.8147E+01	4.8690E+03	1.6970E+00	1.4083E+00	1.0403E+00	1.3788E+00	2.1807E+00	1.6966E+00	2.0813E+00	2.0940E+00
79		1.2145E+00	2.1067E+00	7.8147E+01	4.8690E+03	1.6970E+00	1.4083E+00	1.0403E+00	1.3788E+00	2.1807E+00	1.6966E+00	2.0813E+00	2.0940E+00
80		1.2145E+00	2.1067E+00	7.8147E+01	4.8690E+03	1.6970E+00	1.4083E+00	1.0403E+00	1.3788E+00	2.1807E+00	1.6966E+00	2.0813E+00	2.0940E+00
81		1.2145E+00	2.1067E+00	7.8147E+01	4.8690E+03	1.6970E+00	1.4083E+00	1.0403E+00	1.3788E+00	2.1807E+00	1.6966E+00	2.0813E+00	2.0940E+00
82		1.2145E+00	2.1067E+00	7.8147E+01	4.8690E+03	1.6970E+00	1.4083E+00	1.0403E+00	1.3788E+00	2.1807E+00	1.6966E+00	2.0813E+00	2.0940E+00
83		1.2145E+00	2.1067E+00	7.8147E+01	4.8690E+03	1.6970E+00	1.4083E+00	1.0403E+00	1.3788E+00	2.1807E+00	1.6966E+00	2.0813E+00	2.0940E+00
84		1.2145E+00	2.1067E+00	7.8147E+01	4.8690E+03	1.6970E+00	1.4083E+00	1.0403E+00	1.3788E+00	2.1807E+00	1.6966E+00	2.0813E+00	2.0940E+00
85		1.2145E+00	2.1067E+00	7.8147E+01	4.8690E+03	1.6970E+00	1.4083E+00	1.0403E+00	1.3788E+00	2.1807E+00	1.6966E+00	2.0813E+00	2.0940E+00
86		1.2145E+00	2.1067E+00	7.8147E+01	4.8690E+03	1.6970E+00	1.4083E+00	1.0403E+00	1.3788E+00	2.1807E+00	1.6966E+00	2.0813E+00	2.0940E+00
87		1.2145E+00	2.1067E+00	7.8147E+01	4.8690E+03	1.6970E+00	1.4083E+00	1.0403E+00	1.3788E+00	2.1807E+00	1.6966E+00	2.0813E+00	2.0940E+00
88		1.2145E+00	2.1067E+00	7.8147E+01	4.8690E+03	1.6970E+00	1.4083E+00	1.0403E+00	1.3788E+00	2.1807E+00	1.6966E+00	2.0813E+00	2.0940E+00
89		1.2145E+00	2.1067E+00	7.8147E+01	4.8690E+03	1.6970E+00	1.4083E+00	1.0403E+00	1.3788E+00	2.1807E+00	1.6966E+00	2.0813E+00	2.0940E+00
90		1.2145E+00	2.1067E+00	7.8147E+01	4.8690E+03	1.6970E+00	1.4083E+00	1.0403E+00	1.3788E+00	2.1807E+00	1.6966E+00	2.0813E+00	2.0940E+00
91		1.2145E+00	2.1067E+00	7.8147E+01	4.8690E+03	1.6970E+00	1.4083E+00	1.0403E+00	1.3788E+00	2.1807E+00	1.6966E+00	2.0813E+00	2.0940E+00
92		1.2145E+00	2.1067E+00	7.8147E+01	4.8690E+03	1.6970E+00	1.4083E+00	1.0403E+00	1.3788E+00	2.1807E+00	1.6966E+00	2.0813E+00	2.0940E+00
93		1.2145E+00	2.1067E+00	7.8147E+01	4.8690E+03	1.6970E+00	1.4083E+00	1.0403E+00	1.3788E+00	2.1807E+00	1.6966E+00	2.0813E+00	2.0940E+00
94		1.2145E+00	2.1067E+00	7.8147E+01	4.8690E+03	1.6970E+00	1.4083E+00	1.0403E+00	1.3788E+00	2.1807E+00	1.6966E+00	2.0813E+00	2.0940E+00
95		1.2145E+00	2.1067E+00	7.8147E+01	4.8690E+03	1.6970E+00	1.4083E+00	1.0403E+00	1.3788E+00	2.1807E+00	1.6966E+00	2.0813E+00	2.0940E+00
96		1.2145E+00	2.1067E+00	7.8147E+01	4.8690E+03	1.6970E+00	1.4083E+00	1.0403E+00	1.3788E+00	2.1807E+00	1.6966E+00	2.0813E+00	2.0940E+00
97		1.2145E+00	2.1067E+00	7.8147E+01	4.8690E+03	1.6970E+00	1.4083E+00	1.0403E+00	1.3788E+00	2.1807E+00	1.6966E+00	2.0813E+00	2.0940E+00

Figure J.3. VEL_PRFL Excel Data Collection Worksheet (TTR Exit Data)

APPENDIX K. FORTRAN PROGRAMS



```
program shrink99
*
* This inputs data and multiplies it by 0.99 for a 99%
* shrink factor.
*
  real x(810),p(810)
  open (unit=2,file='hotstrt.dat',status='old')
  open (unit=15,file='lsrt.togin',status='new')
  read(2,*) (x(i),i=1,810)
  do 20 i=1,810
    p(i)=x(i)*0.99
  20 continue
*
* -- print the data out in blocks
*
  write (15,*) (p(i),i=1,56)
  write (15,*)
  write (15,*) (p(i),i=57,113)
  write (15,*)
  write (15,*) (p(i),i=114,170)
  write (15,*)
  write (15,*) (p(i),i=171,226)
  write (15,*)
  write (15,*) (p(i),i=227,324)
  write (15,*)
  write (15,*) (p(i),i=325,422)
  write (15,*)
  write (15,*) (p(i),i=423,519)
  write (15,*)
  write (15,*) (p(i),i=520,616)
  write (15,*)
  write (15,*) (p(i),i=617,713)
  write (15,*)
  write (15,*) (p(i),i=714,810)
  close(2)
  close(15)
  stop
end
```

Figure K 2. SHRINK99.F


```

'===== ROTOR STATOR STAGE ROTOR.
sn11 im=180 jw=25 km=45 itl=20 ill=85 lend
sn12 natg=4 cfl= 4.0 avisc1=0.0 avisc2=1.5 avisc3=1.5 ir=1
     epl=0.65 epj=0.75 epk=0.75 lvd=1 itmag=1000 lend
sn13 lbca=3 lbca=3 lscat=0 lscat=1 lscat=50 lscat=1 lscat=1
     on=0.0 ptt=0.665 lgc=1 emax=0.332 emty=-0.713 expt=0 alex=+41.9
     lend
sn14 em=0.055971 pr=0.678 lgc=1 emax=0.332 emty=-0.713 expt=0 alex=+41.9
     lend
sn15 ill=2 tw=0 renc=664075.6 pnt=7 pnt=7 pnt=7 pnt=7 pnt=7 pnt=7 pnt=7
     attp=0 emax=14. jedge=15 kedge=11 lftin=0 dblh=0.0
     dblt=0.0 xrl=1.5 xrt=2.65 kmg=11 lftin=0 dblh=0.0
sn16 lol=1 loz=151 oar=0. ixjb=0 nj=1 nko=3 jo=1 ko=13 l7 21 lend

```

```

'===== STATOR STAGE STATOR.
sn11 im=151 jw=31 km=45 itl=20 ill=70 lend
sn12 natg=4 cfl= 4.0 avisc1=0.0 avisc2=1.5 avisc3=1.5 ir=1
     epl=0.65 epj=0.75 epk=0.75 lvd=1 itmag=1000 lend
sn13 lbca=3 lbca=3 lscat=0 lscat=1 lscat=50 lscat=1 lscat=1
     on=0.0 ptt=0.665 lgc=1 emax=0.332 emty=0.0 expt=0 alex=-65
     lend
sn14 em=0.055971 pr=0.678 lgc=1 emax=0.332 emty=0.0 expt=0 alex=-65
     lend
sn15 ill=2 tw=0 renc=664075.6 pnt=7 pnt=7 pnt=7 pnt=7 pnt=7 pnt=7 pnt=7
     attp=0 emax=14. jedge=15 kedge=11 lftin=0 dblh=0.0
     dblt=0.0 xrl=1.5 xrt=2.65 kmg=11 lftin=0 dblh=0.0
sn16 lol=1 loz=151 oar=0. ixjb=0 nj=1 nko=3 jo=1 ko=13 l7 21 lend

```

Figure L 3. RVC3D.IN for both the Stator and Rotor

LIST OF REFERENCES

1. Studevan, C.C., "Design of a Cold-Flow Test Facility for the High-Pressure Fuel Turbopump Turbine of the Space Shuttle Main Engine," Master's Thesis, Naval Postgraduate School, Monterey, California, December 1993.
2. Rutkowski, R.J., "Cold-flow Simulation of the Alternate Turbopump Development Turbine of the Space Shuttle Main Engine High Pressure Fuel Turbopump," Master's Thesis, Naval Postgraduate School, Monterey, California, March 1994.
3. Chima, R.V., "RVC3D (Rotor Viscous Code 3-D)," User's Manual, March 1992.
4. National Instruments, "Getting Started with Your AT-GPIB/TNT and the NI-488.2 Software for Windows," User's Manual, Part Number 320719B-01, August 1994.
5. National Instruments, "DAQ PC-DIO-24," User's Manual, Part Number 320288-01, July 1993.
6. National Instruments, "DAQ PC-LPM-16," User's Manual, Part Number 320287-01, November 1993.
7. National Instruments, "LabVIEW for Windows," User's Manual, Part Number 320534-01, August 1993.
8. Eargle T., "Performance Evaluation of an Air Research T-18A40 Turbocharger with Applications to the Transonic Compressor Test Rig," Naval Postgraduate School, Monterey, California, TPL TN 79-04 September 1979.
9. Kaiser M.J., "T-18A40 Turbocharger Performance," Naval Postgraduate School, Monterey, California, TPL TN 80-02 July 1980.
10. Hewlett-Packard Company, "Model 3456A Digital Voltmeter," User's Manual, Revision B, Part Number 03456-90054, February 1982.
11. Hewlett-Packard Company, "5335A Universal Frequency Counter," User's Manual, Fourth Edition, Part Number 05335-90021, August 1988.
12. Scanivalve Corporation, "Digital Interface Unit SDIU MK1 &MK5," Operations Manual, Second Edition, 1994.

13. Hewlett-Packard Company, "Model 3495A Scanner," Programming and Service Manual, Part Number 03495-90012, August 1978.
14. Omega Engineering Inc. "Temperature Measurement Handbook and Encyclopedia," Catalog, 1985.
15. Fishe, R., Fax Transmission, Power Machine Co., 08 May 93.
16. AIRPAX Corporation, "TACHTROL 3 Tachometer," Operations Manual, 1994.
17. Vavra, M.H., "Determination of Flow Rates of Allis-Chalmers Axial Flow Compressor VA-312 of Propulsion Laboratories by Means of Square-Edged Orifices," Naval Postgraduate School, Monterey, California, TN 63T-2 1963.
18. Spitz, J.W., "Laser Anemometry and Viscous Computation of the Flow Through an Annular Turbine Cascade" Master's Thesis, Naval Postgraduate School, Monterey, California, March 1994.
19. Fischer & Porter, "Series 53EL4000 Electronic Controller," Instruction Bulletin, Revision 2, September 1974.
20. Gaddis, S.W., Hudson, S.T., and Johnson, P.D., "Cold-Flow Testing of the Space Shuttle Main Engine Alternate Turbine Development High Pressure Fuel Turbine Model," ASME Paper 92-GT-280, June 1991.
21. Cohen, H., Rogers, G.F.C., and Saravanamuttoo, H.I.H., "Gas Turbine Theory," Second Edition, Longman Group Limited 1972.
22. Instructional Manual Waterbrake Dynamometer, Model 061-109, Kahn Companies, No. 9755, 1976.
23. Glassman, A.J., "TURBINE DESIGN and APPLICATION," Volume one, NASA SP-290, 1973.
24. Chima, R.V., "TCGRID (Turbomachinery C-Grid)," User's Manual, March 1992.
25. Walatka, P.P., and Buning, P., "PLOT3D" User's Manual, NASA TM 101067, March 1989.
26. Chima, R.V., and Yokota, J.W., "Numerical Analysis of Three-Dimensional Viscous Flows in Turbomachinery," AIAA Journal Vol. 28, No. 5 May 1990.

27. Shreeve, R.P., Class Notes, AA4431 Turbomachines: Analysis, Design and Experiment, Naval Postgraduate School, Monterey, CA, 1994.

INITIAL DISTRIBUTION LIST

		No. Copies
1.	Defense Technical Information Center Cameron Station Alexandria VA 22304-6145	2
2.	Library, Code 052 Naval Postgraduate School Monterey CA 93943-5002	2
3.	The Chairman Department of Aeronautics and Astronautics Code AA Naval Postgraduate School 699 Dyer Road-Room 137 Monterey CA 93943	1
4.	Assoc Prof. Garth V. Hobson Department of Aeronautics and Astronautics Code AA Naval Postgraduate School 699 Dyer Road-Room 137 Monterey CA 93943	10
5.	Professor Raymond P. Shreeve Department of Aeronautics and Astronautics Code AA Naval Postgraduate School 699 Dyer Road-Room 137 Monterey CA 93940	1
6.	Naval Air Warfare Center AIR-4.4.T (Attn: Mr. C. Gordon) Washington DC 20361-5360	1
7.	Naval Air Warfare Center Aircraft Division AIR-4.4.3.1 (Attn: D. Parish) Propulsion and Power Engineering, Building 106 Patuxent River, MD 20670-5304	1
8.	Philip A. Greco 6016 Royal Estates PL Jacksonville FL 32211	2